Supporting Information

A sensitive zinc probe operating via enhancement of excited-state intramolecular charge transfer

G. Dinesh Kumar,[a] Marzena Banasiewicz,[b] Antoni Wrzosek,[c] Omar O'Mari,[d] Monika Zochowska,[c] Valentine I. Vullev,*[d] Denis Jacquemin,*[e] Adam Szewczyk,*[c] and Daniel T. Gryko*[a]

[a] Institute of Organic Chemistry, Polish Academy of Sciences, Kasprzaka 44/52, 01-224 Warsaw, Poland. E-mail: dtgryko@icho.edu.pl

[b] Institute of Physics, Polish Academy of Sciences, Al. Lotników 32/46, 02-668 Warsaw, Poland.

[c] Nencki Institute of Experimental Biology of Polish Academy of Sciences, Pasteur 3, 02-093 Warsaw, Poland. E-mail: a.szewczyk@nencki.gov.pl.

[d] Department of Bioengineering, University of California, Riverside, 900 University Ave., Riverside, CA 92521, USA. Email: vullev@ucr.edu

[e] CEISAM UMR 6230, CNRS, Université de Nantes, 44000 Nantes, France. E-mail: denis.Jacquemin@univ-nantes.fr

Table of contents

Section S1: General Information

All reagents and solvents were purchased from commercial sources and were used as received unless otherwise noted. Reagent grade solvents (CH_2Cl_2, hexanes) were distilled prior to use. Transformations with moisture- and oxygen-sensitive compounds were performed under a stream of argon. The reaction progress was monitored by means of thin-layer chromatography (TLC), which was performed on Kieselgel 60. The identity and purity of prepared compounds were proved by ^{1}H NMR and ^{13}C NMR as well as by mass spectrometry (via EI-MS or ESI-MS). HRMS (ESI-TOF) and HRMS (EI): double-focusing magnetic sector instruments with EBE geometry were utilized. NMR spectra were measured on 400 or 500 or 600 MHz instruments. Chemical shifts (δ, ppm) were determined with tetramethylsilane (TMS) as the internal reference; J values are given in Hz. All melting points for crystalline products were measured with an automated melting point apparatus and are given without correction.

UV/Vis absorption spectra were recorded on a PerkinElmer Lambda 35 Spectrometer. Fluorescence spectra were recorded on a FLS1000 of Edinburgh Instruments. All linear optical studies were performed with freshly prepared air-equilibrated solutions at room temperature (298 K). Acetonitrile was spectrophotometric grade and was used without further purification. Quartz cells (10 mm) were used for the measurements of absorption and emission spectra. As a standard, Rh6G (Φ_{fl} = 0.94 in EtOH) was used to determine fluorescence quantum yields.

Section S2: Experimental Procedure

All reagents and solvents were purchased from commercial sources and were used as received unless otherwise noted. Reagent grade solvents (DCM, hexanes) were distilled prior to use. Transformations with moisture- and oxygen-sensitive compounds were performed under a stream of argon. The reaction progress was monitored by means of thin-layer chromatography (TLC), which was performed on Kieselgel 60. The identity and purity of prepared compounds were proved by ^{1}H NMR and ^{13}C NMR as well as by mass spectrometry (via EI-MS or ESI-MS). HRMS (ESI-TOF) and HRMS (EI): double-focusing magnetic sector instruments with EBE geometry were utilized. NMR spectra were measured on 400 or 500 or 600 MHz instruments. Chemical shifts (δ, ppm) were determined with tetramethylsilane (TMS) as the internal reference; J values are given in Hz. All melting points for crystalline products were measured with an automated melting point apparatus and are given without correction. Pyrrolidone **1** was obtained following the literature procedure.[1]

Synthesis of nitriles:

2-(bis(pyridin-2-ylmethyl)amino)isonicotinonitrile (2a)

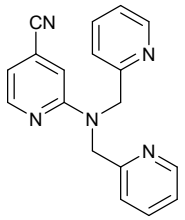

2a

A mixture commercially available 2-fluoro-4-cyanopyridine (0.5 g, 4 mmol), di-(2-picolyl)amine (0.82 g, 4 mmol) in 5 ml of deoxygenated N,N-dimethylacetamide was heated to 130 °C under argon for overnight. Then reaction mixture was cooled to room temperature, diluted with water (100 mL) and extracted with EtOAc (2×100 mL). The organic phase dried over anhydrous Na_2SO_4 and filtered. The solvent was removed under reduced pressure and the resulting colorless oil was chromatographed on silica gel (hexane/EtOAc = 1: 1) to obtain desired product as colorless oil (1.06 g, 86%). ^{1}H NMR (500 MHz, $CDCl_3$) δ 8.56 (dd, *J* = 9.6 Hz, 2H), 8.27 (d, *J* = 11.2 Hz, 1H), 7.62 (dt, *J* = 3.4 Hz, 2H), 7.22-7.17 (m, 4H), 6.7 (dd, *J* = 8.0 Hz, 2H), 4.98 (s, 4H). ^{13}C NMR (126 MHz, $CDCl_3$) δ 158.2, 157.4, 149.6, 149.3, 136.8, 122.4, 121.4, 121.3, 117.4, 113.3, 108.5, 54.1. HRMS (ESI, *m/z*): $[M+Na]^+$ Calcd. for $C_{18}H_{15}N_5Na$: 324.3530; found, 324.3460.

2-((bis(pyridin-2-ylmethyl)amino)methyl)isonicotinonitrile (2b)

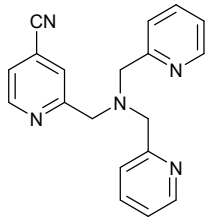

2b

To a mixture of 2-Formylpyridine-4-carbonitrile (1 g, 7.5 mmol) and di-2-picolylamine (1.4 mL, 7.5 mmol) in 1,2-dicloroethane (20 mL), then $NaBH(OAc)_3$ (2.1 g, 9.8 mmol) was added in portions. Then the reaction was stirred at room temperature for overnight, then reaction mixture was first acidified with 1N HCl to pH 4-5, followed by neutralized with 1N NaOH to pH 7-8. The organic phase was separated, and aqueous phase was extracted with DCM (2×100mL). The organic phases were combined and dried over Na_2SO_4 and the solvent was evaporated to give crude product which was purified by column chromatography using DCM/CH3OH (10:1) to obtain the desired product **2b** as a brown liquid (1.94 g, 82%). ^{1}H NMR (500 MHz, $CDCl_3$) δ 8.65 (d, *J* = 5.1 Hz, 1H), 8.52 (m, 2H), 7.85 (s, 1H), 7.65 (dt, *J* = 7.6 Hz, 2H), 7.49 (d, *J* = 7.8 Hz, 2H), 7.32 (dd, *J* = 5.1 Hz, 1H), 7.14 (m, 2H), 3.9 (s, 2H), 3.8(s, 4H). ^{13}C NMR (126 MHz, $CDCl_3$) δ 161.8, 158.6, 149.8, 149.3, 136.5, 124.6, 123.2, 123.1, 122.2, 120.1, 116.8, 60.5, 59.6. HRMS (ESI, *m/z*): $[M+Na]^+$ Calcd. for $C_{19}H_{17}N_5Na$: 338.1382; found, 338.1380.

ethyl 4-hydroxy-2-(4-methoxyphenyl)-1-(3-morpholinopropyl)-5-oxo-2,5-dihydro-1H-pyrrole-3-carboxylate (5)

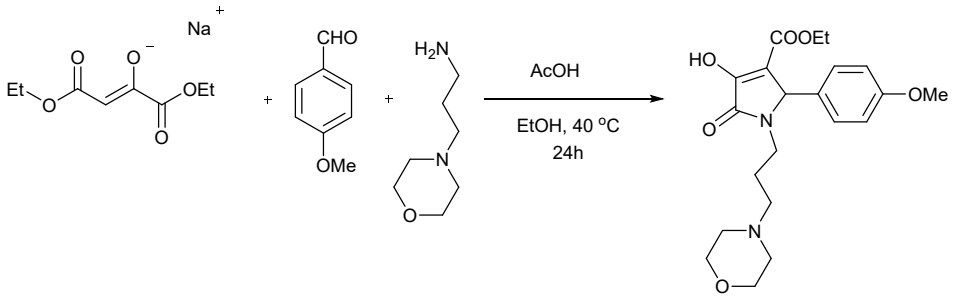

5

A 250 mL round bottom flask equipped with a magnetic stirring bar, was charged with ethanol (100 mL), 4-methoxy benzaldehyde (6.5 mL, 53 mmol) and (3-Aminopropyl)morpholine (7.8 mL, 53 mmol), reaction mixture was kept at room temperature, with constant stirring for 15 minutes. Next diethyl oxalacetate (10.0 g, 53 mmol) was added in one portion, followed by dropwise addition of acetic acid (6.1 mL, 106 mmol). Reaction mixture was heat up to 40 °C, and vigorously stirred overnight. Then reaction mixture was cooled to room temperature and diluted with water (200 mL), and extracted with DCM (200mL×2). Organic phase were dried over anhydrous Na_2SO_4, filtered and concentrated in vacuo. Yellowish solid was recrystallized from EtOAc to obtain product **5** as white crystals (15.6 g, 72%); mp 171-172 °C.^{1}H NMR (600 MHz, $CDCl_3$) δ 7.10 (d, *J* = 8.6 Hz, 2H), 6.86 (d, *J* = 8.7 Hz, 2H), 5.07 (s, 1H), 4.65 (bs, 2H), 4.14 (q, *J* = 6.3 Hz, 2H), 3.8 (s, 3H), 3.73-3.65 (m, 5H), 2.84-2.79 (m, 1H), 2.49 (s, 3H), 2.46-2.34 (m, 2H), 1.77 – 1.64 (m, 2H), 1.12 (t, *J* = 7.1 Hz, 3H); ^{13}C NMR (151 MHz, $CDCl_3$) δ 166.1, 165.1, 164.8, 159.8, 158.6, 128.9, 127.3, 114.1,

111.6, 66.4, 60.5, 55.7, 55.3, 53.2, 38.6, 24.4, 14.0. HRMS (ESI, *m/z*): $[M+H]^+$ Calcd. for $C_{21}H_{29}N_2O_6$: 405.2026; found, 405.2024.

ethyl 4-hydroxy-2-(4-methoxyphenyl)-1-(3-morpholinopropyl)-5-oxopyrrolidine-3-carboxylate (6)

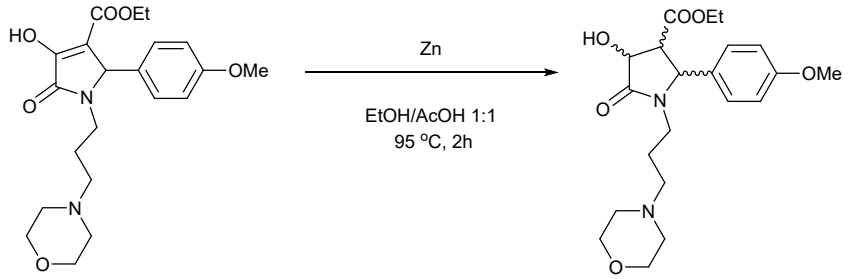

6

Compound **5** (15.0 g, 37.1 mmol) was dissolved in 150 mL mixture of EtOH/AcOH (1:1) and zinc powder (14.6 g, 222.5 mmol) was added and reaction mixture vigorously stirred at 95 °C for 1h. A second portion of zinc powder (14.6 g, 222.5 mmol) was added and stirring was continued at 95 °C until completion of the reaction. After cooling to room temperature reaction mixture was diluted with EtOAc (100 mL) the excess of zinc and the inorganic salts were filtered off. The filtrate was then diluted with water (150 mL). The aqueous layer was extracted with EtOAc (100 mL), and the combined organic phases were washed with saturated $NaHCO_3$ solution until neutral and finally dried over Na_2SO_4, filtered and concentrated in vacuo to obtain liquid product **6** as mixture of diastereoisomers (10.8 g, 72%). Careful analysis of ^1H NMR spectra of crude **6** showed the ratio 2:1 of major isomer **6** with the all-trans configuration in relation to the rest three minor compounds.

Crude compound (10.8 g, 31.9 mmol) was dissolved in dry EtOH (75 mL), freshly powdered K_2CO_3 (8.0 g, 79.7 mmol) was added in one portion. Reaction mixture was stirred at room temperature for 30 minutes. Next reaction mixture was diluted with EtOAc (100 mL) the excess of inorganic salts were filtered off. The filtrate was then washed with water (100 mL x 2), organic phase was dried over Na_2SO_4, filtered and concentrated in vacuum to obtain yellowish liquid product (10.8 g, 99.5 %). ^1H NMR spectra showed 10:1 ratio of major isomer **6a** with the all-trans configuration in relation to the rest two minor compounds.

^1H NMR (500 MHz, $CDCl_3$) δ 7.22 (d, *J* = 8.7 Hz, 2H), 7.03 (bs, 4H), 6.91 (d, *J* = 8.7 Hz, 2H), 4.66 (dd, *J* = 8.4, 7.9 Hz, 2H), 4.14 (q, *J* = 4.8 Hz, 2H), 3.8 (s, 3H), 3.73-3.65 (m, 5H), 3.58-3.50 (m, 1H), 2.75-2.60 (m, 2H), 2.44 – 2.35 (m, 2H), 1.66-1.56 (m, 2H), 1.22 (t, *J* = 7.1 Hz, 3H); ^{13}C NMR (101 MHz, $CDCl_3$) δ 175.6, 173.5, 171.2, 160.0, 129.0, 114.4, 72.2, 65.9, 61.4, 60.9, 55.2, 52.6, 49.2, 38.7, 22.7, 21.4, 14.0. HRMS (ESI, *m/z*): $[M+H]^+$ Calcd. for $C_{21}H_{31}N_2O_6$: 407.2182; found, 407.2183.

ethyl 2-(4-methoxyphenyl)-1-(3-morpholinopropyl)-5-oxo-4-((trimethylsilyl)oxy)pyrrolidine-3-carboxylate (7)

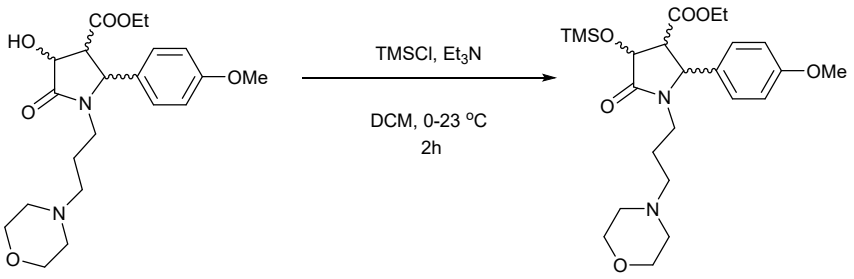

7

To cooled to ~0 °C solution of **6a** (7.0 g, 17.2 mmol) in dry DCM (100 mL), dry Et_3N (4.4 mL, 30.9 mmol) was added, next TMSCl (3.3 mL, 25.8 mmol) was added drop wise. After addition cooling bath was removed, and reaction mixture was allowed to reach room temperature and stirring was continued at room temperature for 1.5 h. Next reaction mixture was diluted with water (100 mL), phases were separated and organic phase was dried over anhydrous Na_2SO_4, filtered and concentrated in vacuo gives brownish oil (6.8 g, 82%) of product **7** without chromatographic purification. ^{1}H NMR spectra showed 10:1 ratio of major isomer **7** with the all-trans configuration in relation to the rest two minor compounds, used for next reaction without further purification.

^{1}H NMR (600 MHz, $CDCl_3$) δ 7.13 (d, *J* = 8.5 Hz, 2H), 6.84 (d, *J* = 8.7 Hz, 2H), 4.55-4.49 (m, 2H), 4.10-4.06 (m, 2H), 3.75 (s, 3H), 3.56 (m, 6H), 2.91 (m, 1H), 2.62-2.58 (m, 1H), 2.22 (bs, 4H), 1.57-1.51 (m, 2H), 1.46-1.4 (m, 1H), 1.15 (t, *J* = 7.2 Hz, 3H), 0.15 (s, 9H). ^{13}C NMR (151 MHz, $CDCl_3$) δ 171.7, 171.6, 159.8, 129.7, 128.8, 114.3, 73.4, 66.8, 61.3, 60.5, 57.1, 55.9, 55.3, 53.5, 39.1, 23.5, 14.1, 1.9, 0.1. HRMS (ESI, *m/z*): $[M+H]^+$ Calcd. for $C_{24}H_{39}N_2O_6Si$: 479.2577; found, 479.2588.

General procedure for the synthesis of DPP derivatives

In flame dried Schlenk flask, a mixture of appropriate nitrile (1 eq.) and lithium *tert*-butoxide (4 eq.) was heated to 110 °C under argon. To this solid mixture, *tert*-amyl alcohol (5 mL) was added in one portion followed by dropwise addition of pyrrolidone **1** or **7** (1 eq.) dissolved in dry toluene (3 mL). The resulting dark solution was left to stir at this temperature for overnight. After cooling to room temperature reaction mixture was diluted with water (100 mL) and extracted with DCM (100 mL), water phase was one more time washed with DCM (50 mL). The combined organic phases were dried over Na_2SO_4, filtered and concentrated in vacuum. The resulting crude compound was chromatographed on silica gel (DCM/MeOH = 9: 1) and crystallization from DCM/n-hexanes allowed to obtain the desired DPP product.

6-(2-(bis(pyridin-2-ylmethyl)amino)pyridin-4-yl)-2-butyl-3-(4-methoxyphenyl)-2,5-dihydropyrrolo[3,4-*c*]pyrrole-1,4-dione (3)

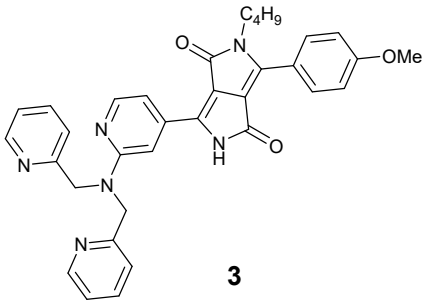

3

2-(bis(pyridin-2-ylmethyl)amino)isonicotinonitrile **2a** (1.5 g, 4.4 mmol), lithium *tert*-butoxide (1.42 g, 17.8mmol) and pyrrolidone **1** (1.82 g, 4.4 mmol) in combined solvent were used to obtain **3** as shiny red crystals (0.4 g, 21%); mp 217 °C. ^{1}H NMR (500 MHz, $CDCl_3$) δ 10.01 (s, 1H), 8.52 (s, 2H), 8.26 (d, *J* = 4.8 Hz, 1H), 7.80 (d, *J* = 7.8 Hz, 2H), 7.59-7.49 (m, 4H), 7.27 (s, 2H), 7.18 (s, 2H), 6.98 (d, *J* = 8.2 Hz, 2H), 5.03 (s, 4H), 3.82 (s, 3H), 3.77 (t, *J* = 7.5 Hz, 2H), 2.66 (br s, 2H), 1.57 (t, *J* = 6.8 Hz, 2H), 1.28 (q, *J* = 7.3 Hz, 2H), 0.87 (t, *J* = 7.3 Hz, 3H). ^{13}C NMR (126 MHz, $CDCl_3$) δ 162.8, 162.7, 162.2, 158.7, 158.1, 150.3, 149.0, 148.9, 141.7, 136.9, 136.0, 130.9, 122.2, 121.7, 120.1, 114.4, 112.0, 110.1, 110.0, 103.3, 55.4, 53.6, 42.0, 31.4, 19.9, 13.6. HRMS (ESI, *m/z*): $[M+H]^+$ Calcd. for $C_{34}H_{33}N_6O_3$: 573.2614; found, 573.2628.

6-(2-((bis(pyridin-2-ylmethyl)amino)methyl)pyridin-4-yl)-2-butyl-3-(4-methoxyphenyl)-2,5-dihydropyrrolo[3,4-*c*]pyrrole-1,4-dione (4)

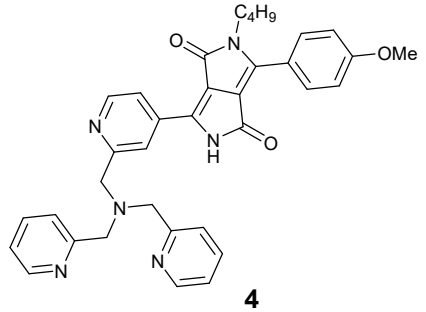

4

2-((bis(pyridin-2-ylmethyl)amino)methyl)isonicotinonitrile **2b** (0.5 g, 1.6 mmol), lithium *tert*-butoxide (0.5 g, 6.3 mmol) and pyrrolidone **1** (0.65 g, 1.6 mmol) in combined solvent were used to obtain **4** as shiny red crystals (0.19 g, 21%); mp 204 °C. ^{1}H NMR (600 MHz, $CDCl_3$) δ 10.3 (s, 1H), 8.99 (s, 1H), 8.78 (d, *J* = 4.0 Hz, 2H), 8.68 (d, *J* = 5.2 Hz, 1H), 8.40 (d, *J* = 4.3 Hz, 1H), 7.9 (d, *J* = 8.9 Hz, 2H), 7.59 (dt, *J* = 7.7 Hz, 2H), 7.41 (d, *J* = 7.7 Hz, 2H), 7.17 (dt, *J* = 5.7 Hz, 6.7 Hz, 2H), 7.09 (d, *J* = 8.8 Hz, 2H), 3.98 (s, 3H), 3.91 (d, *J* = 4.2 Hz, 6H), 3.87 (t, *J* = 7.8 Hz, 2H), 2.66 (br s, 1H), 1.67 (quint, *J* = 7.8 Hz, 2H), 1.33 (m, 2H), 0.91 (t, *J* = 7.0 Hz, 3H). ^{13}C NMR (151 MHz, $CDCl_3$) δ 162.9, 162.4, 162.3, 160.9, 158.6, 150.5, 150.1, 149.5, 141.3, 136.6, 135.0, 130.9, 123.8, 122.5, 120.2, 119.9, 119.2, 114.5, 112.4, 110.3, 59.6, 59.4, 55.5, 42.1, 31.5, 20.0, 13.6. HRMS (ESI, *m/z*): $[M+H]^+$ Calcd. for $C_{35}H_{35}N_6O_3$: 587.2757; found, 587.2781.

6-(2-(bis(pyridin-2-ylmethyl)amino)pyridin-4-yl)-3-(4-methoxyphenyl)-2-(3-morpholinopropyl)-2,5-dihydropyrrolo[3,4-*c*]pyrrole-1,4-dione (8)

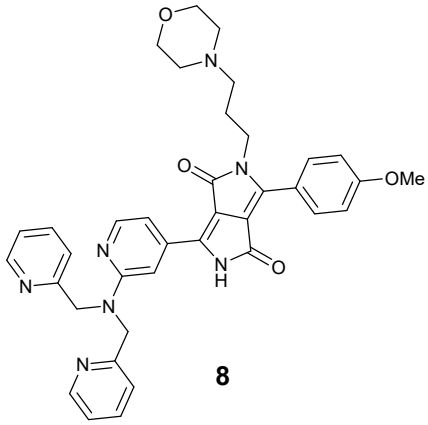

8

2-(bis(pyridin-2-ylmethyl)amino)isonicotinonitrile **2a** (1.0 g, 3.3 mmol), lithium *tert*-butoxide (1.06 g, 13.2 mmol) and pyrrolidone **7** (1.58 g, 3.3 mmol) in combined solvent were used to obtain **8** as shiny red crystals (0.31 g, 15%); mp 230 °C. ^{1}H NMR (500 MHz, $CDCl_3$) δ 10.02 (s, 1H), 8.51 (d, *J* = 3.7 Hz, 2H), 8.29 (d, *J* = 5.2 Hz, 1H), 7.81 (d, *J* = 8.0 Hz, 2H), 7.57 (d, *J* = 7.2 Hz, 2H), 7.50 (d, *J* = 5.0 Hz, 2H), 7.23 (d, *J* = 7.7 Hz, 2H), 7.12 (d, *J* = 6.0 Hz, 2H), 6.98 (d, *J* = 8.5 Hz, 2H), 5.01 (s, 4H), 3.88 (d, *J* = 7.4 Hz ,2H), 3.81 (s, 3H), 3.58 (t, *J* = 4.0 Hz ,4H), 2.28 (bs, 6H), 1.75 (m, 2H). ^{13}C NMR (126 MHz, $CDCl_3$) δ 162.8, 162.2, 159.0, 158.3, 150.0, 149.3, 149.2, 141.9, 136.6, 135.9, 130.9, 122.0, 121.4, 120.1, 114.4, 111.9, 110.1, 109.1, 103.1, 66.9, 59.9, 55.4, 53.6, 40.5, 26.9, 25.9. HRMS (ESI, *m/z*): $[M+H]^+$ Calcd. for $C_{37}H_{38}N_7O_4$: 644.2985; found, 644.2988.

6-(2-((bis(pyridin-2-ylmethyl)amino)methyl)pyridin-4-yl)-3-(4-methoxyphenyl)-2-(3-morpholinopropyl)-2,5-dihydropyrrolo[3,4-*c*]pyrrole-1,4-dione (9)

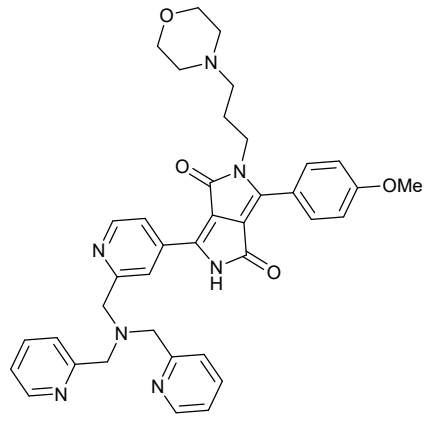

9

2-((bis(pyridin-2-ylmethyl)amino)methyl)isonicotinonitrile **2b** (0.5 g, 1.6 mmol), lithium *tert*-butoxide (0.5 g, 6.3 mmol) and pyrrolidone **7** (0.76 g, 1.6 mmol) in combined solvent were used to obtain **9** as shiny red crystals (0.14 g, 14%); mp 194 °C. ^{1}H NMR (500 MHz, $CDCl_3$) δ 10.34 (s, 1H), 8.96 (s, 1H), 8.74 (d, *J* = 4.0 Hz, 2H), 8.66 (d, *J* = 5.0 Hz, 1H), 8.35 (d, *J* = 4.4 Hz, 1H), 7.88 (d, *J* = 8.9 Hz, 2H), 7.58 (td, *J* = 7.6,

2H), 7.40 (d, *J* = 7.7 Hz, 2H), 7.15 (td, *J* = 5.5, 5.0, 6.6 Hz, 2H), 7.03 (d, *J* = 8.8 Hz, 2H), 3.96 (m, 4H), 3.88 (d, *J* = 7.9 Hz ,7H), 3.61 (bs, 4H), 2.34 (bs, 6H), 1.84 (bs, 2H). ^{13}C NMR (126 MHz, $CDCl_3$) δ 162.9, 162.4, 162.3, 160.9, 158.6, 150.5, 149.9, 149.5, 141.5, 136.6, 134.9, 130.9, 123.8, 122.5, 120.1, 119.8, 119.3, 114.5, 112.3, 110.5, 66.7, 59.6, 59.4, 55.9, 55.5, 53.5, 45.8, 40.6, 25.9, 8.6. HRMS (ESI, *m/z*): $[M+H]^+$ Calcd. for $C_{38}H_{40}N_7O_4$: 658.3142; found, 658.3164.

Preparation of mitochondrial probe 10:

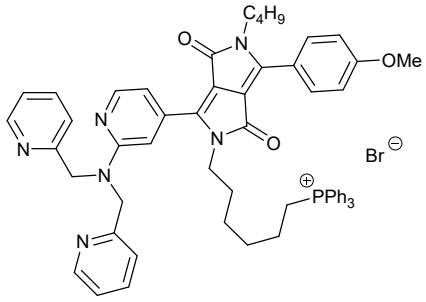

10

A suspension of DPP **3** (0.3 g, 0.52 mmol) and *t*-BuOK (0.15 g, 1.3 mmol) in dry NMP (10 mL) was stirred at 75 °C under argon atmosphere for 15 min. then 1,6-dibromohexane (0.25 mL, 1.6 mmol) was added and the mixture was stirred at 75 °C under argon for 3 h. After cooling to room temperature reaction mixture was diluted with water (100 mL) and extracted with DCM (100 mL), water phase was one more time washed with DCM (50 mL). The combined organic phases were dried over Na_2SO_4, filtered and concentrated in vacuum. The product was purified by column chromatography over silica gel using a step gradient of MeOH in DCM as eluent (from 0% to 10%). Compound was obtained as an orange red semi solid (300 mg, 78%); HRMS (ESI, m/z): $[M+Na]^+$Calcd.for $C_{40}H_{43}BrN_6O_3Na$: 757.2478; found, 757.2467.

Alkylated crude compound of **3** (300 mg, 0.41 mmol) and triphenylphosphine (1.06 g, 4.1 mmol) were added into a flask containing 5 mL of acetonitrile. The mixture was refluxed for 72 h. After removal of solvent in vacuo, the remaining solid was purified by column chromatography with gradient solvent from CH_2Cl_2 to CH_2Cl_2/MeOH (v/v = 9/1). Compound **10** was obtained as orange-red crystals by recrystallization from diethyl ether (130 mg, 35%); mp 105 °C. ^{1}H NMR (600 MHz, CD_3CN): δ 8.9 (s, 2H), 8.8 (s, 1H), 8.35-8.26 (m, 4H), 8.03 (d, *J* = 6.0 Hz, 2H), 7.79-7.65 (m, 17H), 7.20 (d, *J* = 9.6 Hz, 2H), 6.99 (d, *J* = 9.6 Hz, 2H), 5.53 (s, 4H), 3.86 (s, 3H), 3.64 (t, *J* = 7.8 Hz, 4H), 3.4-3.2 (m, 6H), 1.39-1.27 (m, 8H), 0.88 (t, *J* = 9.0 Hz, 3H). ^{13}C NMR (126 MHz, $CDCl_3$) δ 162.2, 161.7, 158.6, 149.4, 148.7, 144.3, 137.0, 135.0, 133.7, 130.9, 130.3, 130.2, 122.2, 121.3, 118.8, 117.3, 114.3, 111.1, 108.2, 104.8, 65.3, 55.4, 54.5, 54.3, 41.2, 40.8, 31.0, 29.7, 28.5, 27.8, 25.2, 24.8, 21.9, 21.4, 19.5, 14.6, 12.9; HRMS (ESI, *m/z*): $[M+H]^+$ Calcd. for $C_{58}H_{58}N_6O_3P$: 917.4308; found, 917.4303.

Section S3: Absorption and emission spectra

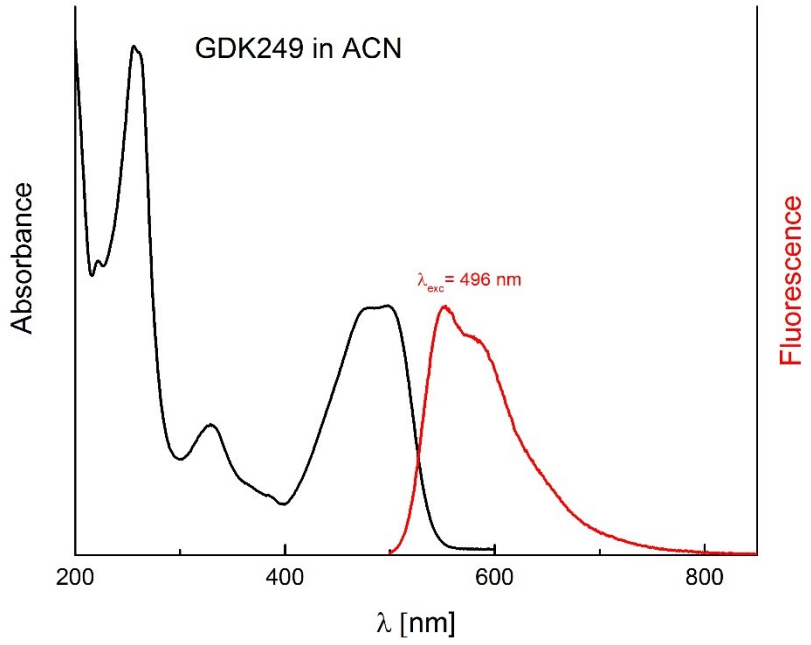

Fig. S1. The absorption and emission spectra of DPP **3** in CH_3CN.

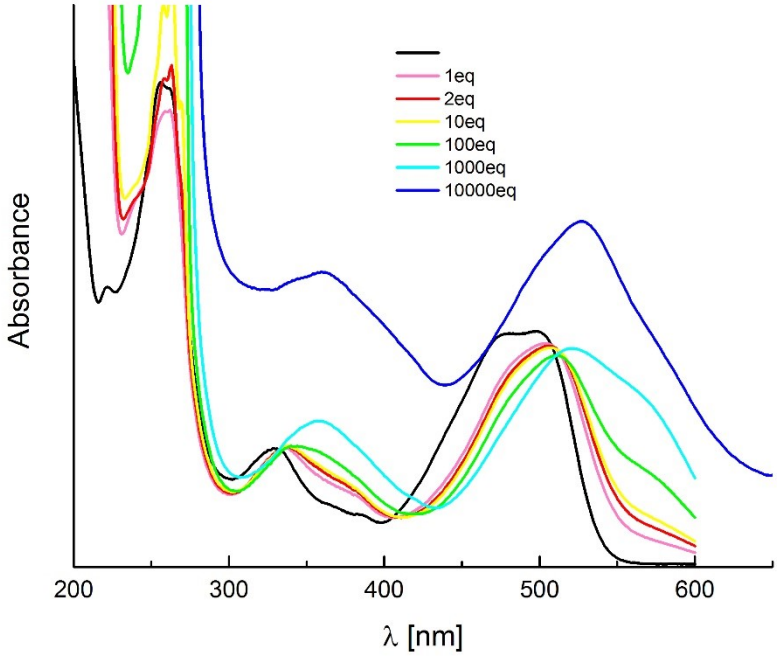

Fig. S2.The effect of $PhSO_3H$ addition on the absorption spectra of DPP **3** measured in CH_3CN.

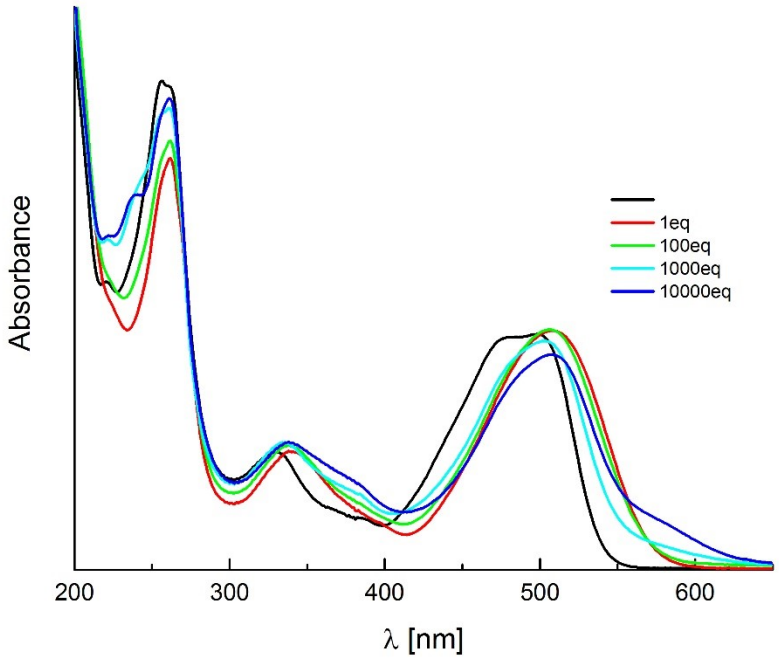

Fig. S3.The effect of cadmium perchlorate addition on the absorption spectra of DPP **3** measured in CH_3CN.

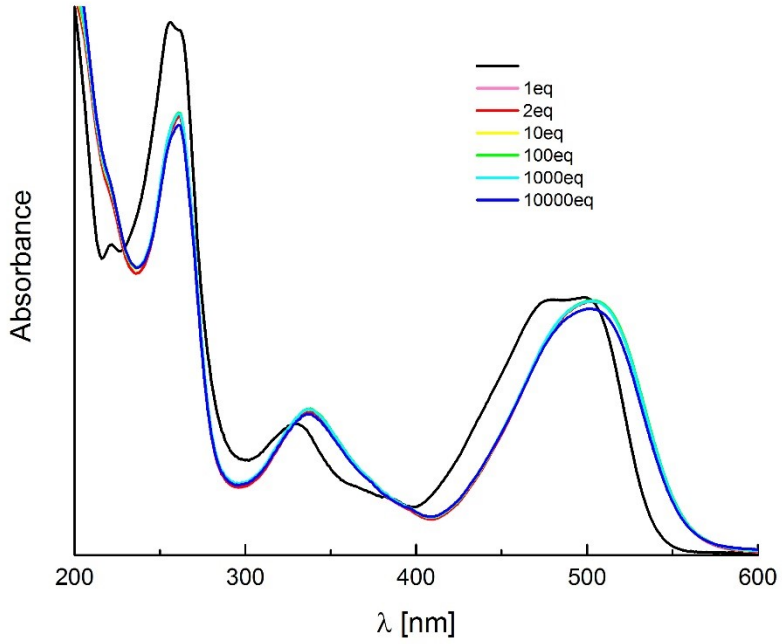

Fig. S4.The effect of zinc perchlorate addition on the absorption spectra of DPP **3** measured in CH_3CN.

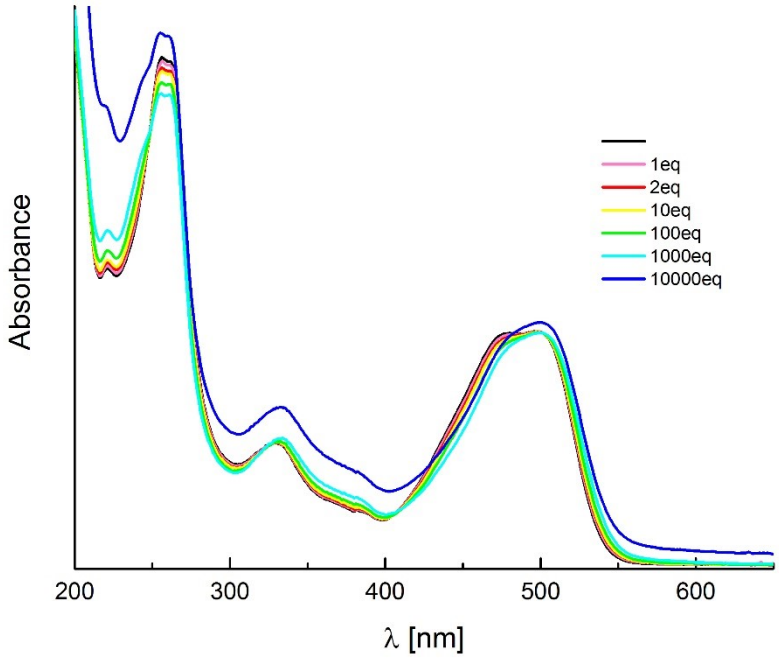

Fig. S5.The effect of magnesium perchlorate addition on the absorption spectra of DPP **3** measured in CH_3CN.

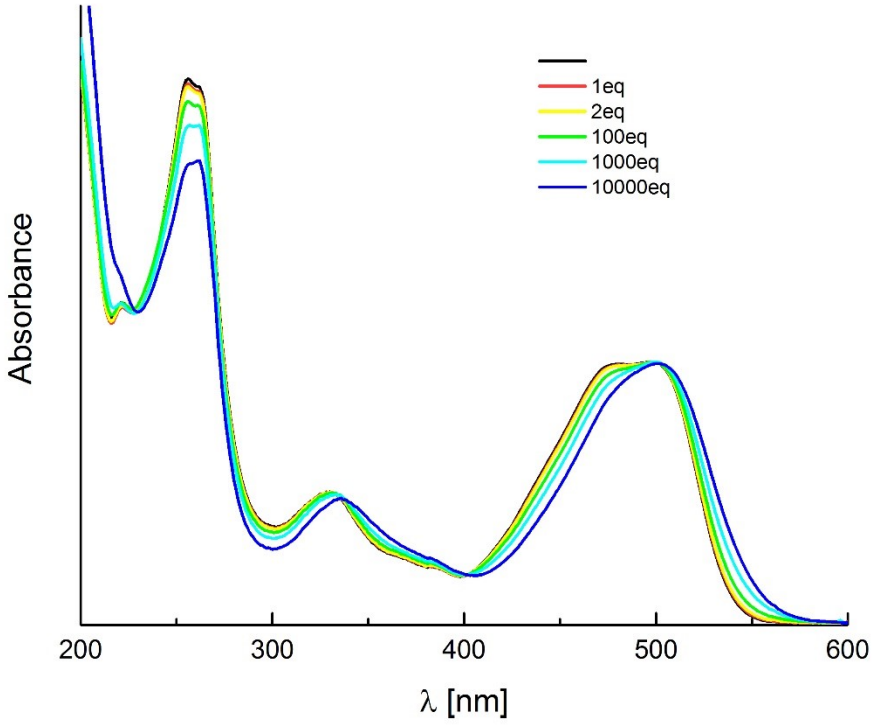

Fig. S6.The effect of calcium perchlorate addition on the absorption spectra of DPP **3** measured in CH_3CN.

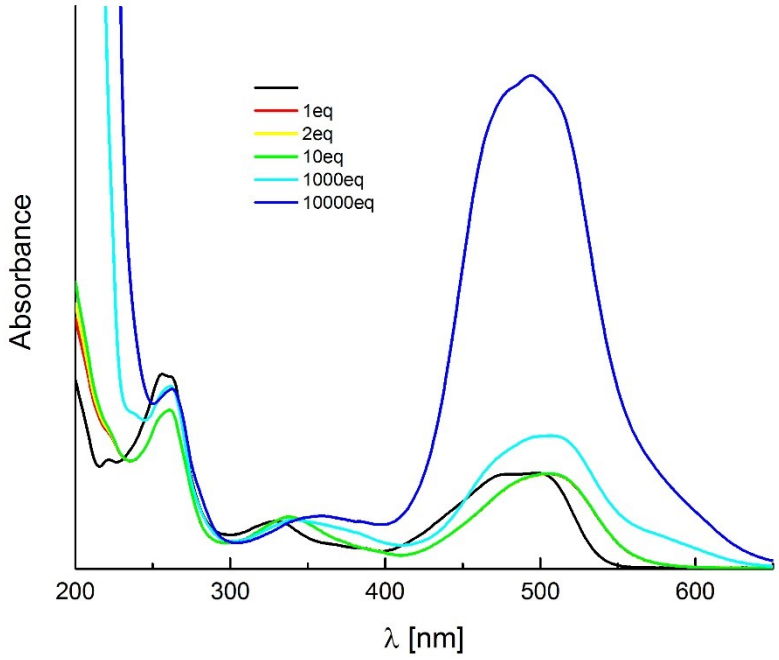

Fig. S7.The effect of cobalt perchlorate addition on the absorption spectra of DPP **3** measured in CH_3CN.

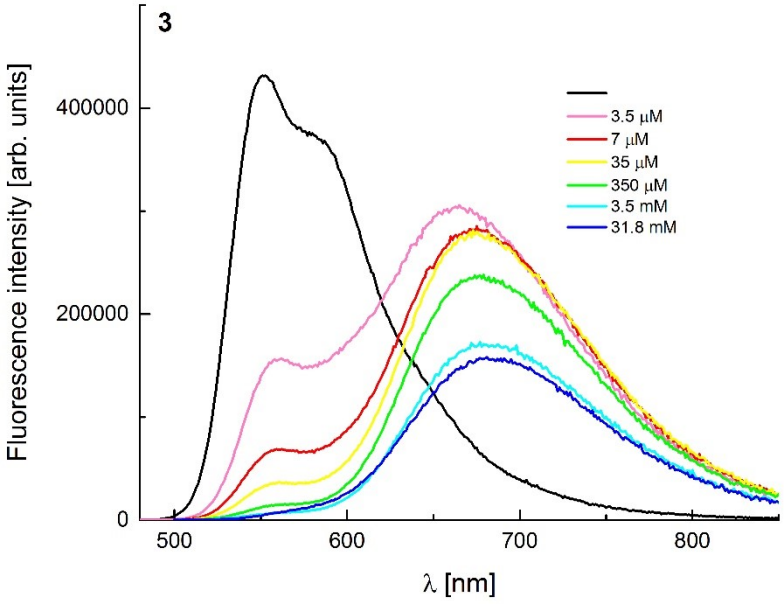

Fig. S8. The effect of $PhSO_3H$ addition on the emission spectra of DPP **3** measured in CH_3CN.

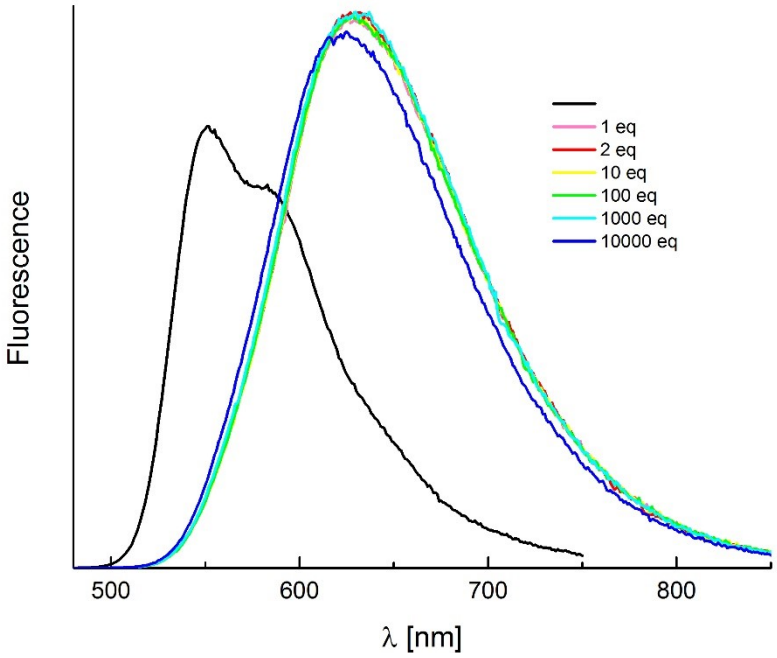

Fig. S9. The effect of zinc perchlorate addition on the emission spectra of DPP **3** measured in CH_3CN.

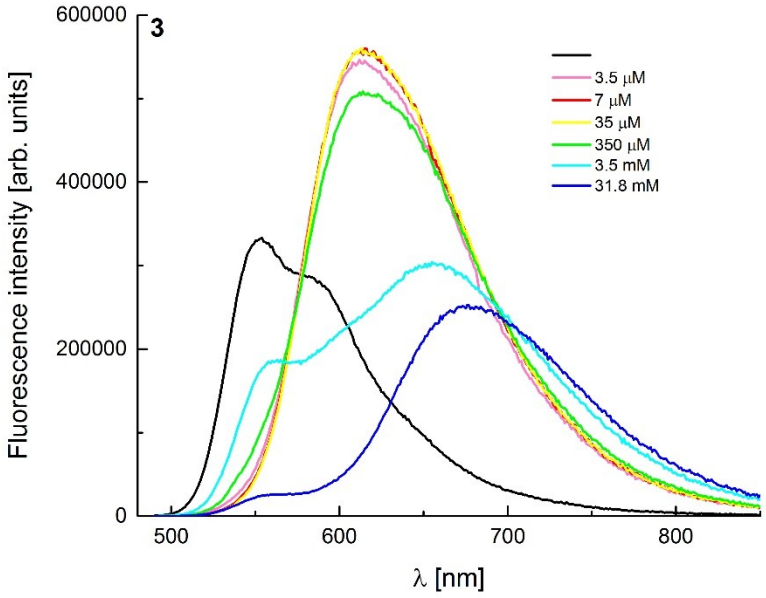

Fig. S10. The effect of cadmium perchlorate addition on the emission spectra of DPP **3** measured in CH_3CN.

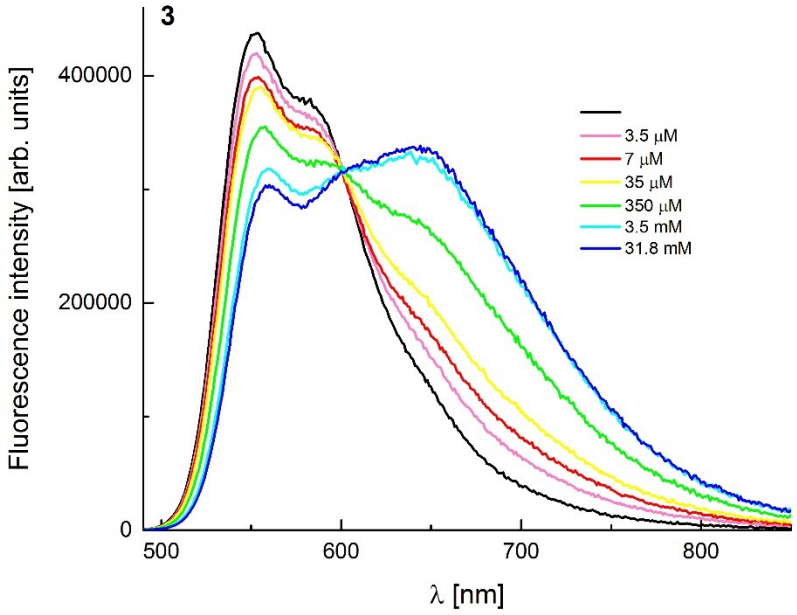

Fig. S11. The effect of magnesium perchlorate addition on the emission spectra of DPP **3** measured in CH_3CN.

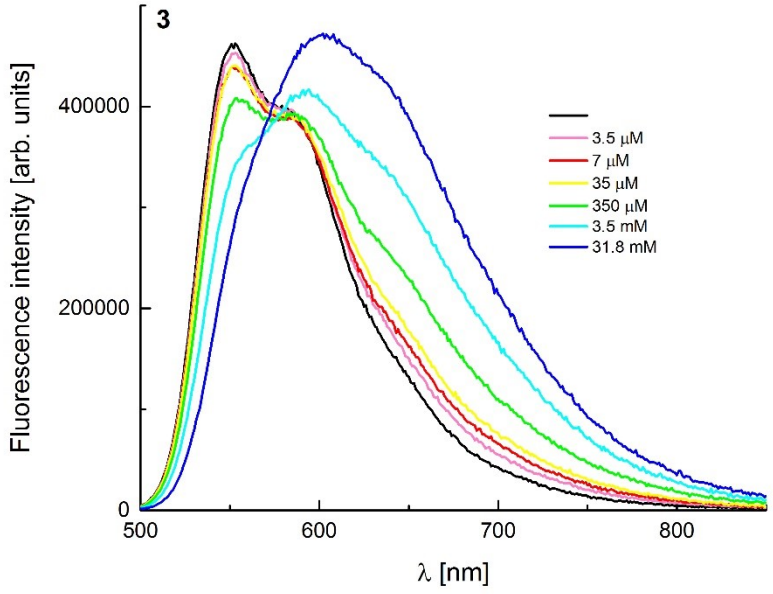

Fig. S12. The effect of calcium perchlorate addition on the emission spectra of DPP **3** measured in CH_3CN.

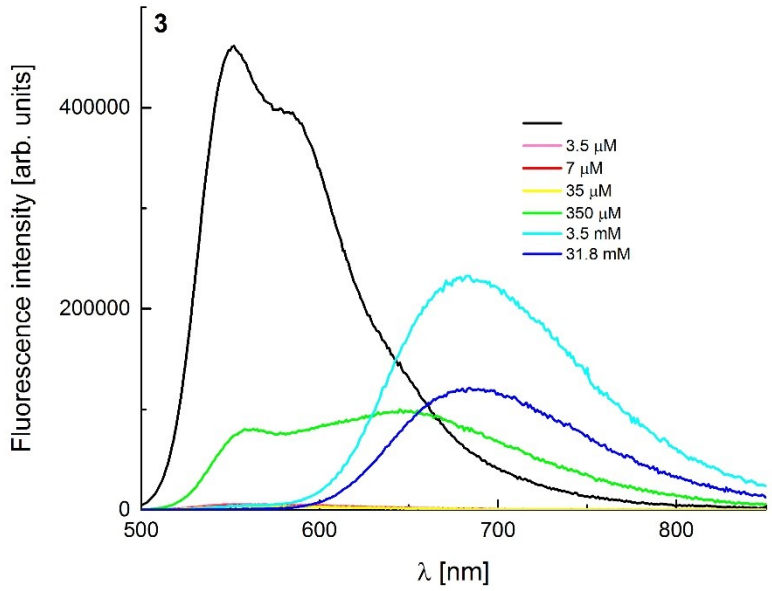

Fig. S13. The effect of cobalt perchlorate addition on the emission spectra of DPP **3** measured in CH_3CN.

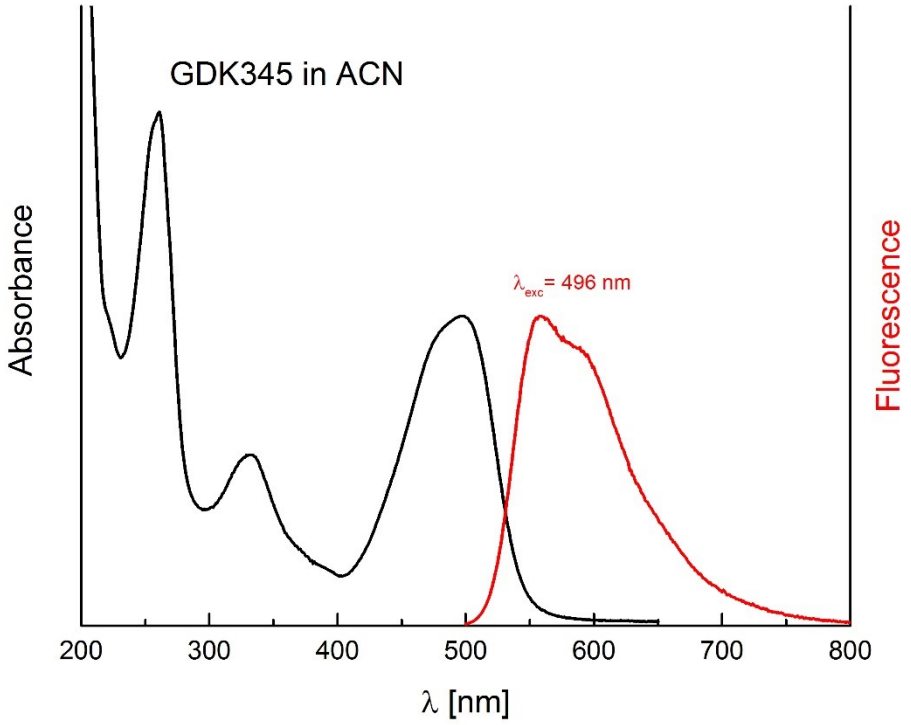

Fig. S14. The absorption and emission spectra of DPP **4** in CH_3CN.

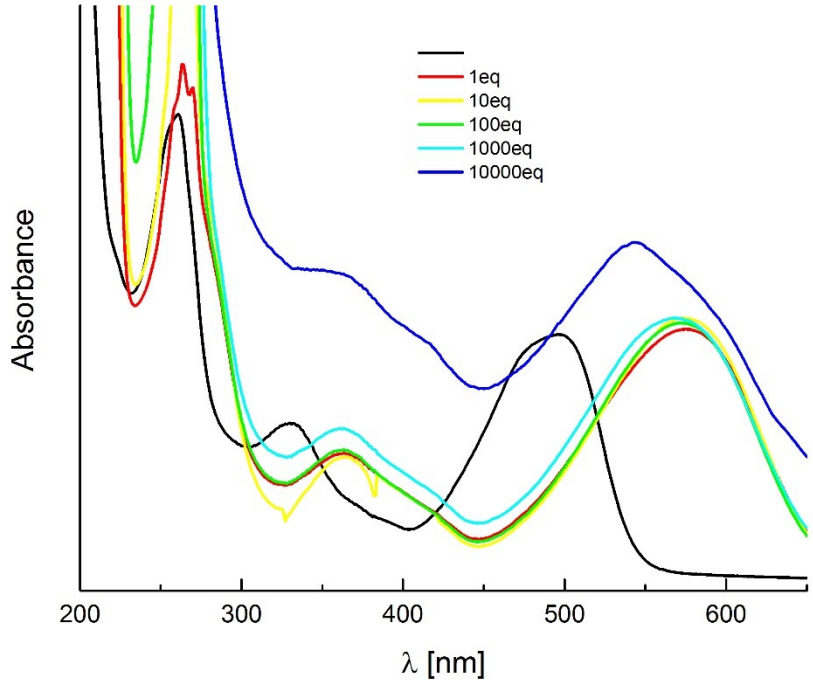

Fig. S15.The effect of $PhSO_3H$ addition on the absorption spectra of DPP **4** measured in CH_3CN.

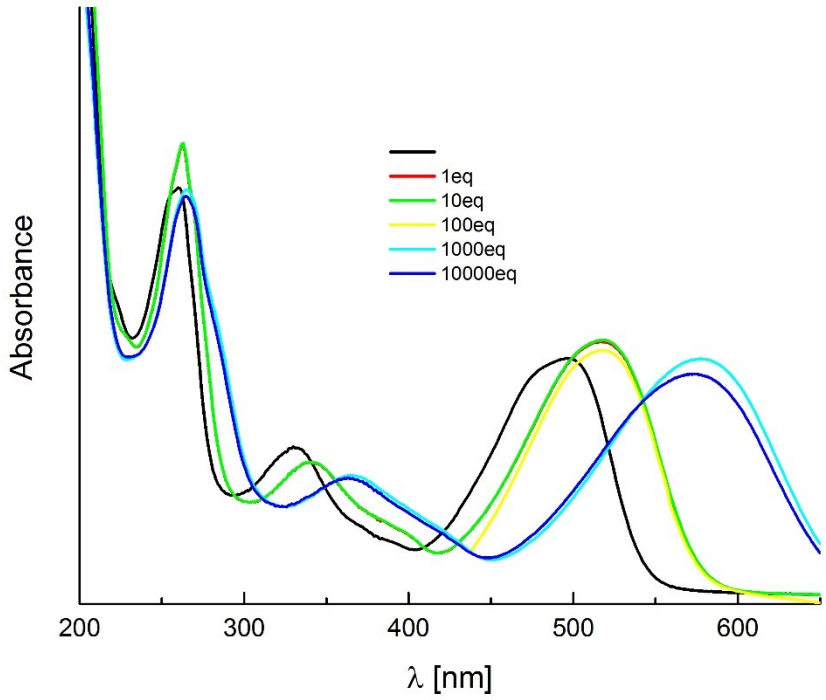

Fig. S16.The effect of cadmium perchlorate addition on the absorption spectra of DPP **4** measured in CH_3CN.

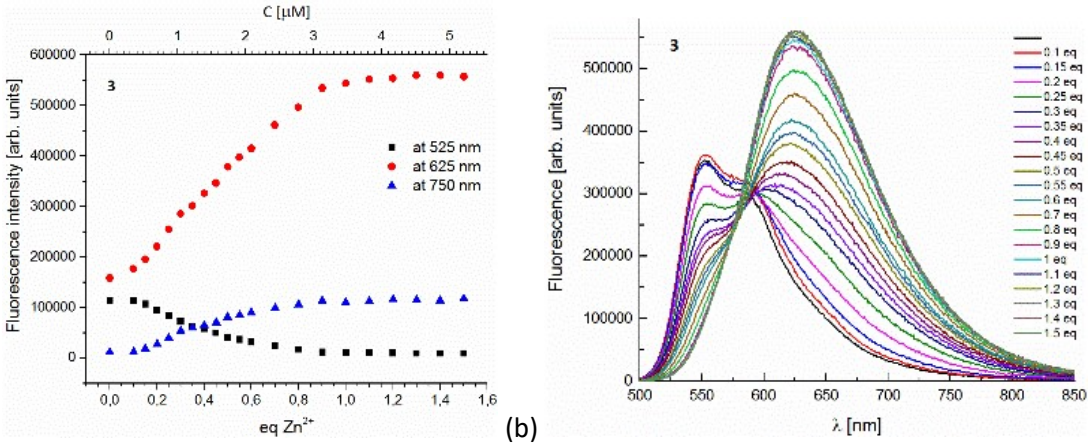

Fig S17. Fluorescence titration for compound **3**. a: Titration curve; b: Fluorescence spectrum

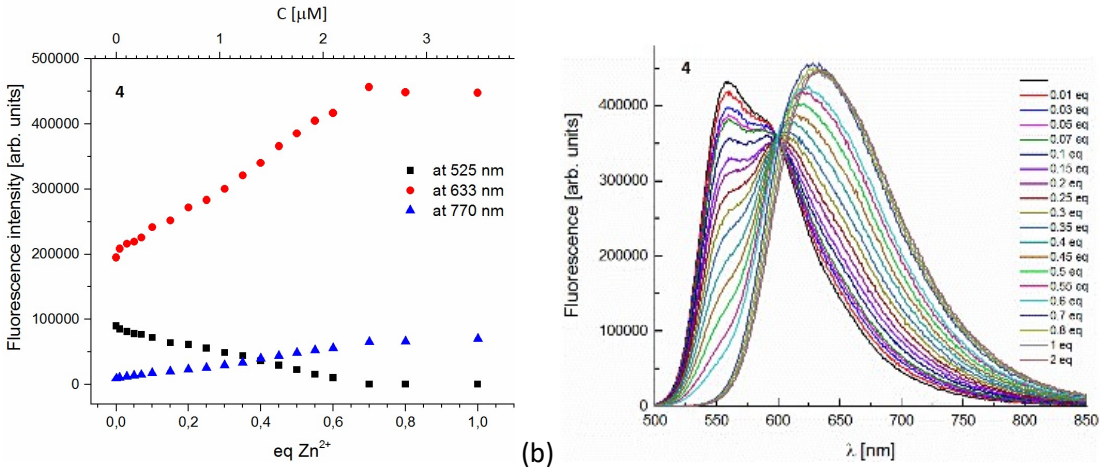

Fig S18. Fluorescence titration for compound **4**. a: Titration curve; b: Fluorescence spectrum

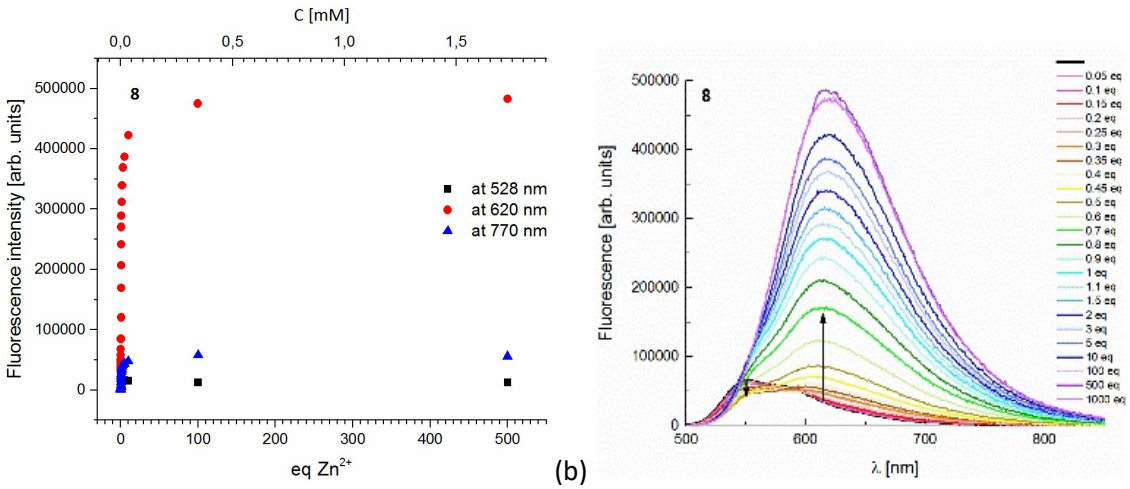

Fig S19. Fluorescence titration for compound **8**. a: Titration curve; b: Fluorescence spectrum

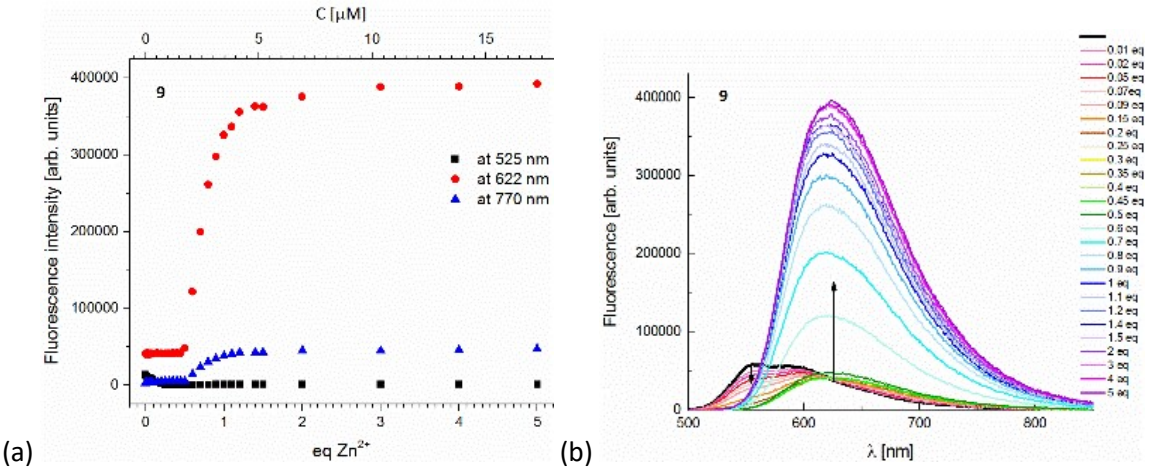

Fig S20. Fluorescence titration for compound **9**. a: Titration curve; b: Fluorescence spectrum

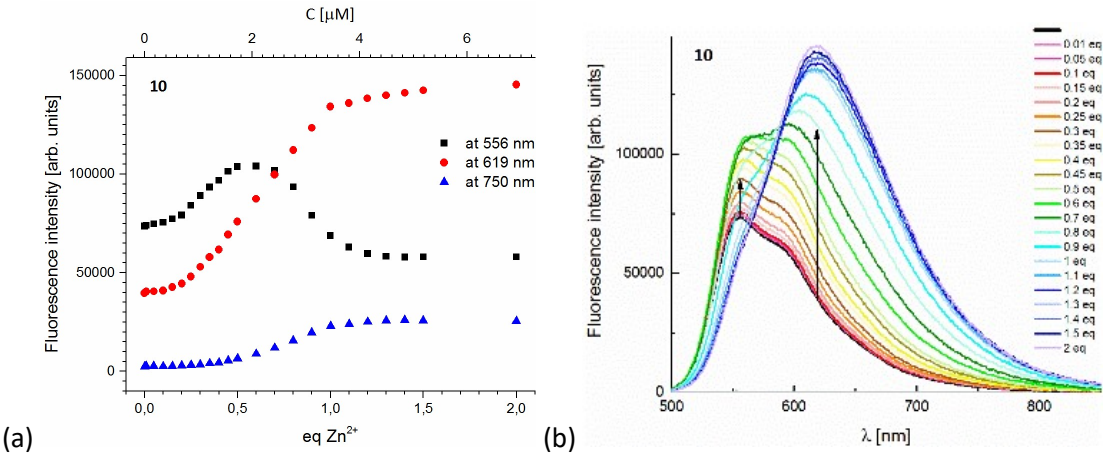

Fig S21. Fluorescence titration for compound **10**. a: Titration curve; b: Fluorescence spectrum

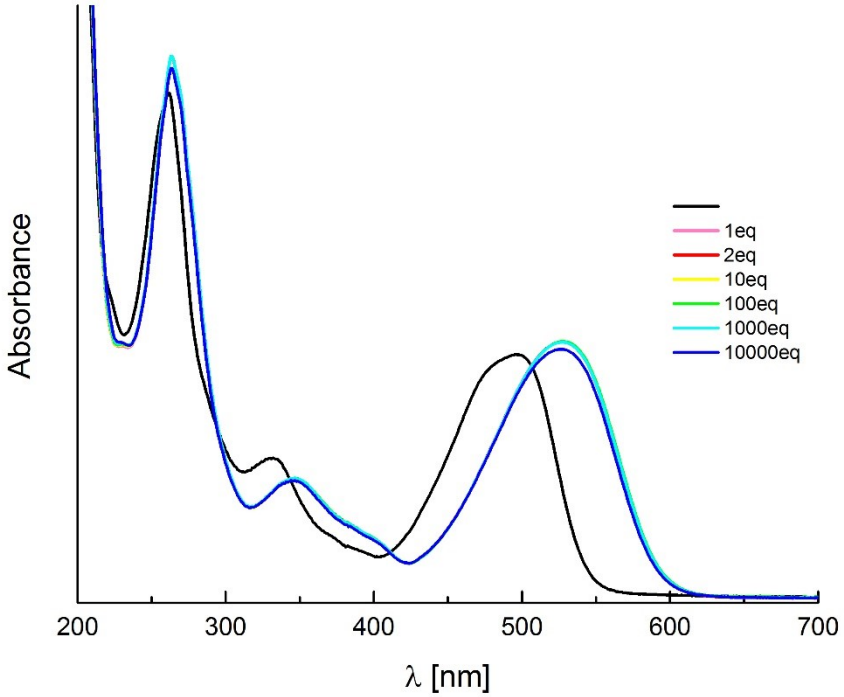

Fig. S22.The effect of zinc perchlorate addition on the absorption spectra of DPP **4** measured in CH_3CN.

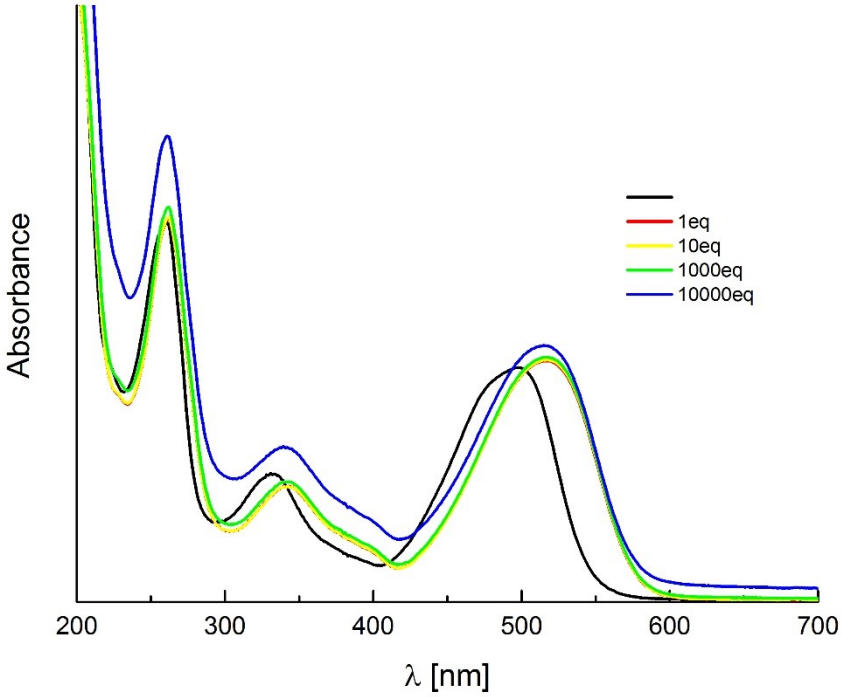

Fig. S23.The effect of magnesium perchlorate addition on the absorption spectra of DPP **4** measured in CH_3CN.

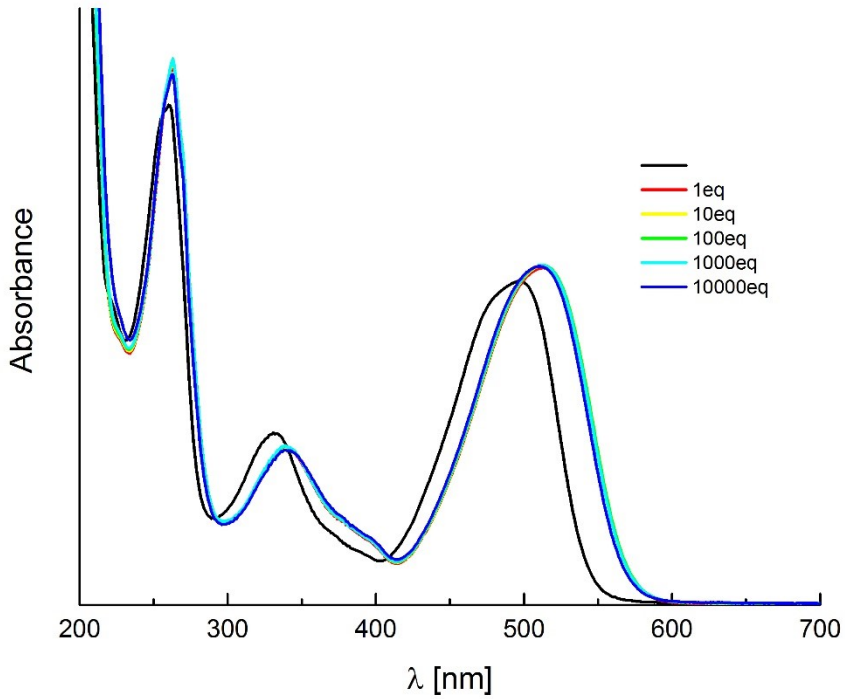

Fig. S24.The effect of calcium perchlorate addition on the absorption spectra of DPP **4** measured in CH_3CN.

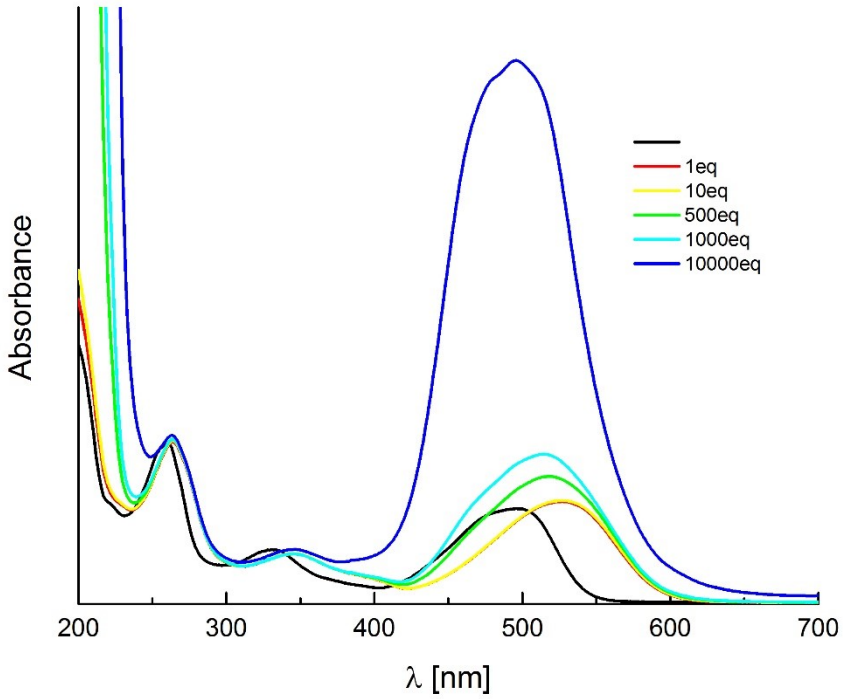

Fig. S25.The effect of cobalt perchlorate addition on the absorption spectra of DPP **4** measured in CH_3CN.

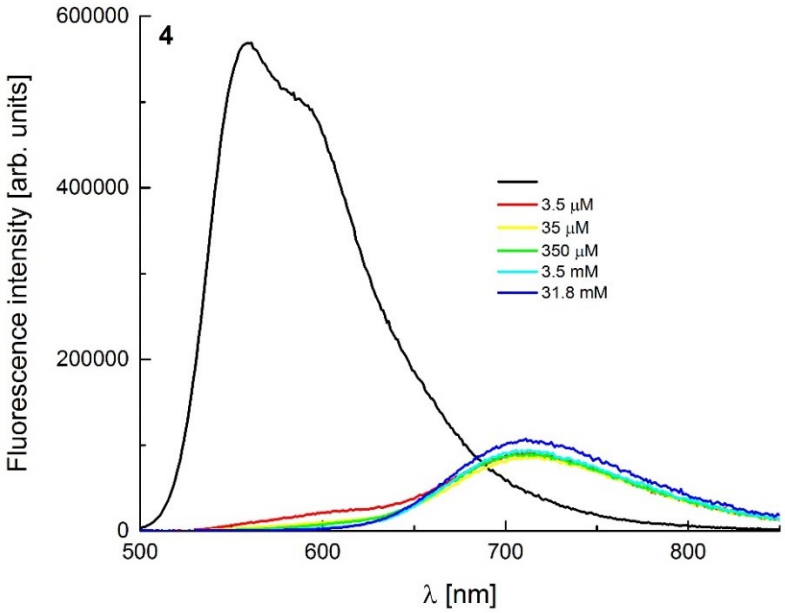

Fig. S26. The effect of $PhSO_3H$ addition on the emission spectra of DPP **4** measured in CH_3CN.

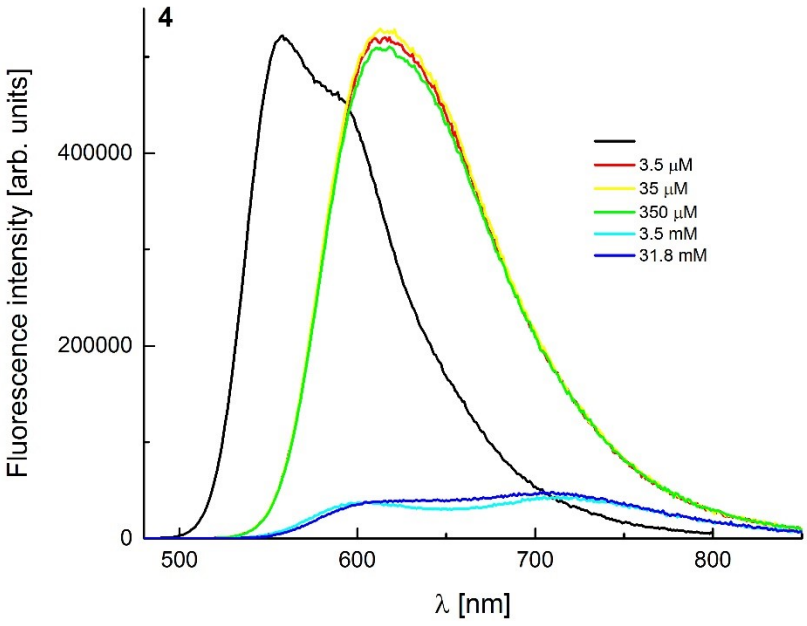

Fig. S27. The effect of cadmium perchlorate addition on the emission spectra of DPP **4** measured in CH_3CN.

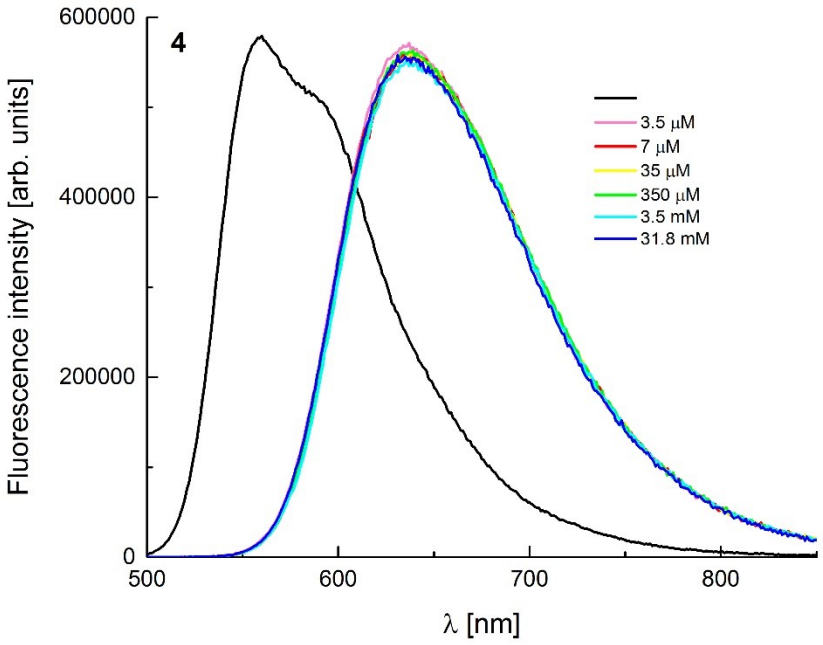

Fig. S28. The effect of zinc perchlorate addition on the emission spectra of DPP **4** measured in CH_3CN.

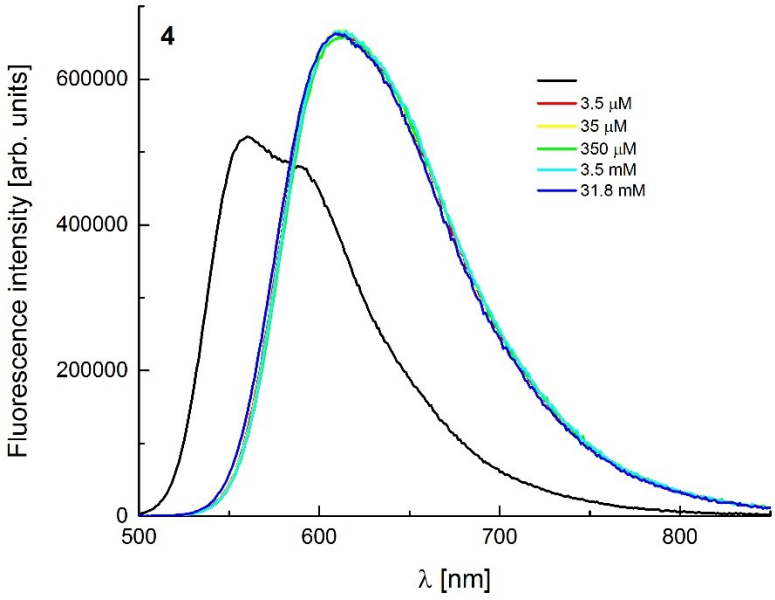

Fig. S29. The effect of magnesium perchlorate addition on the emission spectra of DPP **4** measured in CH_3CN.

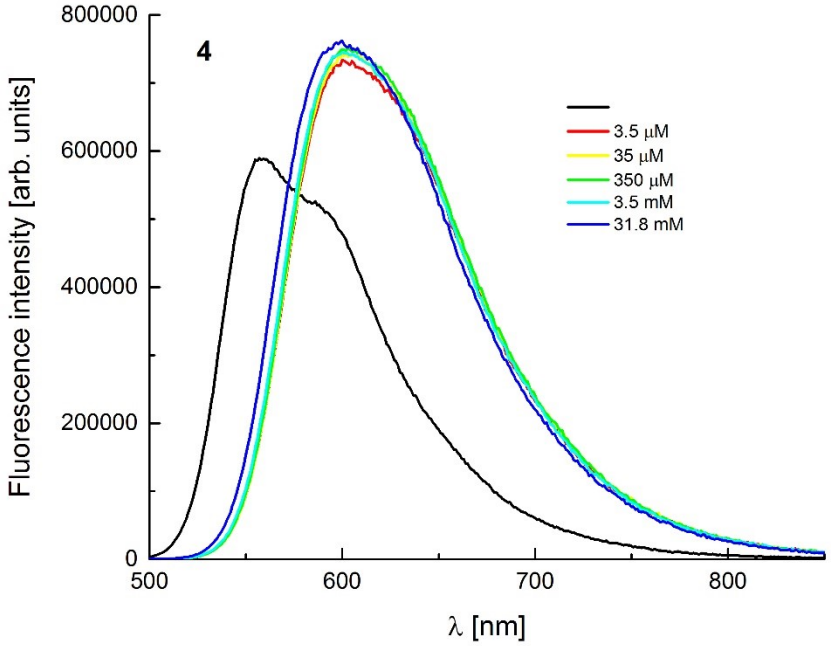

Fig. S30. The effect of calcium perchlorate addition on the emission spectra of DPP **4** measured in CH_3CN.

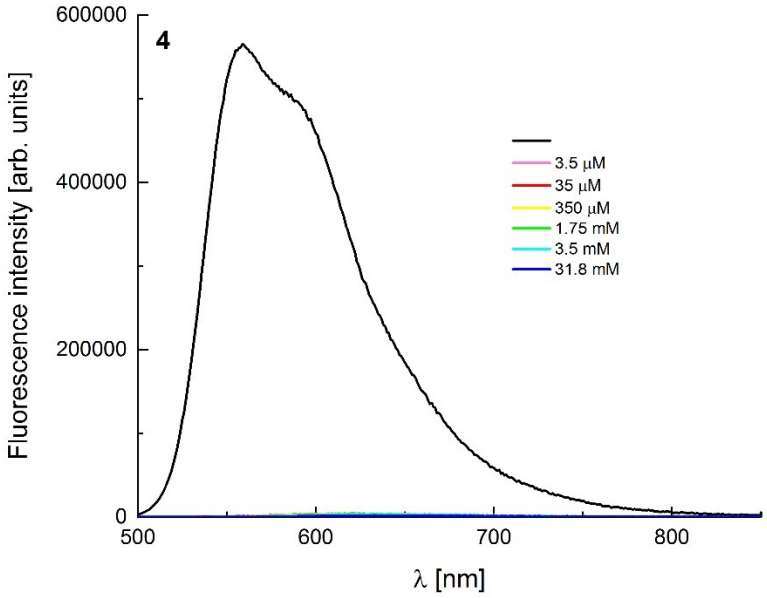

Fig. S31. The effect of cobalt perchlorate addition on the emission spectra of DPP **4** measured in CH_3CN.

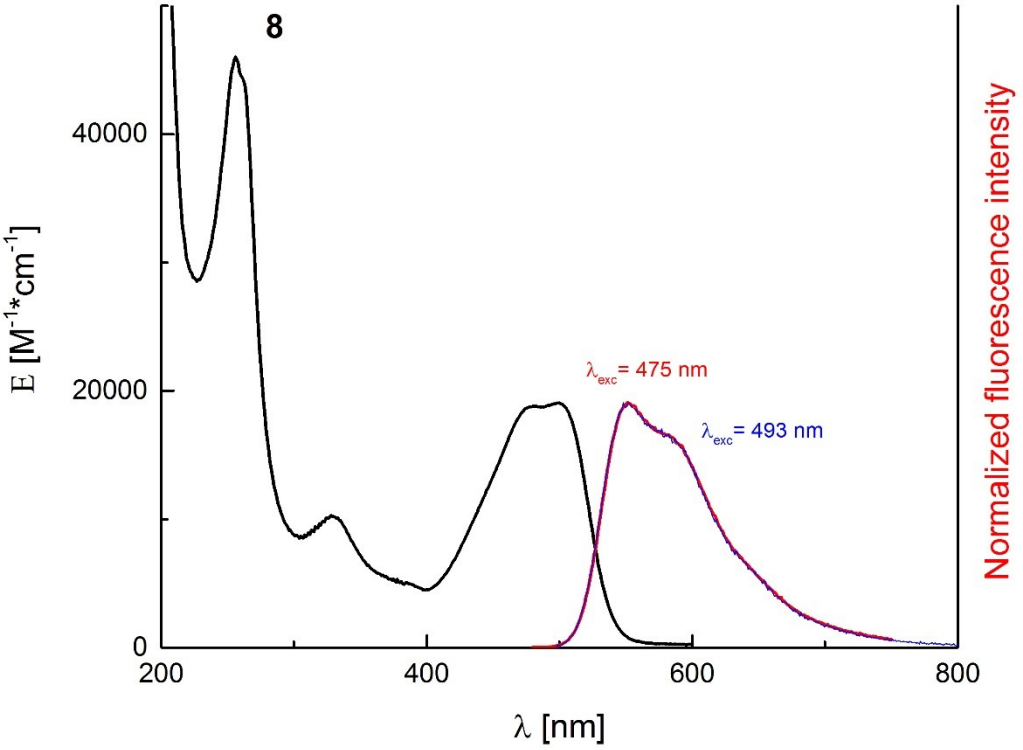

Fig. S32. The absorption and emission spectra of DPP **8** in CH_3CN.

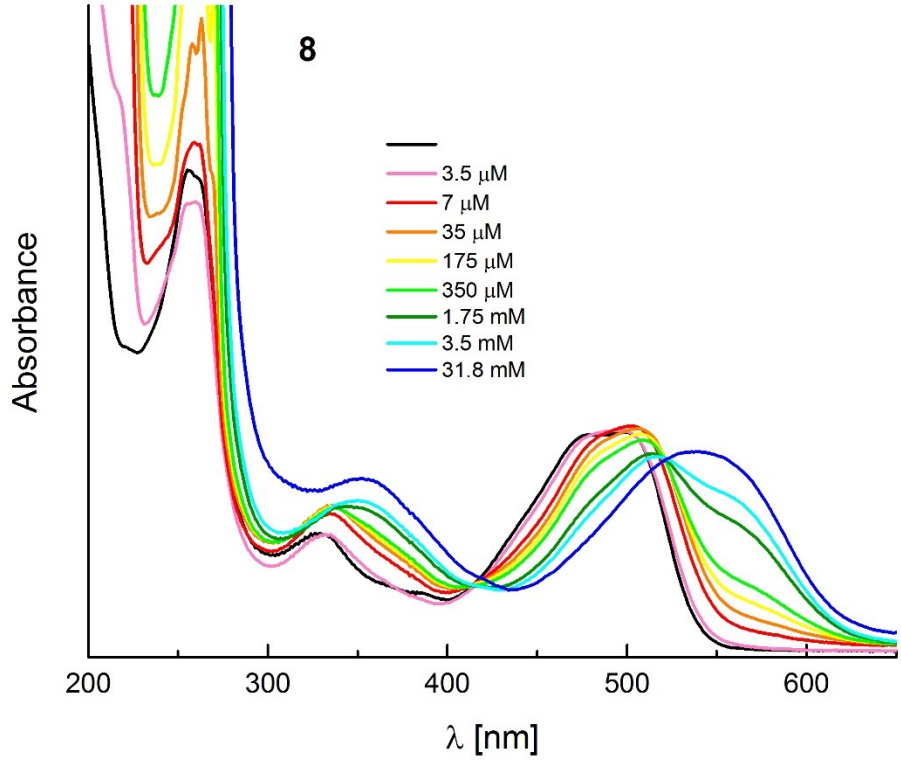

Fig. S33.The effect of $PhSO_3H$ addition on the absorption spectra of DPP **8** measured in CH_3CN.

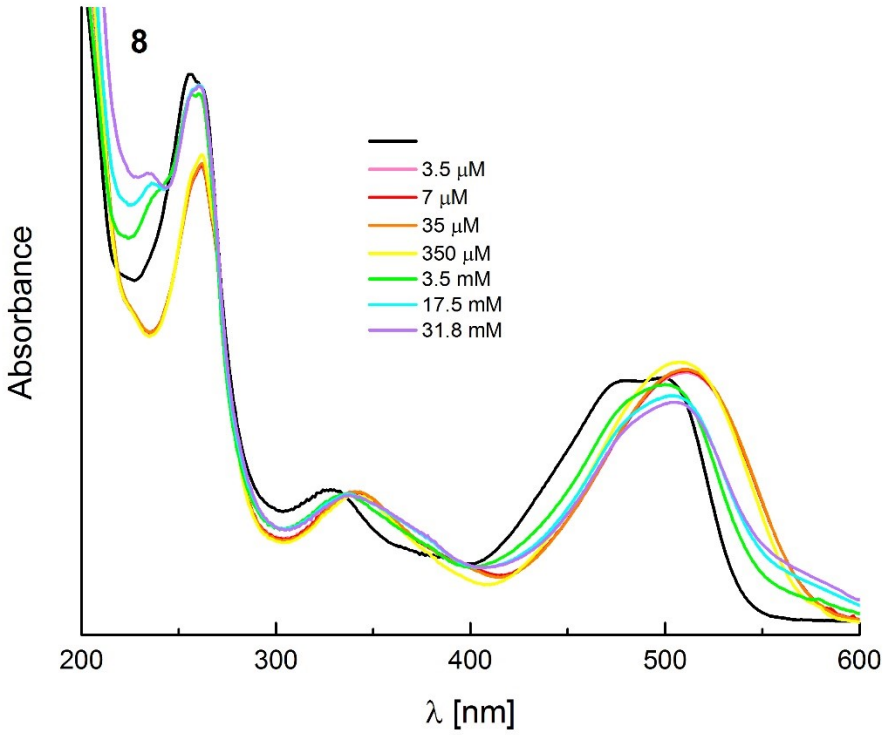

Fig. S34.The effect of cadmium perchlorate addition on the absorption spectra of DPP **8** measured in CH_3CN.

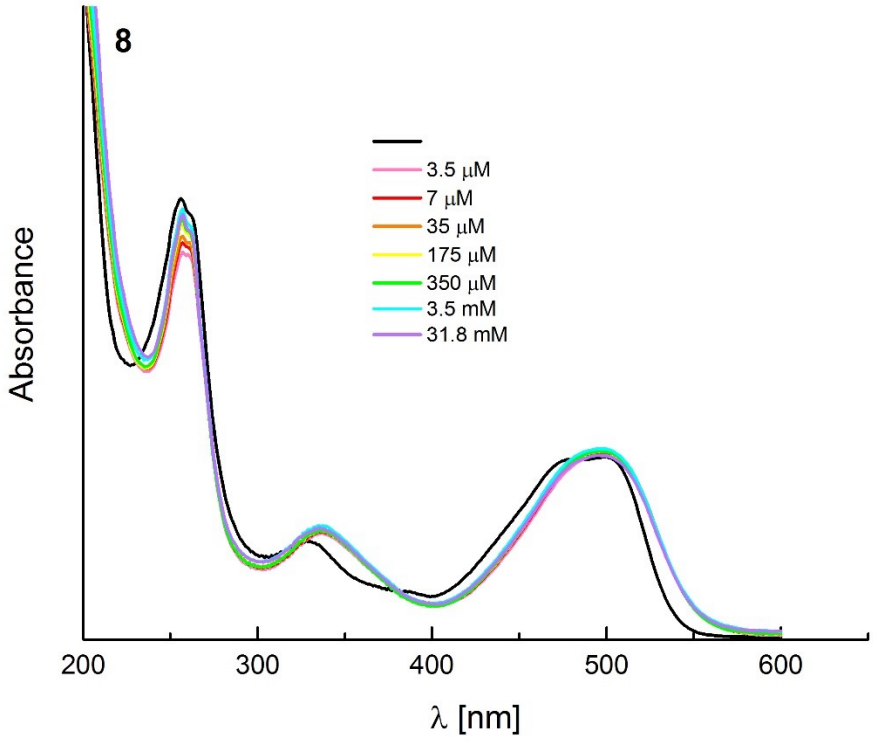

Fig. S35.The effect of zinc perchlorate addition on the absorption spectra of DPP **8** measured in CH_3CN.

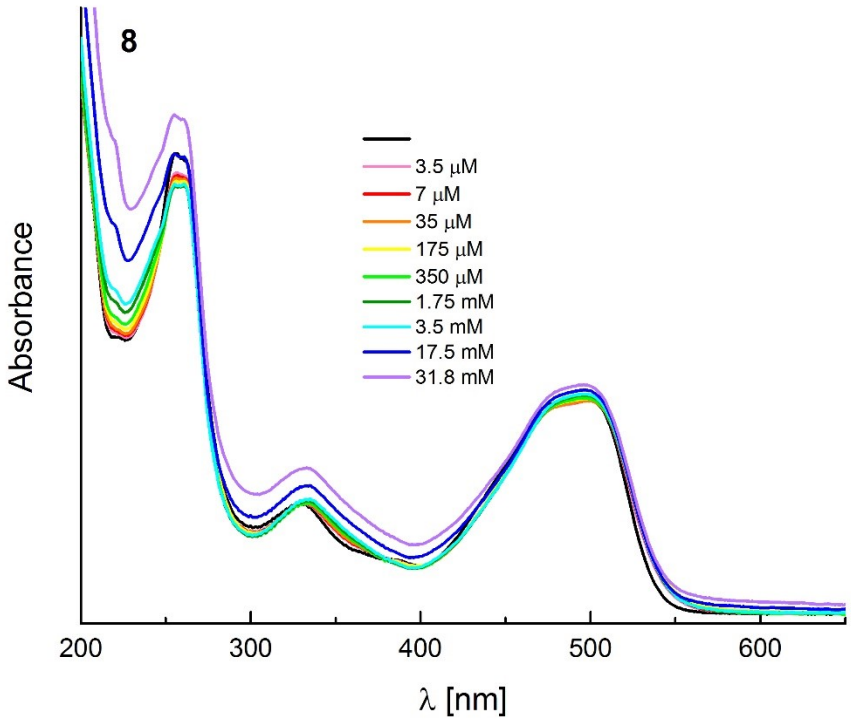

Fig. S36.The effect of magnesium perchlorate addition on the absorption spectra of DPP **8** measured in ACN.

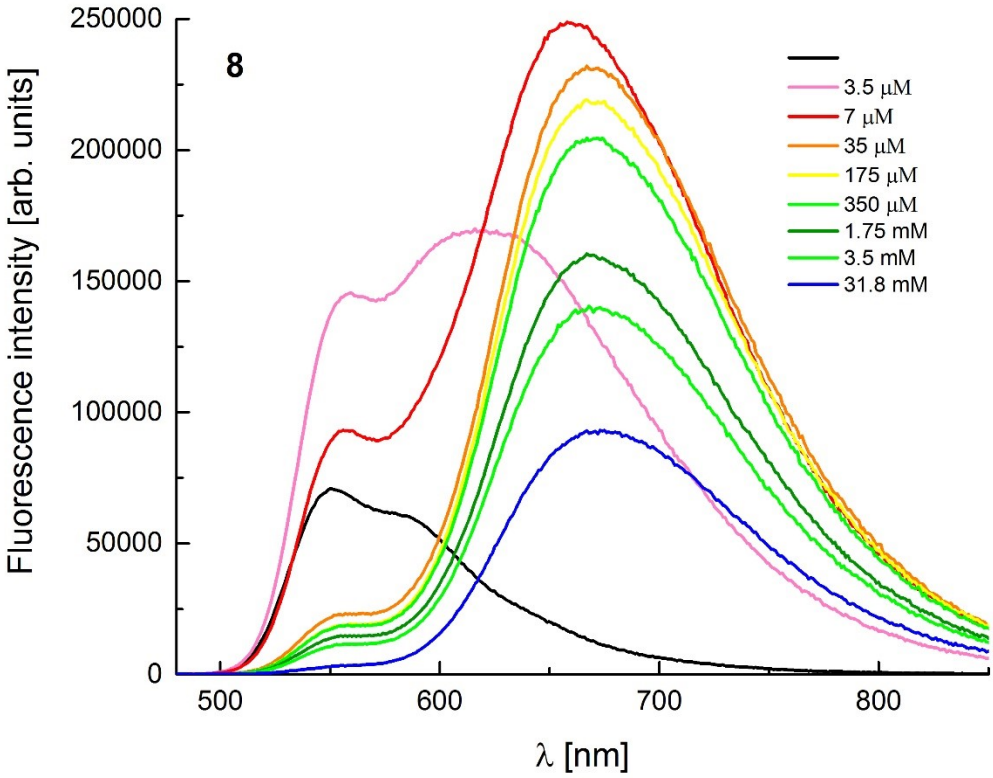

Fig. S37. The effect of $PhSO_3H$ addition on the emission spectra of DPP **8** measured in CH_3CN.

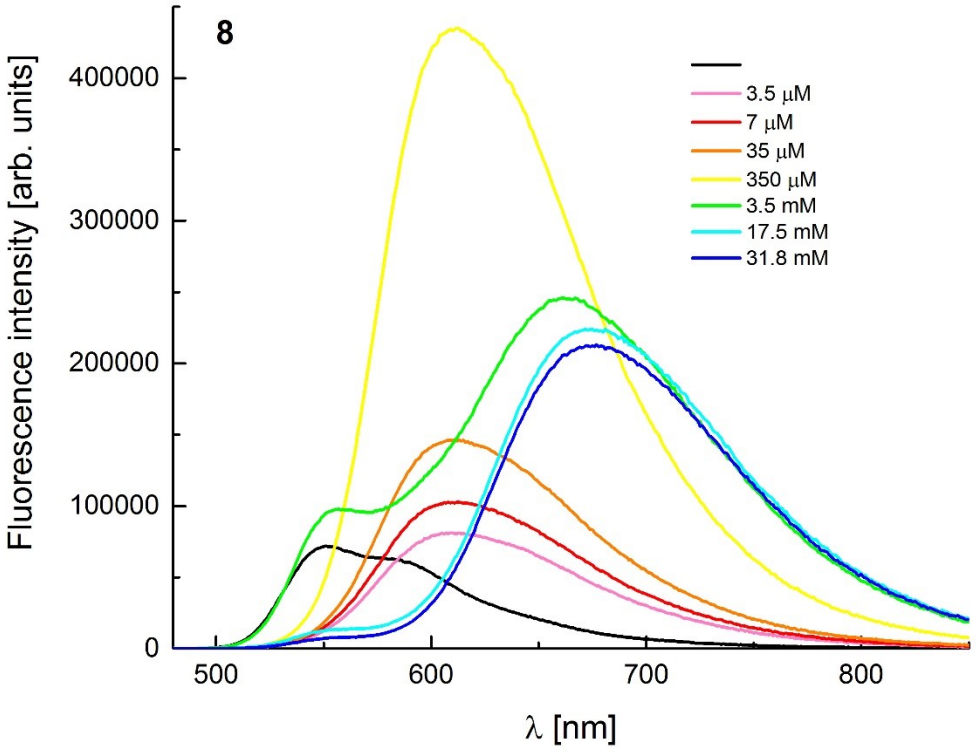

Fig. S38. The effect of cadmium perchlorate addition on the emission spectra of DPP **8** measured in CH_3CN.

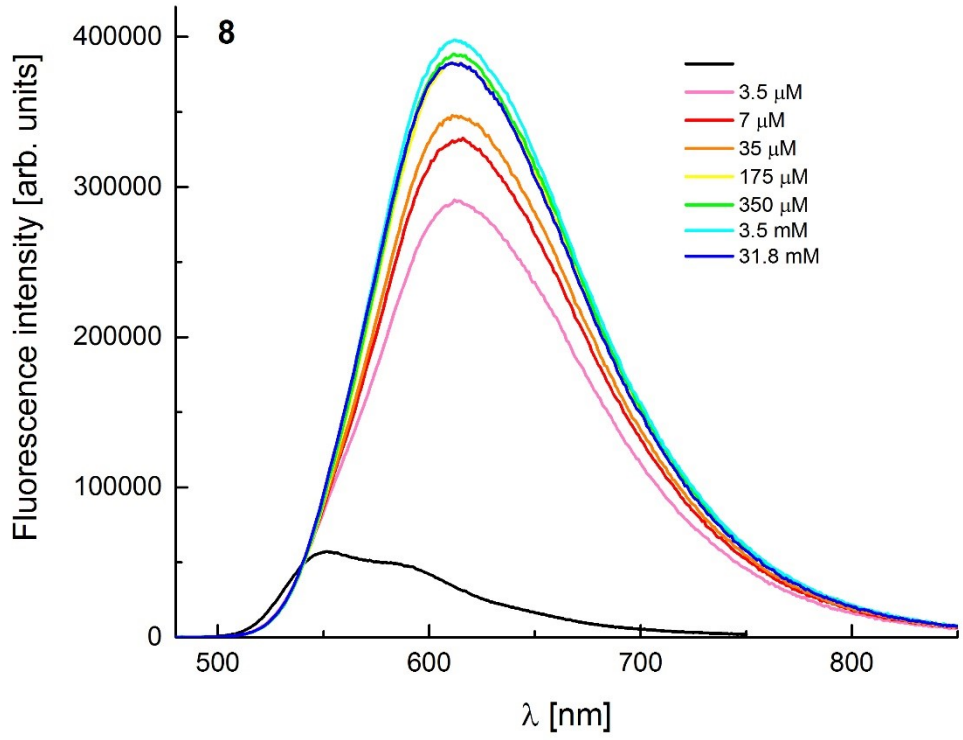

Fig. S39. The effect of zinc perchlorate addition on the emission spectra of DPP **8** measured in CH_3CN.

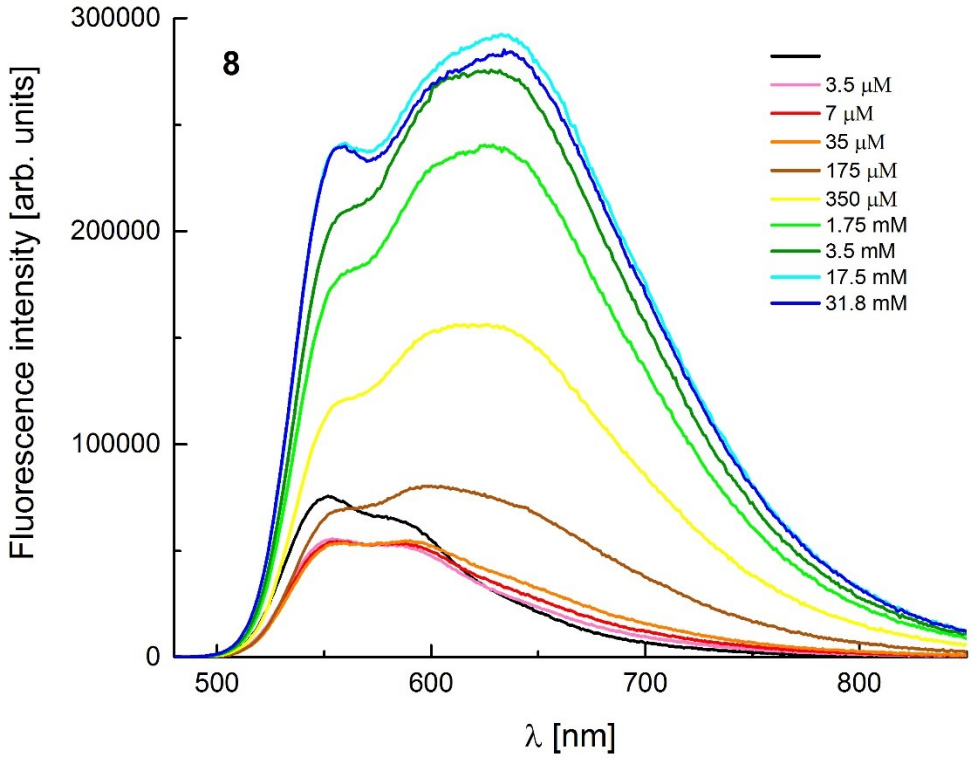

Fig. S40. The effect of magnesium perchlorate addition on the emission spectra of DPP **8** measured in CH_3CN.

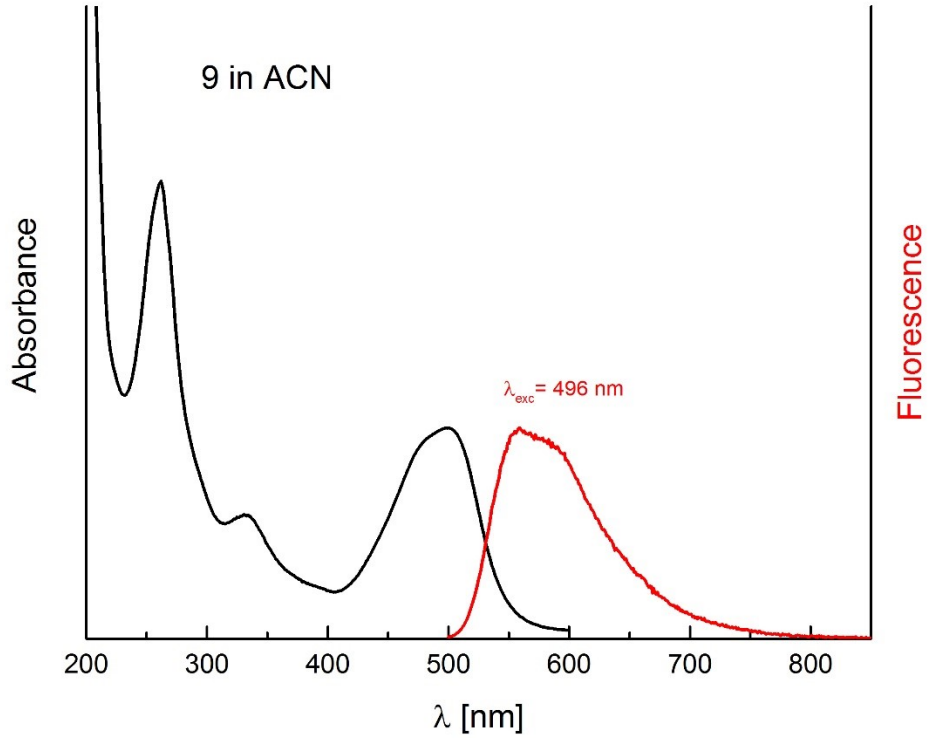

Fig. S41. The absorption and emission spectra of DPP **9** in CH_3CN.

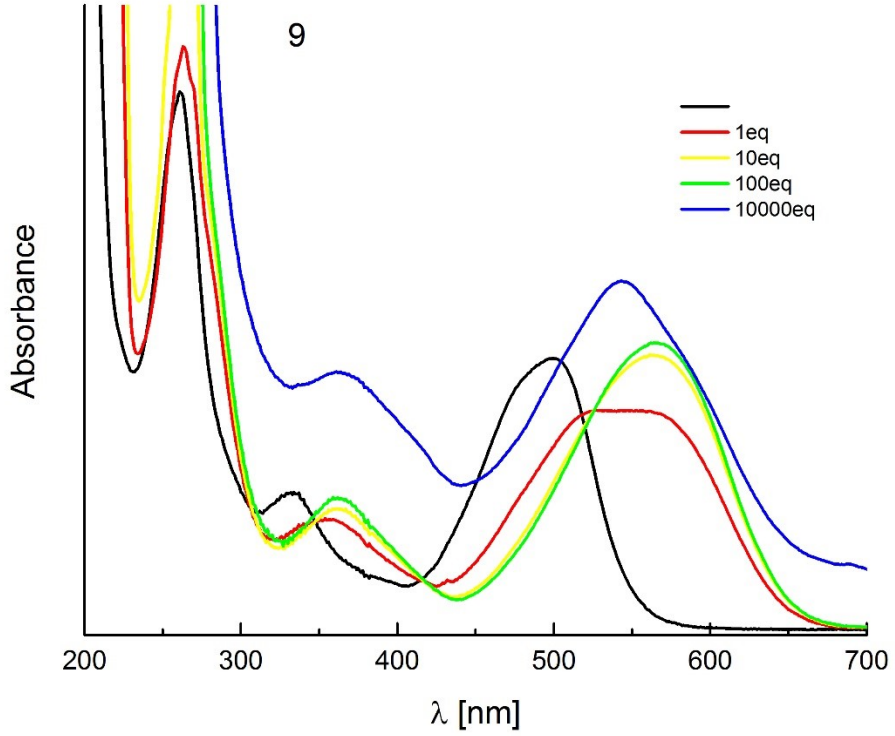

Fig. S42.The effect of $PhSO_3H$ addition on the absorption spectra of DPP **9** measured in CH_3CN.

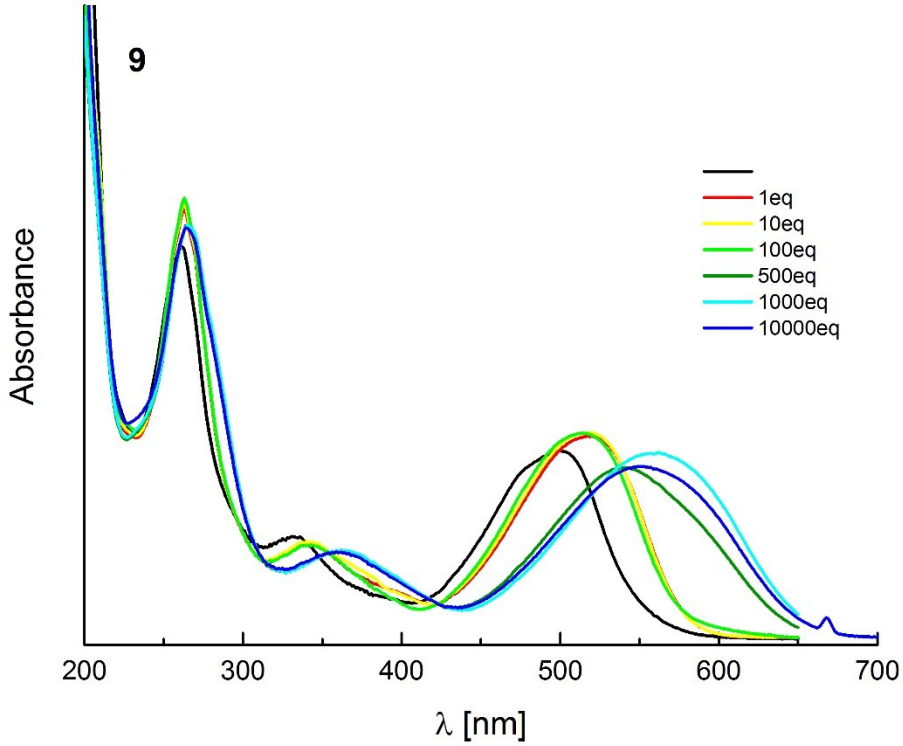

Fig. S43.The effect of cadmium perchlorate addition on the absorption spectra of DPP **9** measured in CH_3CN.

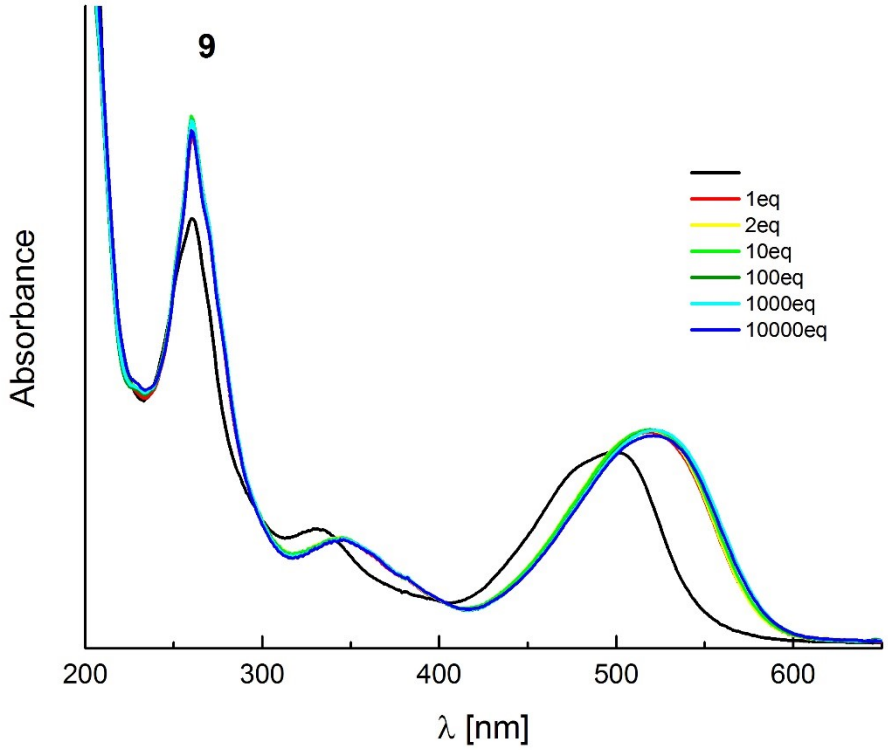

Fig. S44.The effect of zinc perchlorate addition on the absorption spectra of DPP **9** measured in CH_3CN.

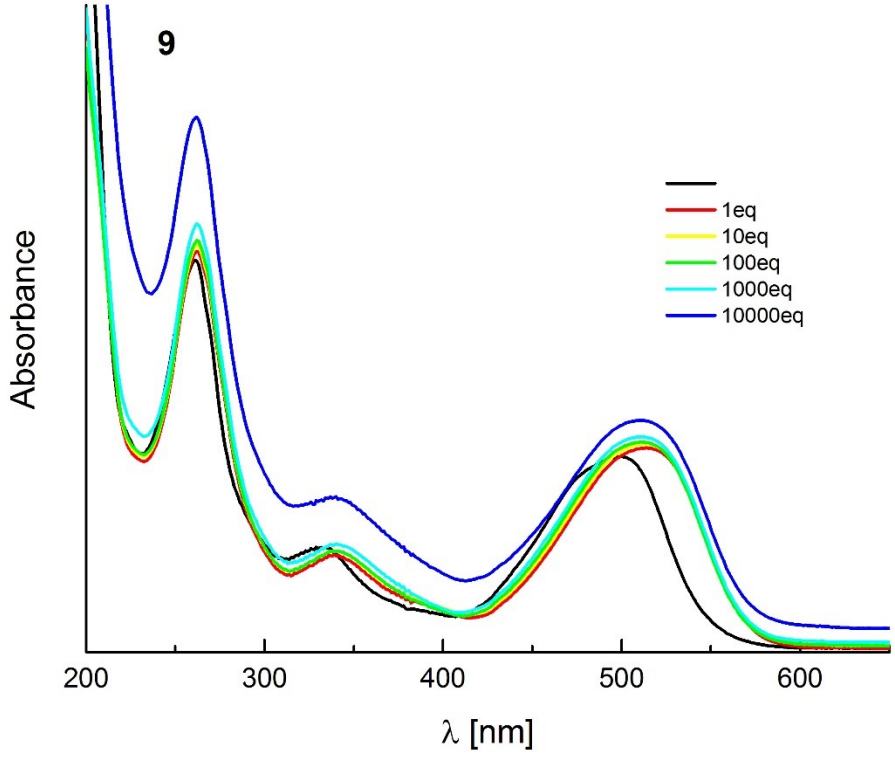

Fig. S45.The effect of magnesium perchlorate addition on the absorption spectra of DPP **9** measured in CH_3CN.

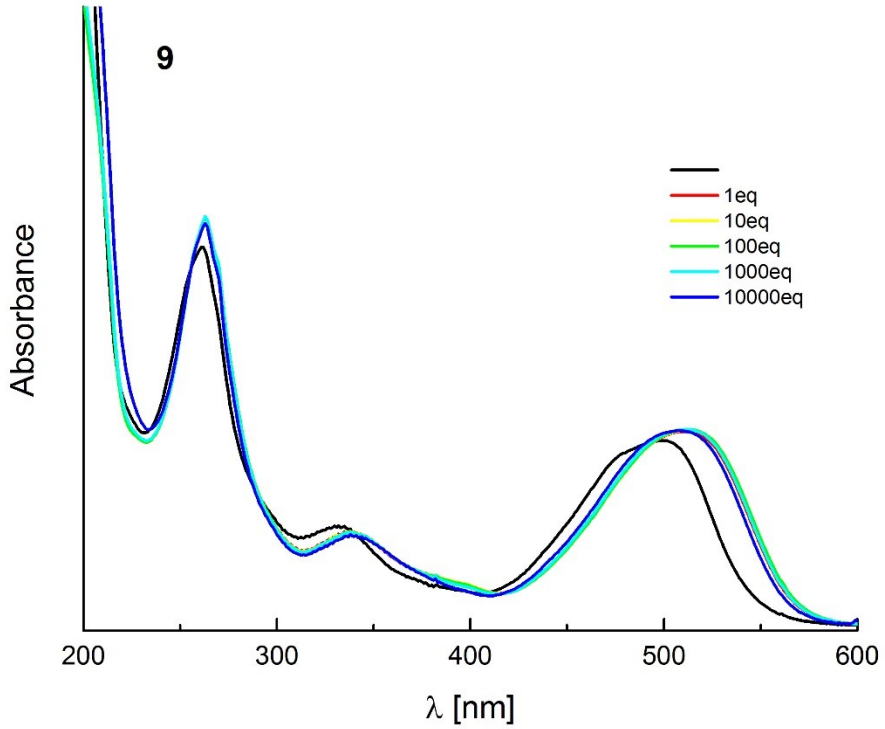

Fig. S46.The effect of calcium perchlorate addition on the absorption spectra of DPP **9** measured in CH_3CN.

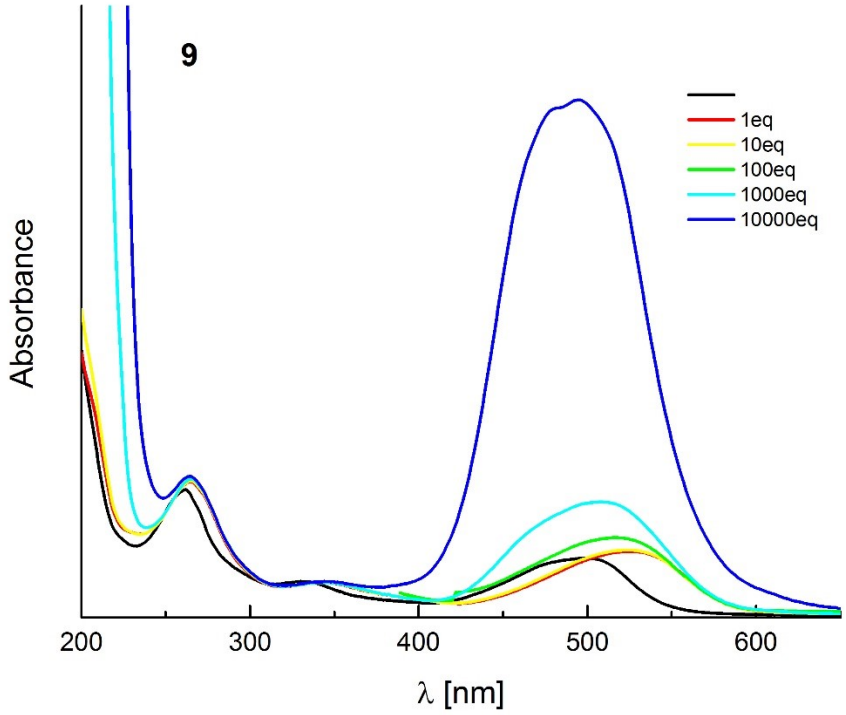

Fig. S47.The effect of cobalt perchlorate addition on the absorption spectra of DPP **9** measured in CH_3CN.

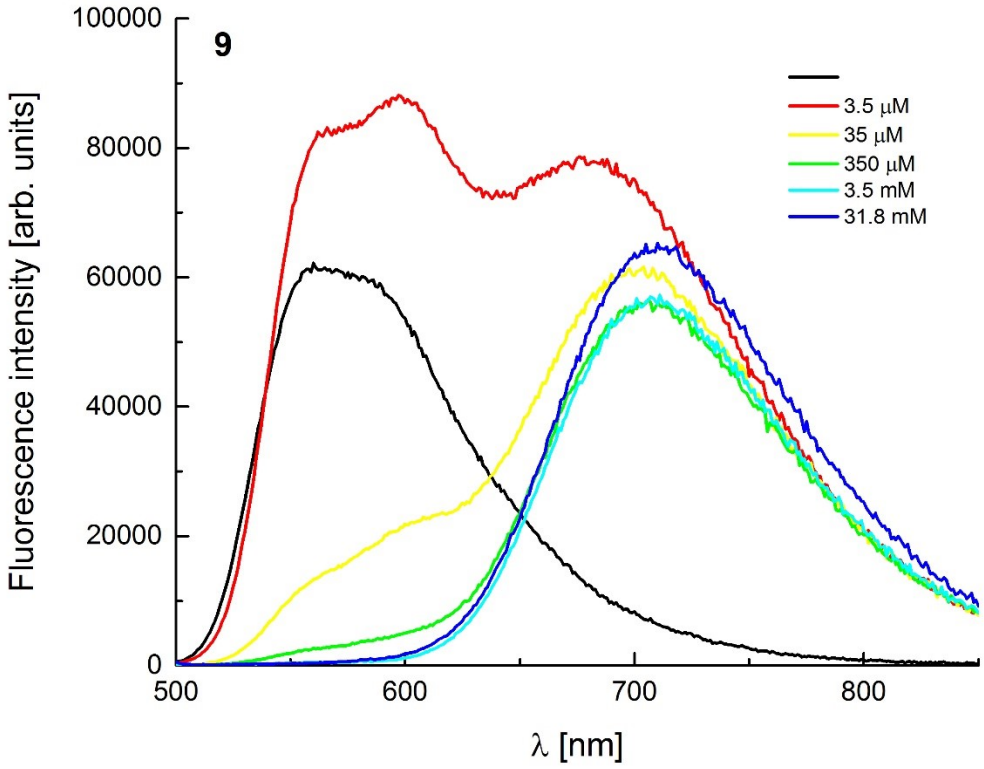

Fig. S48. The effect of $PhSO_3H$ addition on the emission spectra of DPP **9** measured in CH_3CN.

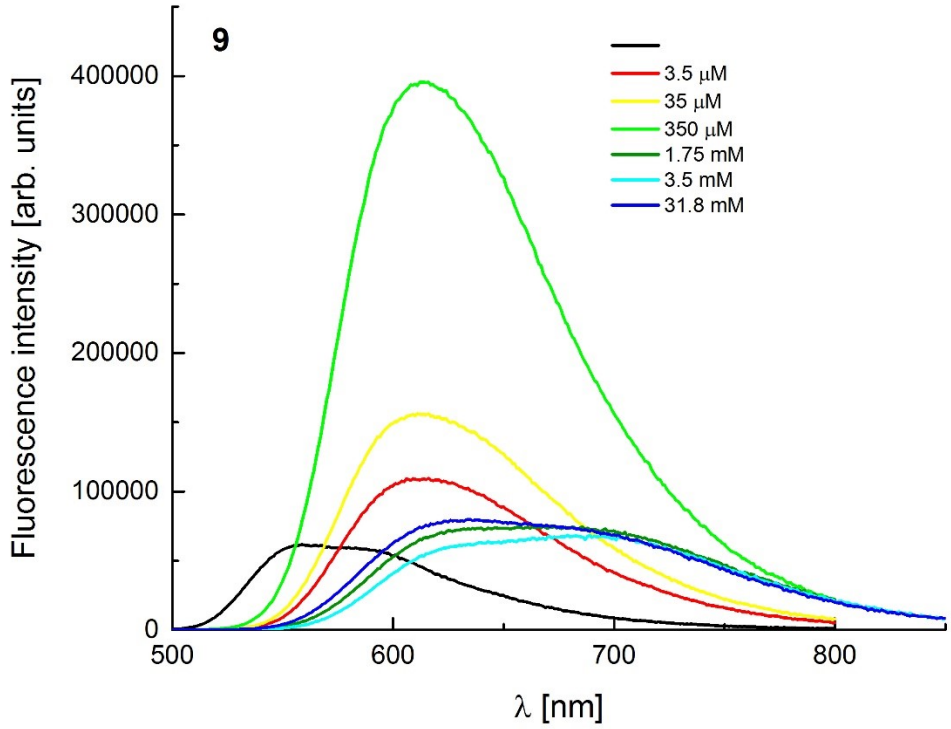

Fig. S49. The effect of cadmium perchlorate addition on the emission spectra of DPP **9** measured in CH_3CN.

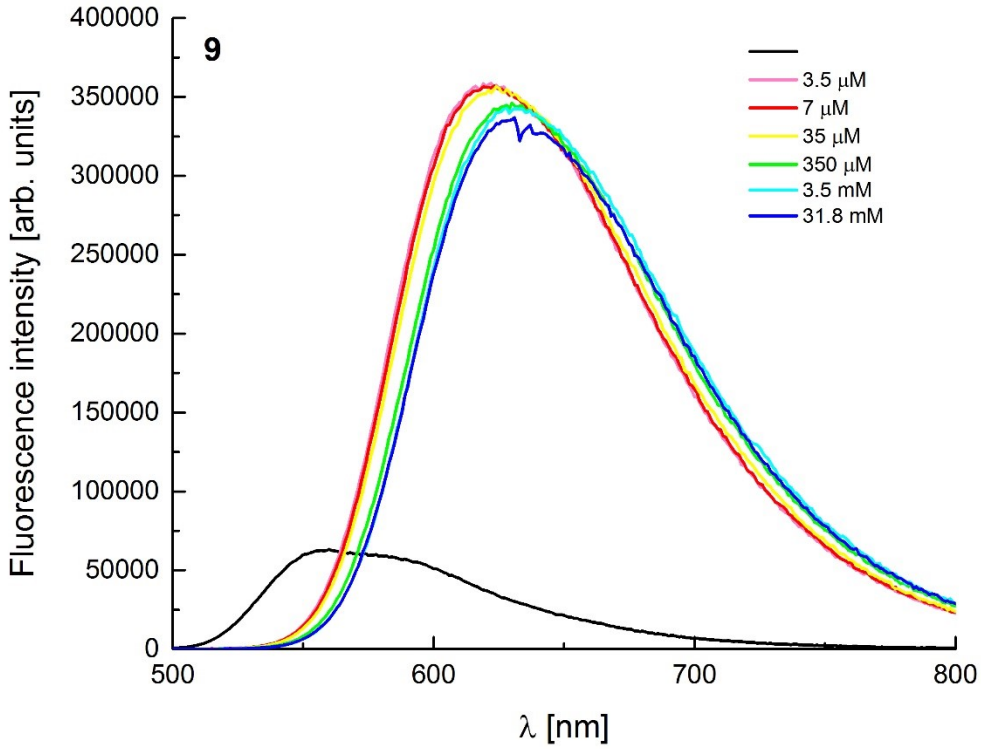

Fig. S50. The effect of zinc perchlorate addition on the emission spectra of DPP **9** measured in CH_3CN.

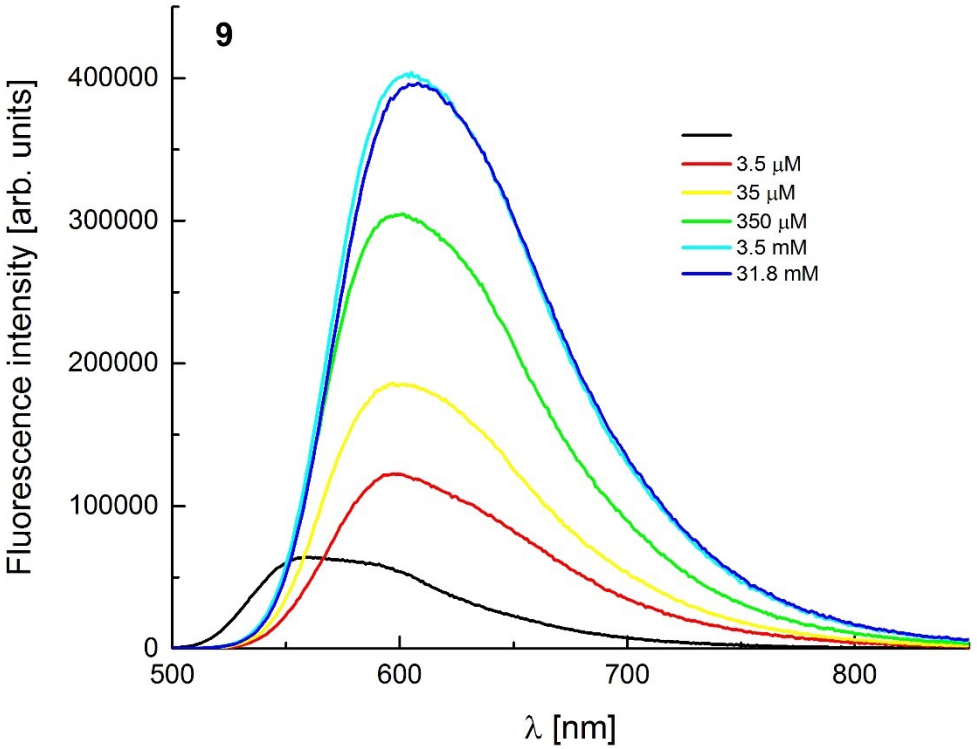

Fig. S51. The effect of magnesium perchlorate addition on the emission spectra of DPP **9** measured in CH_3CN.

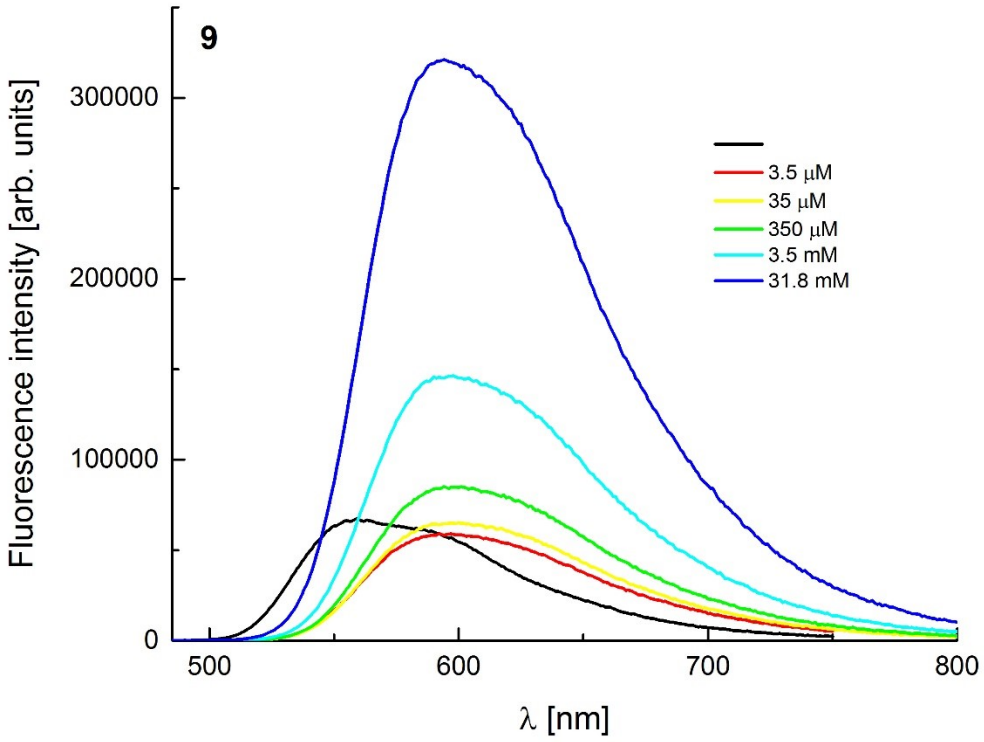

Fig. S52. The effect of calcium perchlorate addition on the emission spectra of DPP **9** measured in CH_3CN.

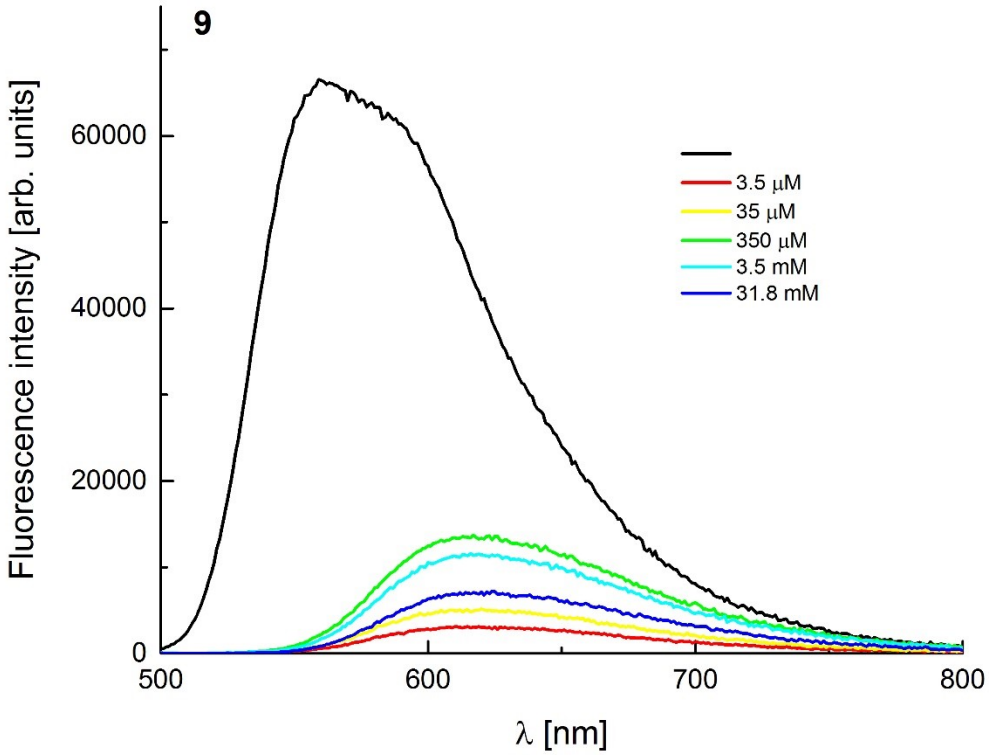

Fig. S53. The effect of cobalt perchlorate addition on the emission spectra of DPP **9** measured in CH_3CN.

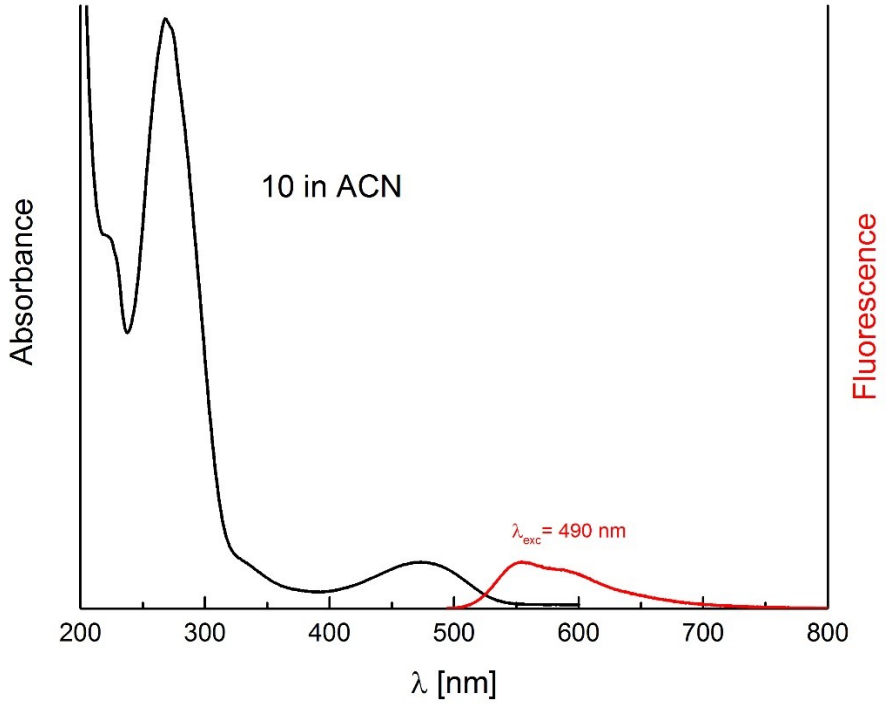

Fig. S54. The absorption and emission spectra of DPP **10** in CH_3CN.

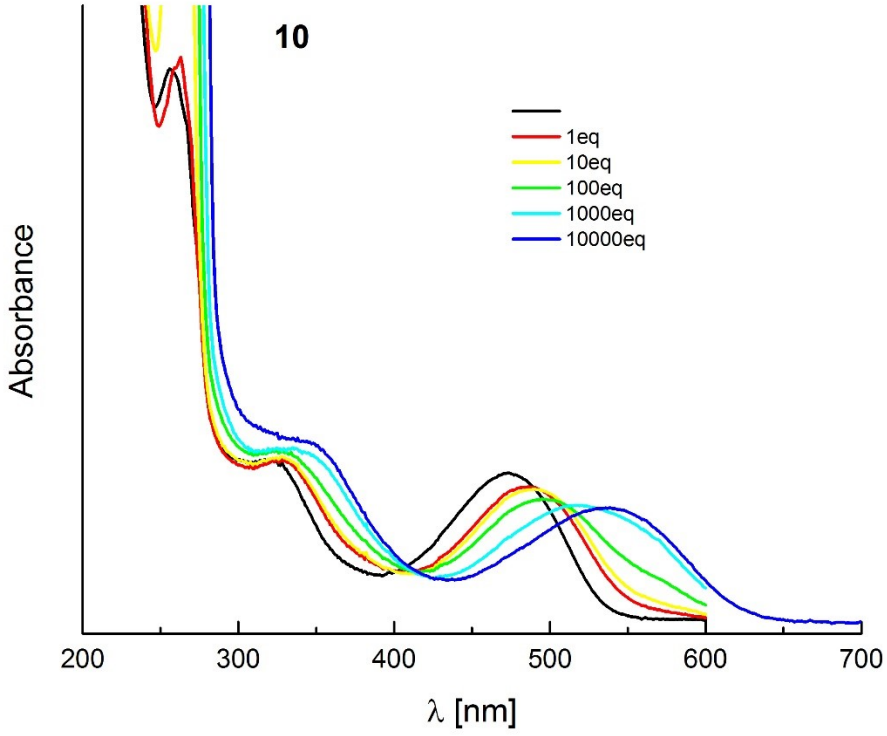

Fig. S55.The effect of $PhSO_3H$ addition on the absorption spectra of DPP **10** measured in CH_3CN.

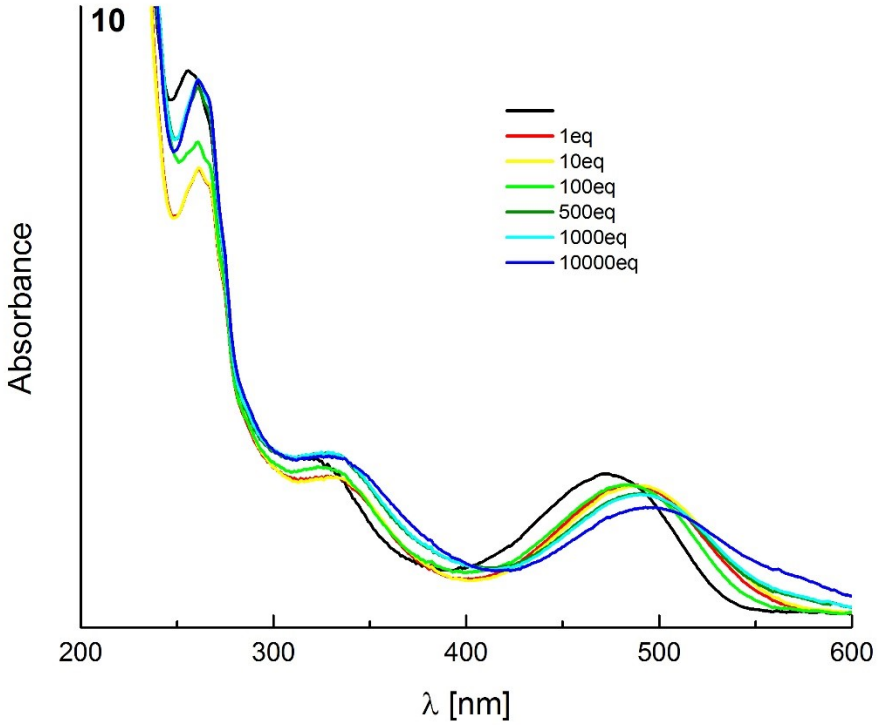

Fig. S56.The effect of cadmium perchlorate addition on the absorption spectra of DPP **10** measured in CH_3CN.

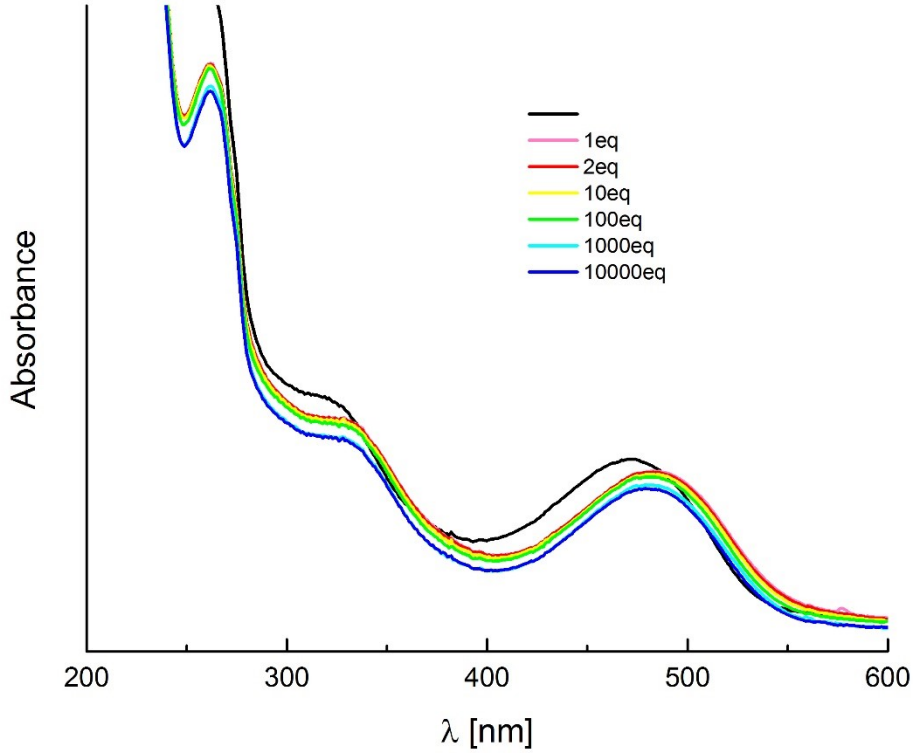

Fig. S57.The effect of zinc perchlorate addition on the absorption spectra of DPP **10** measured in CH_3CN.

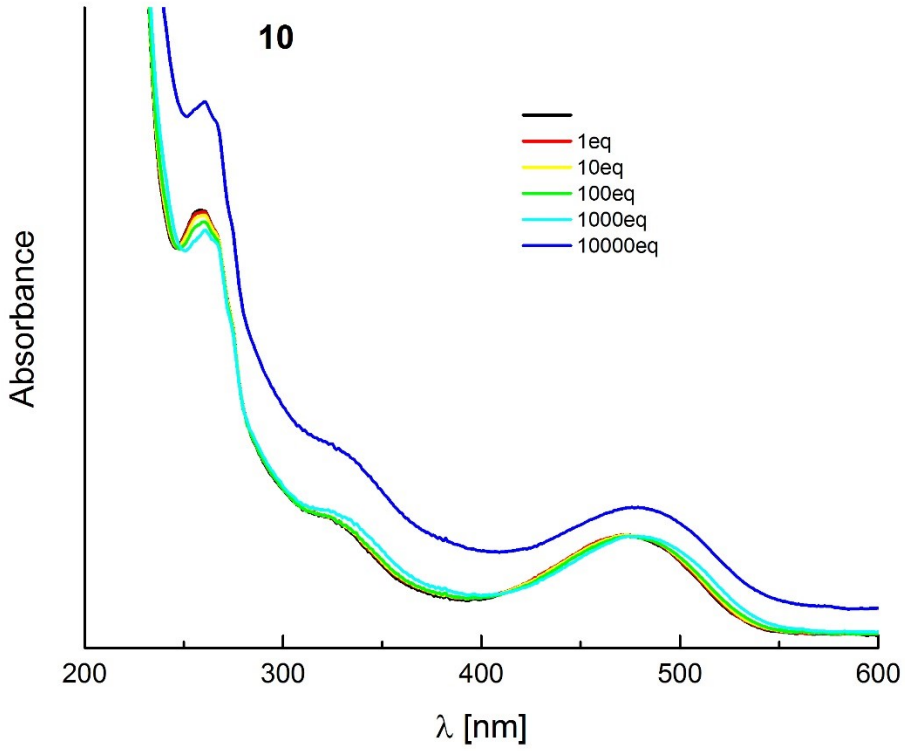

Fig. S58.The effect of magnesium perchlorate addition on the absorption spectra of DPP **10** measured in CH_3CN.

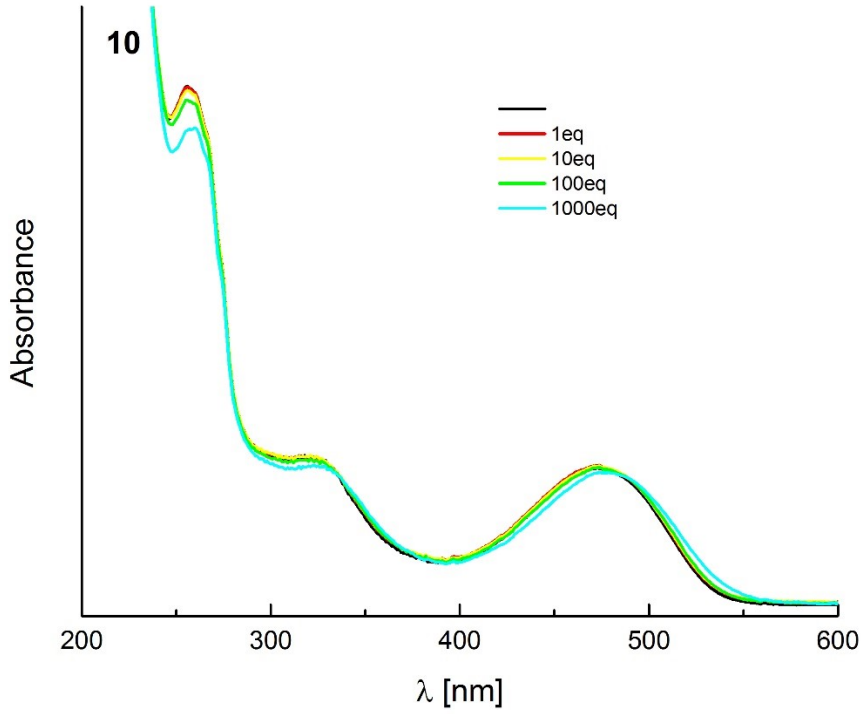

Fig. S59.The effect of calcium perchlorate addition on the absorption spectra of DPP **10** measured in CH_3CN.

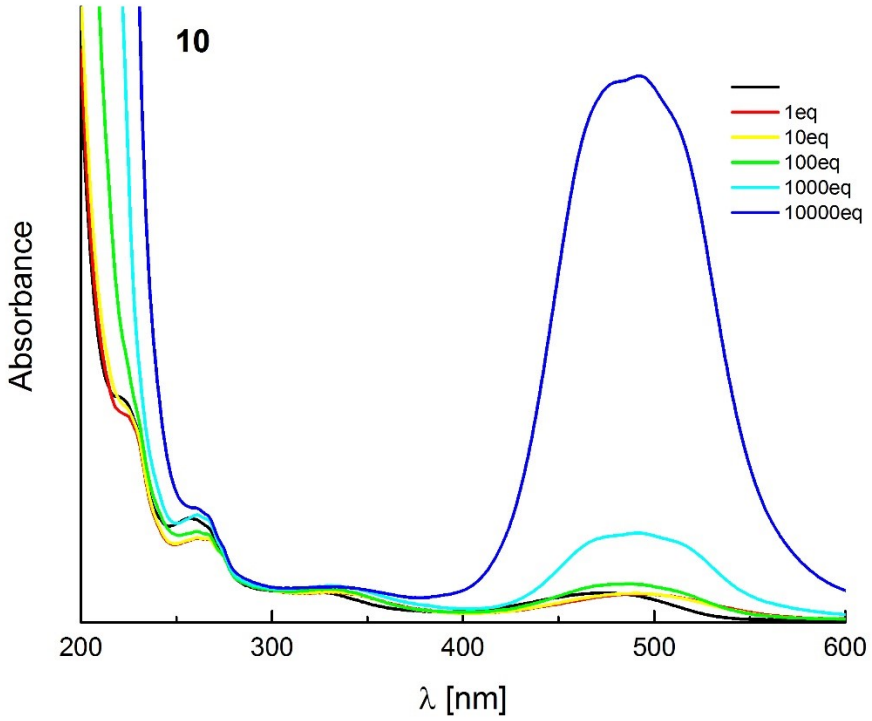

Fig. S60.The effect of cobalt perchlorate addition on the absorption spectra of DPP **10** measured in CH_3CN.

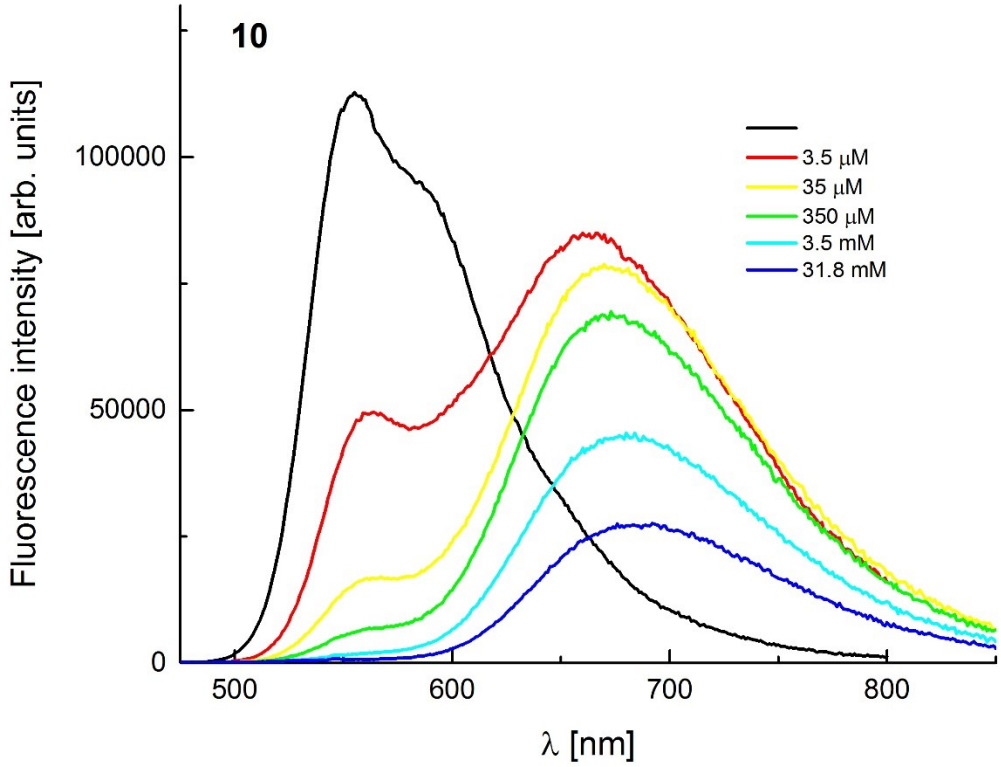

Fig. S61. The effect of $PhSO_3H$ addition on the emission spectra of DPP **10** measured in CH_3CN.

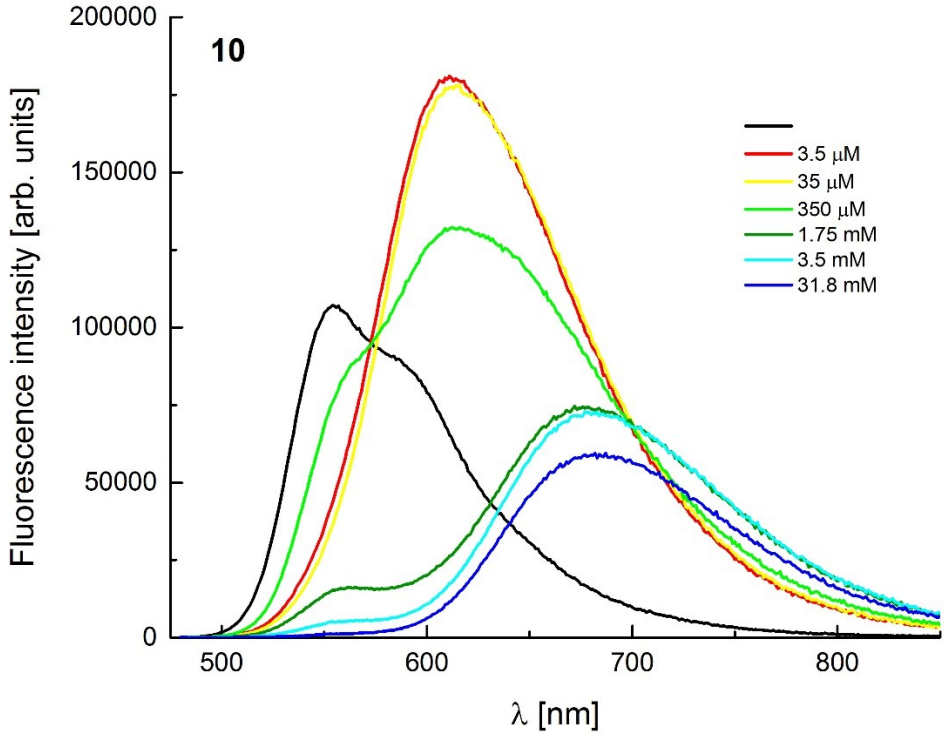

Fig. S62. The effect of cadmium perchlorate addition on the emission spectra of DPP **10** measured in CH_3CN.

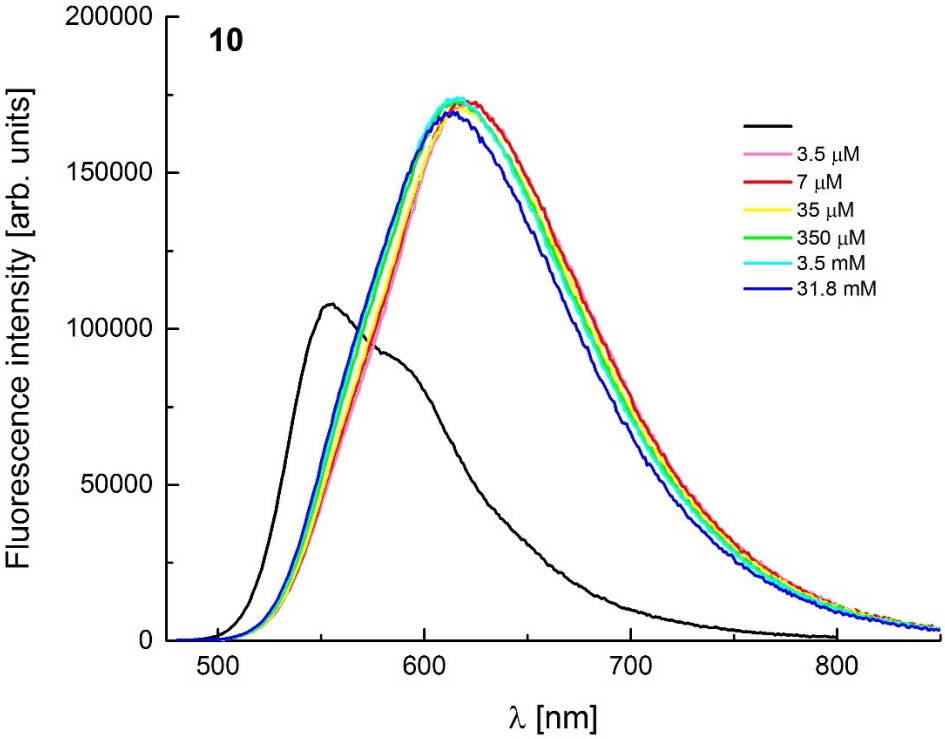

Fig. S63. The effect of zinc perchlorate addition on the emission spectra of DPP **10** measured in CH_3CN.

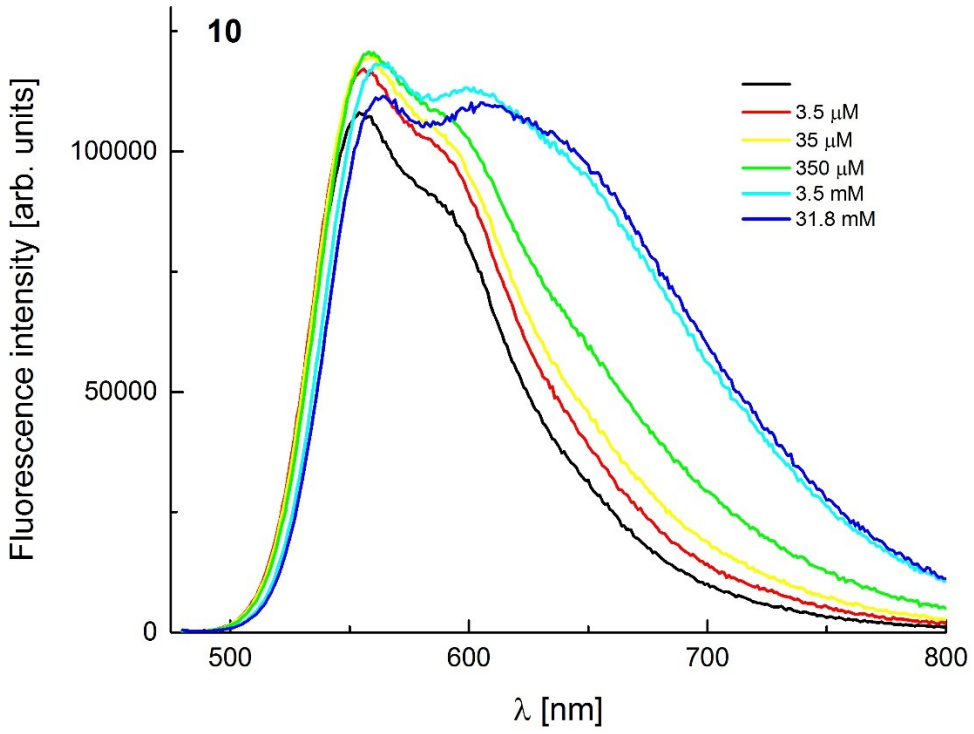

Fig. S64. The effect of magnesium perchlorate addition on the emission spectra of DPP **10** measured in CH_3CN.

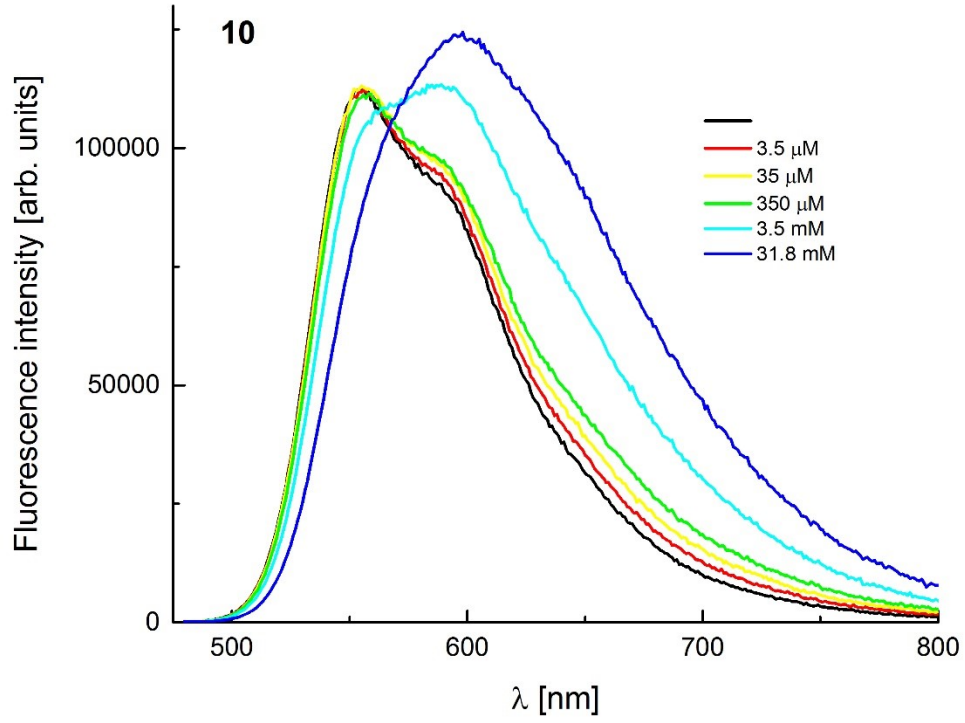

Fig. S65. The effect of calcium perchlorate addition on the emission spectra of DPP **10** measured in CH_3CN.

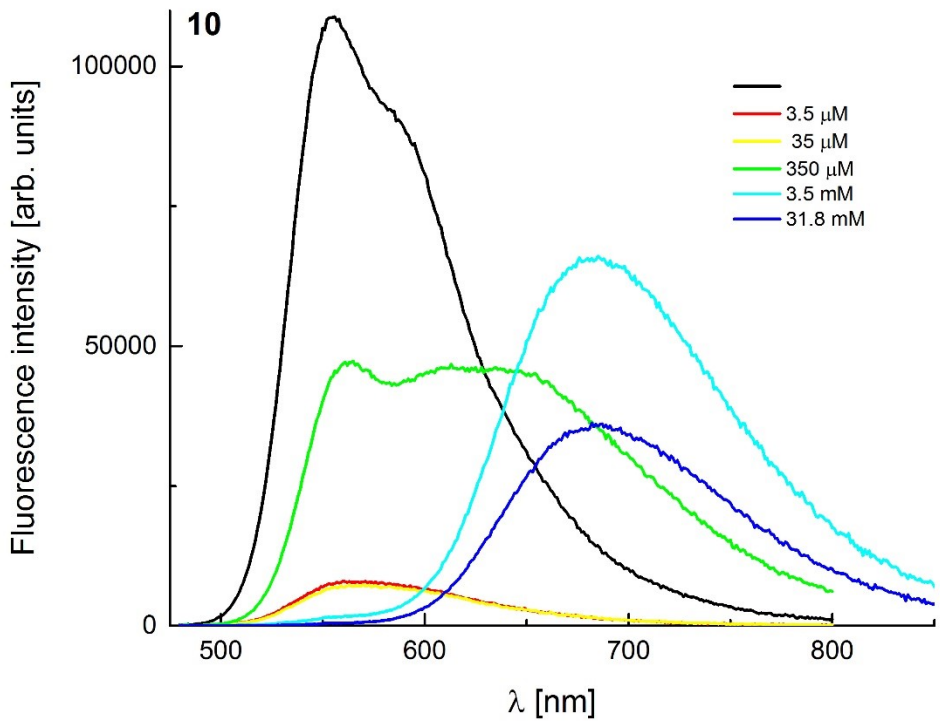

Fig. S66. The effect of cobalt perchlorate addition on the emission spectra of DPP **10** measured in CH_3CN.

Section S4: Water solubility and binding constants

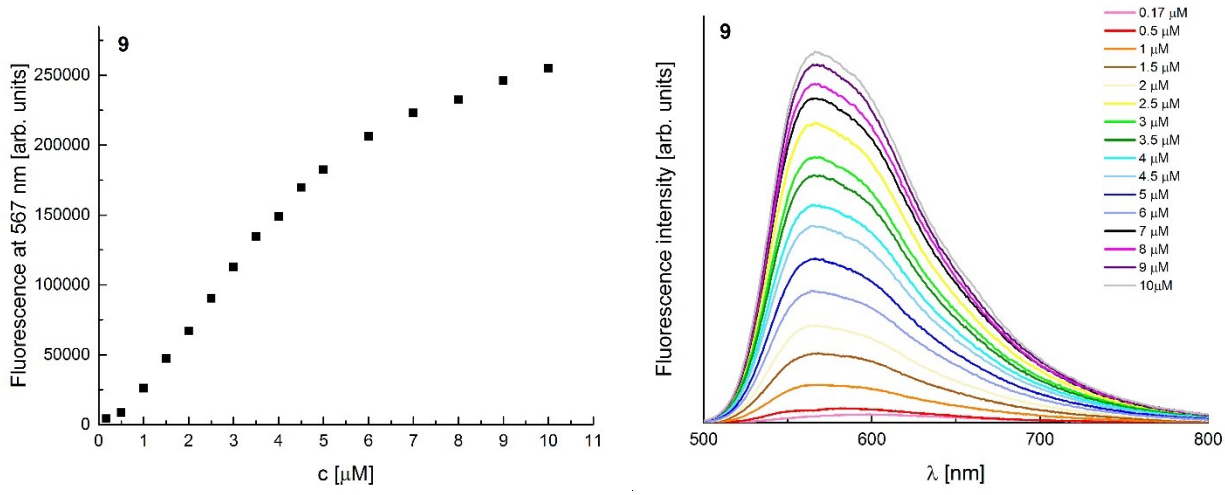

Fig. S67. Plot of fluorescence intensity against concentration of DPP **9** in water.

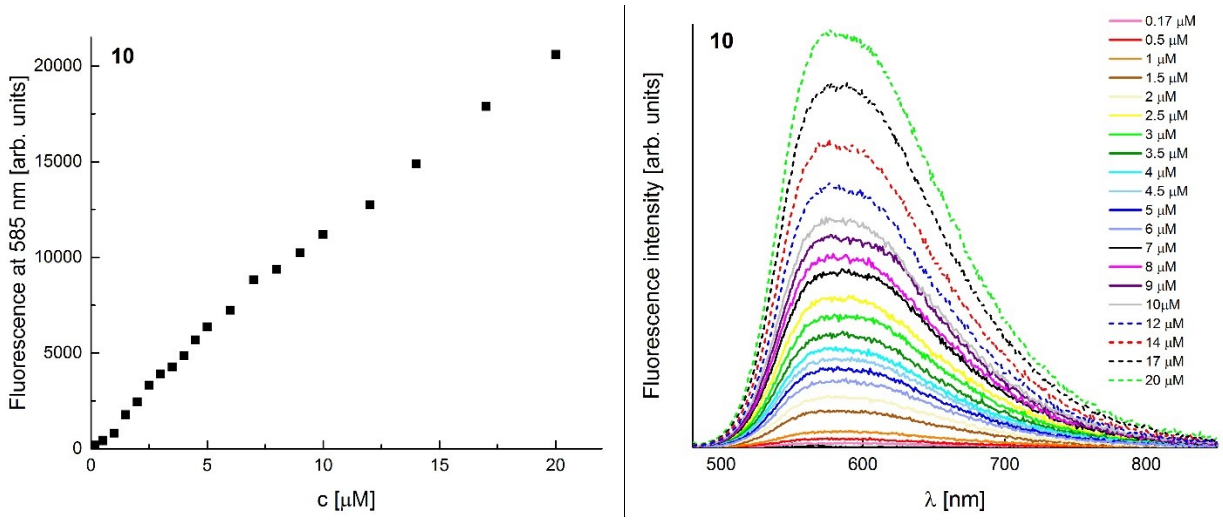

Fig. S68. Plot of fluorescence intensity against concentration of DPP **10** in water.

Section S5: Imaging

Cell culture conditions. The rat embryonic cardiomyoblast-derived H9C2 cell lines were cultured at 37°C in a humidified atmosphere containing 5% CO_2 in DMEM supplemented with 10% foetal bovine serum (FBS), 2 mM glutamine, 100 U/ml penicillin, and 100 µg/ml streptomycin.

Fluorescence localization of diketopyrrolopyrrole-based zinc probes within the cells. The cardiac H9C2 cells were loaded with fluorophores in DMEM medium supplemented with 10% FBS, 2 mM glutamine, 100 U/ml penicillin, and 100 µg/ml streptomycin at 37°C in a humidified atmosphere containing 5% CO_2 for 15 to 30 minutes with the diketopyrrolopyrrole-based zinc probe at the final concentration ranging from 200 to 500 nM. The final concentration of the MitoTracker™ Green FM was 150 nM, and Lysosyme probe was 100 nM. The fluorophores were dissolved in DMSO. Before measurements, the incubation medium was replaced with FluoroBrite™ DMEM. The measurements were performed with use of Olympus IX83 confocal microscope with the water objective 60x UPLSAPO 60XW. Registered data were transferred to the ImageJ and analyzed for presentation.

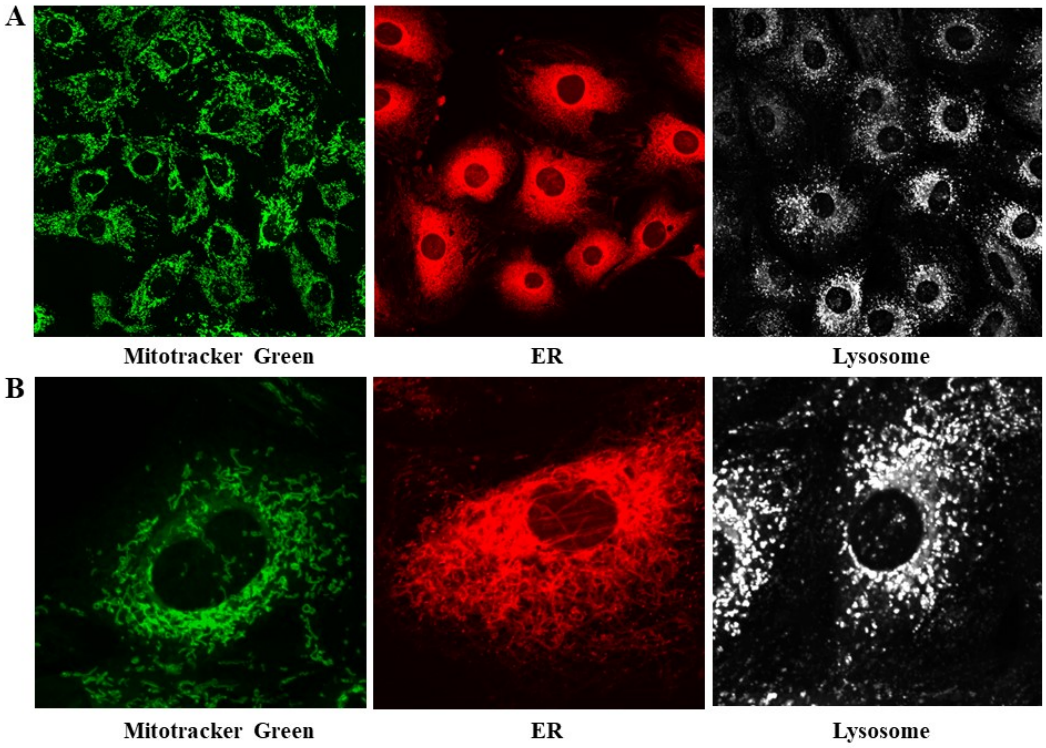

Fig. S69. Confocal imaging of the location of organellar fluorescent markers in H9C2 cells line. A. Localization of fluorescent markers for mitochondria (Mitotracker Green), endoplasmic reticulum (ER), and lysosomes, respectively, in H9C2 cells. B. Three-fold magnification of the selected Region of Interest (ROI), respectively for the individual fluorescent markers.

Section S6: Additional computational results

To ascertain the quality of the TD-DFT results, we have considered three smaller models of the investigated probes, denoted **M3**, and **M4** (see Fig. **S64**) for which CC2/*aug-cc*-pVTZ single point calculations were achievable.

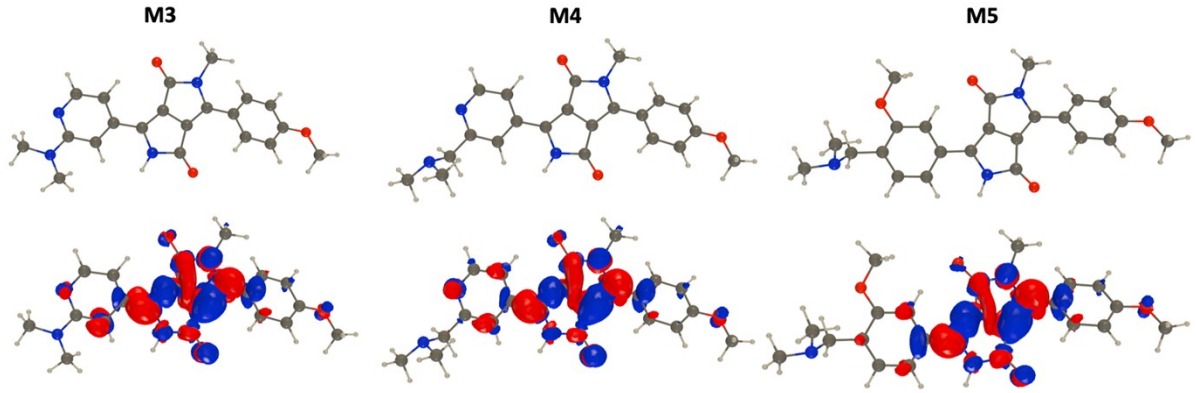

Fig. S70: Representation of the model probes used to test the reliability of the TD-DFT approach. We also provide the density difference plots (contour threshold: 0.001 au).

The cLR^2-PCM-TD-DFT protocol returns vertical absorption at 452, 461, and 453 nm for **M3**, and **M4** respectively. When adding the difference between CC2/*aug*-cc-pVTZ and TD-DFT results computed in gas phase, the values are increases slightly to 464, 473, and 463 nm, respectively. For vertical fluorescence, the cLR^2-PCM-TD-DFT values are 549, 557, and 542 nm, for for **M3**, and **M4**, respectively, whereas the CC2-corrected results are 552, 562, and 541 nm. Again, the values are very close and this hints that the selected functional is well suited for the systems under investigation.

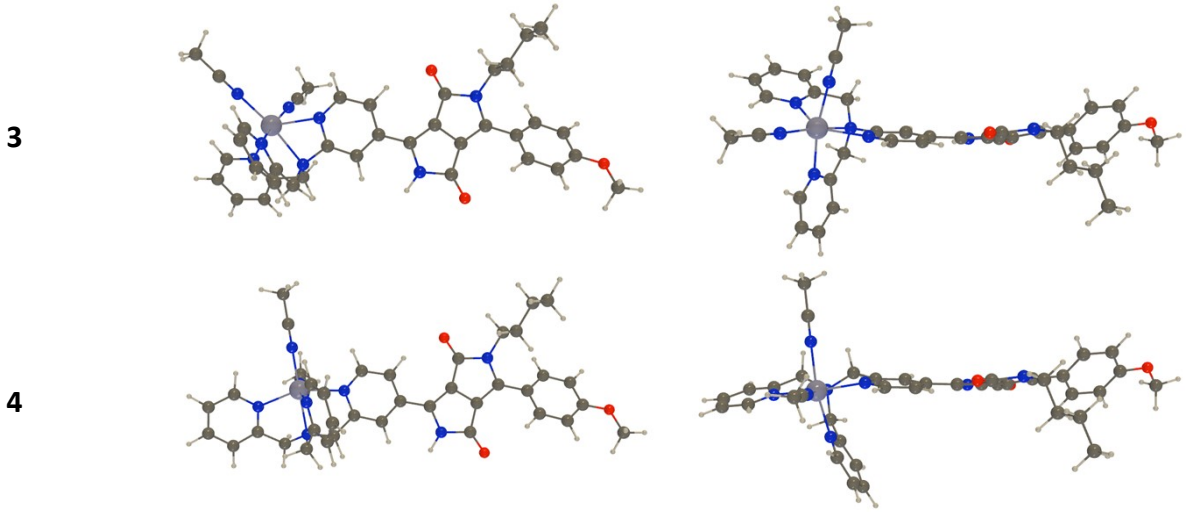

Fig. S71: Optimal geometries of the molecules **3**, **4** with a Zn^{++} ion complexed and explicit ACN molecules added to complete the coordination sphere of the cation. Side (left) and top (right) views.

Section S7: ^{1}H, ^{13}C and HRMS spectra

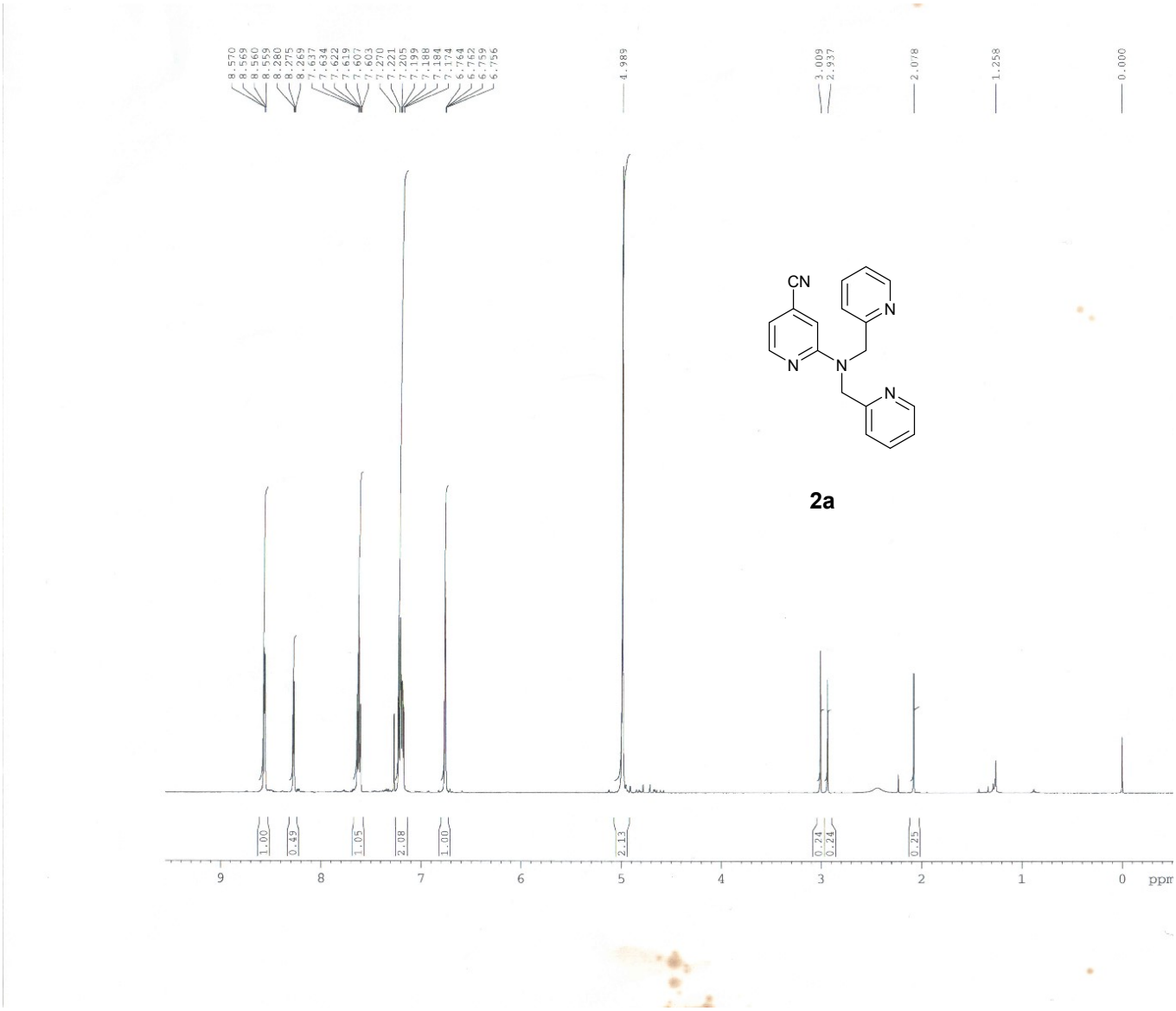

^{1}H-NMR spectra of **2a** in $CDCl_3$

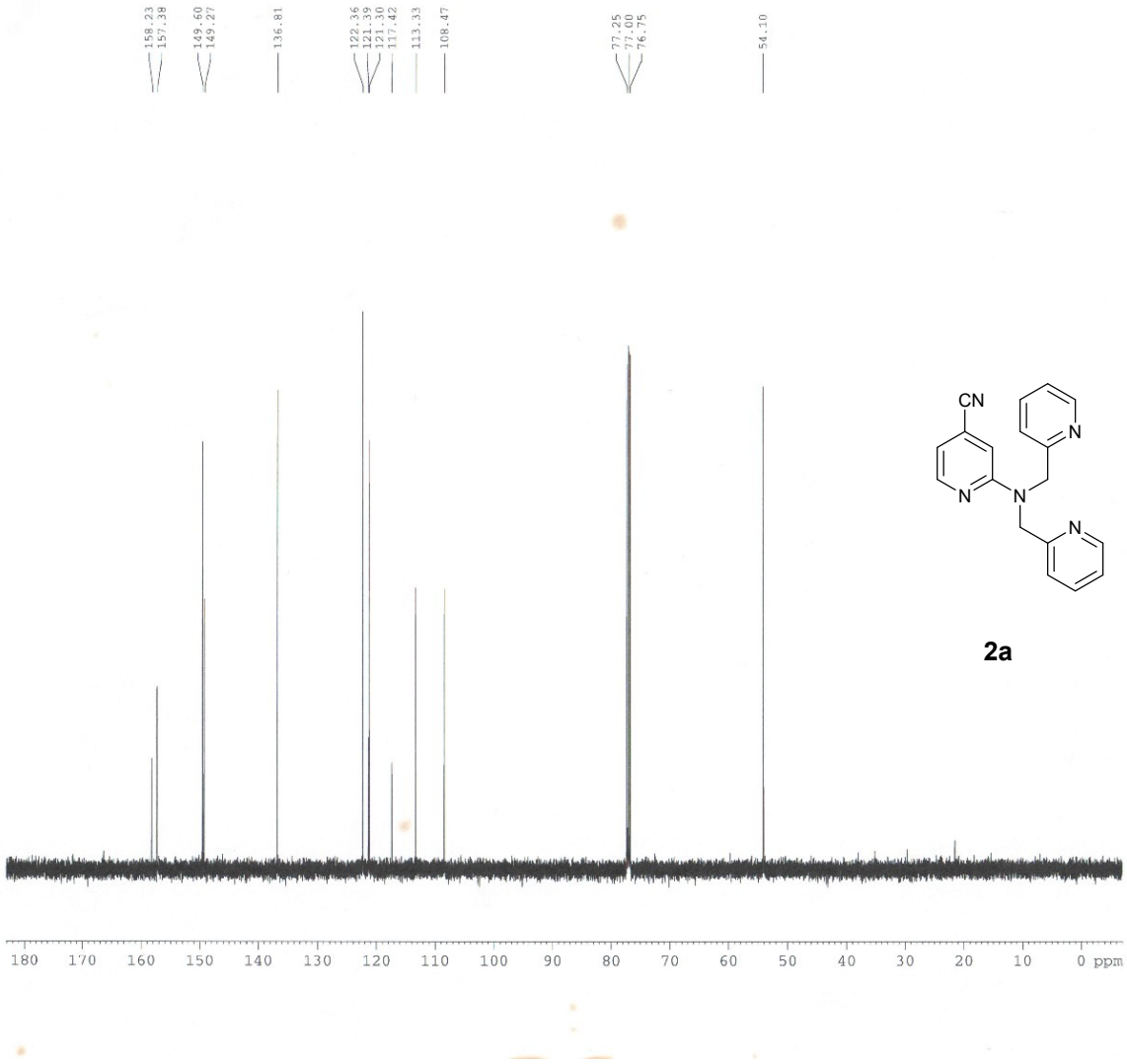

^{13}C-NMR spectra of **2a** in $CDCl_3$

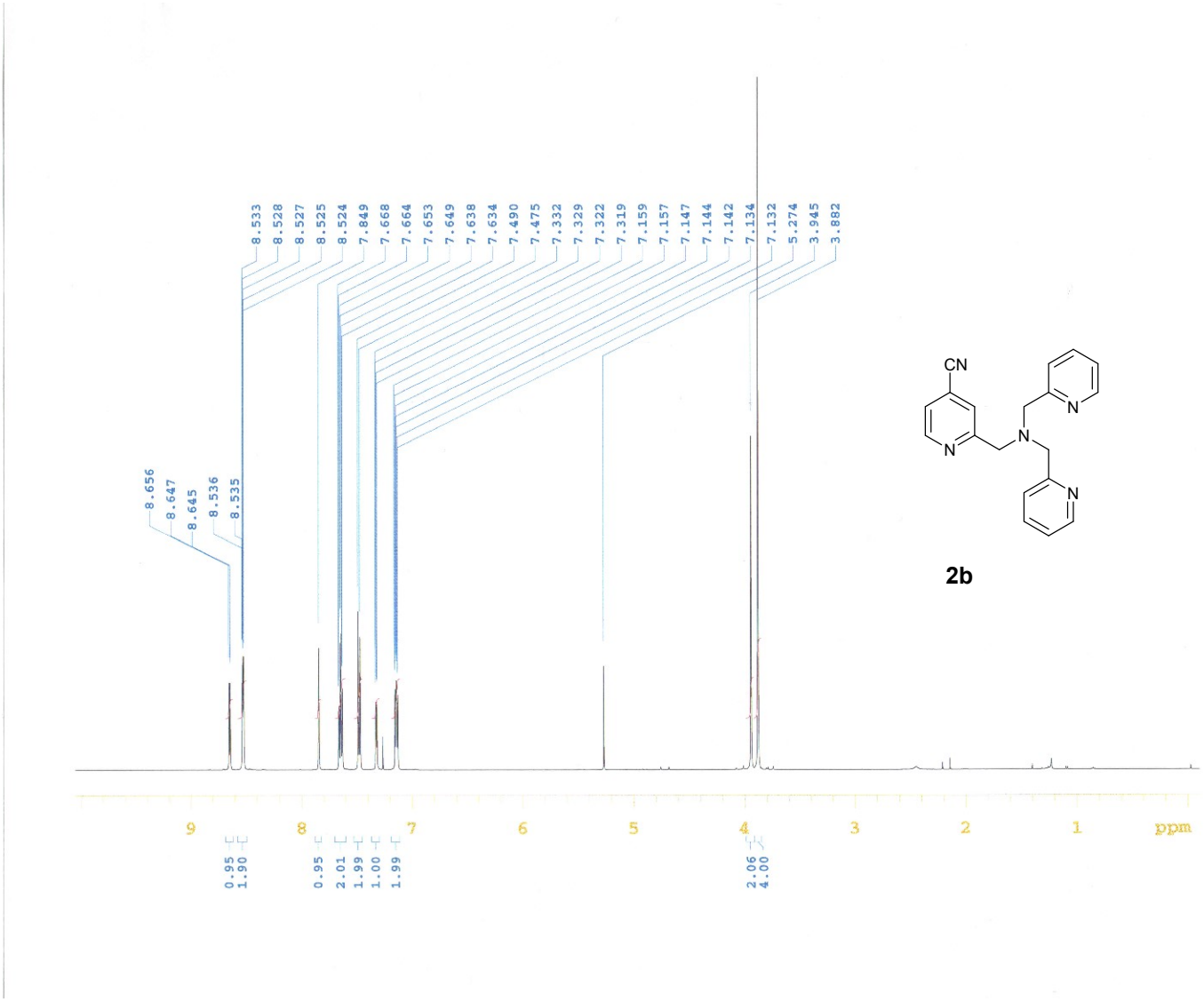

^{1}H-NMR

spectra of **2b** in $CDCl_3$

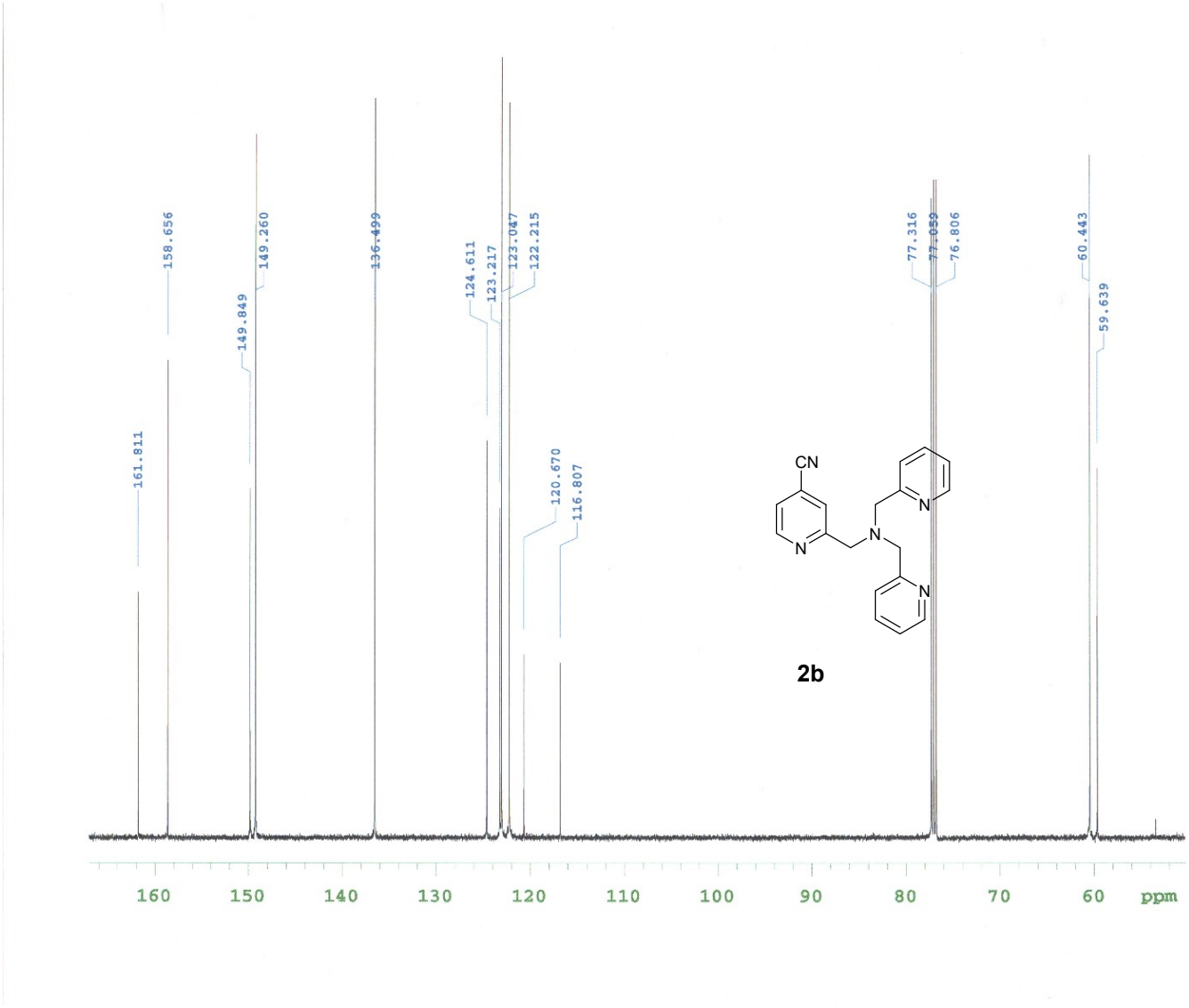
161.811
158.656
149.849
149.260
136.499
124.611
123.217
123.047
122.215
120.670
116.807
77.316
77.059
76.806
60.443
59.639
CN
N
N
N
2b
160
150
140
130
120
110
100
90
80
70
60
ppm

^{13}C-NMR

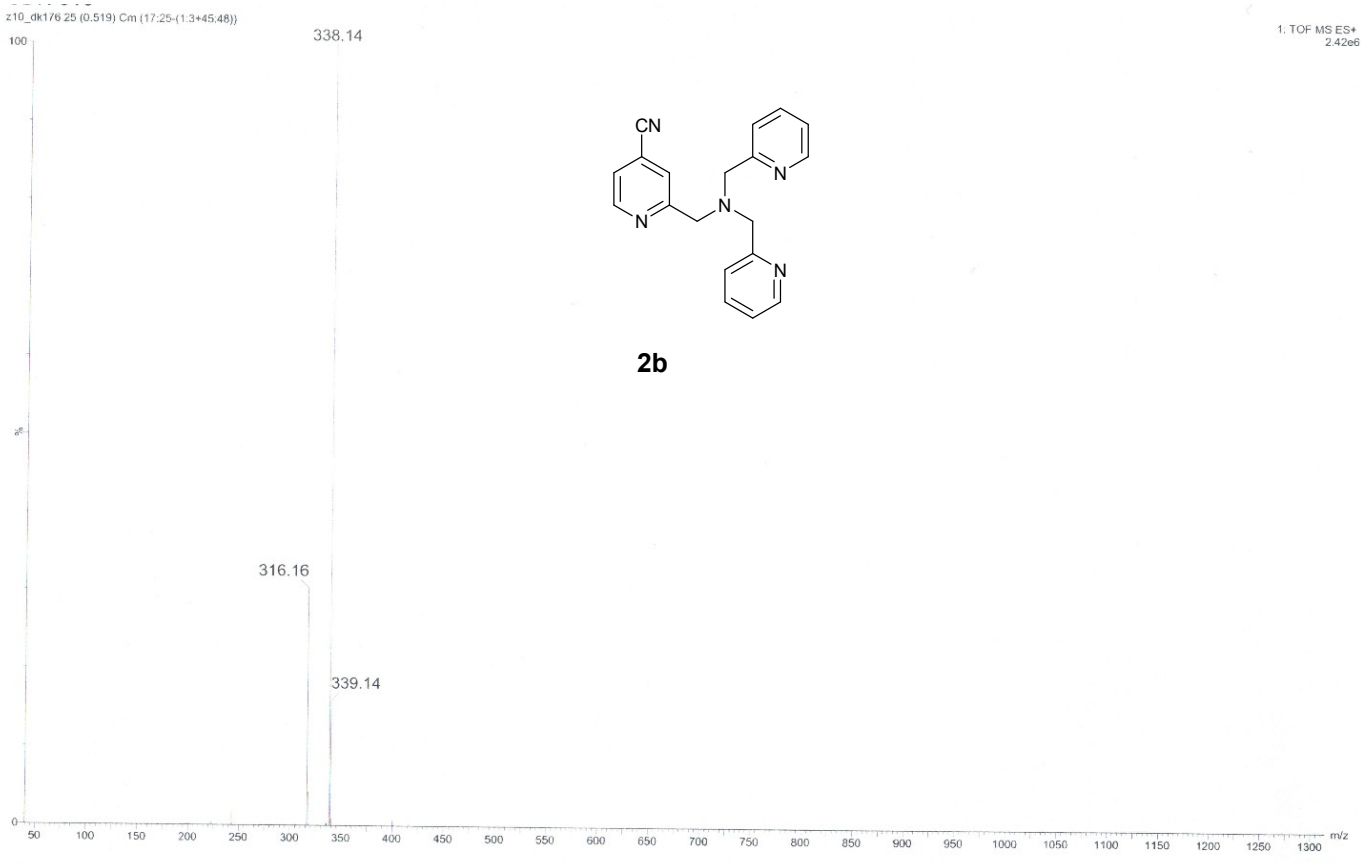

spectra of **2b** in $CDCl_3$

HRMS (ESI, m/z) spectra of **2b**

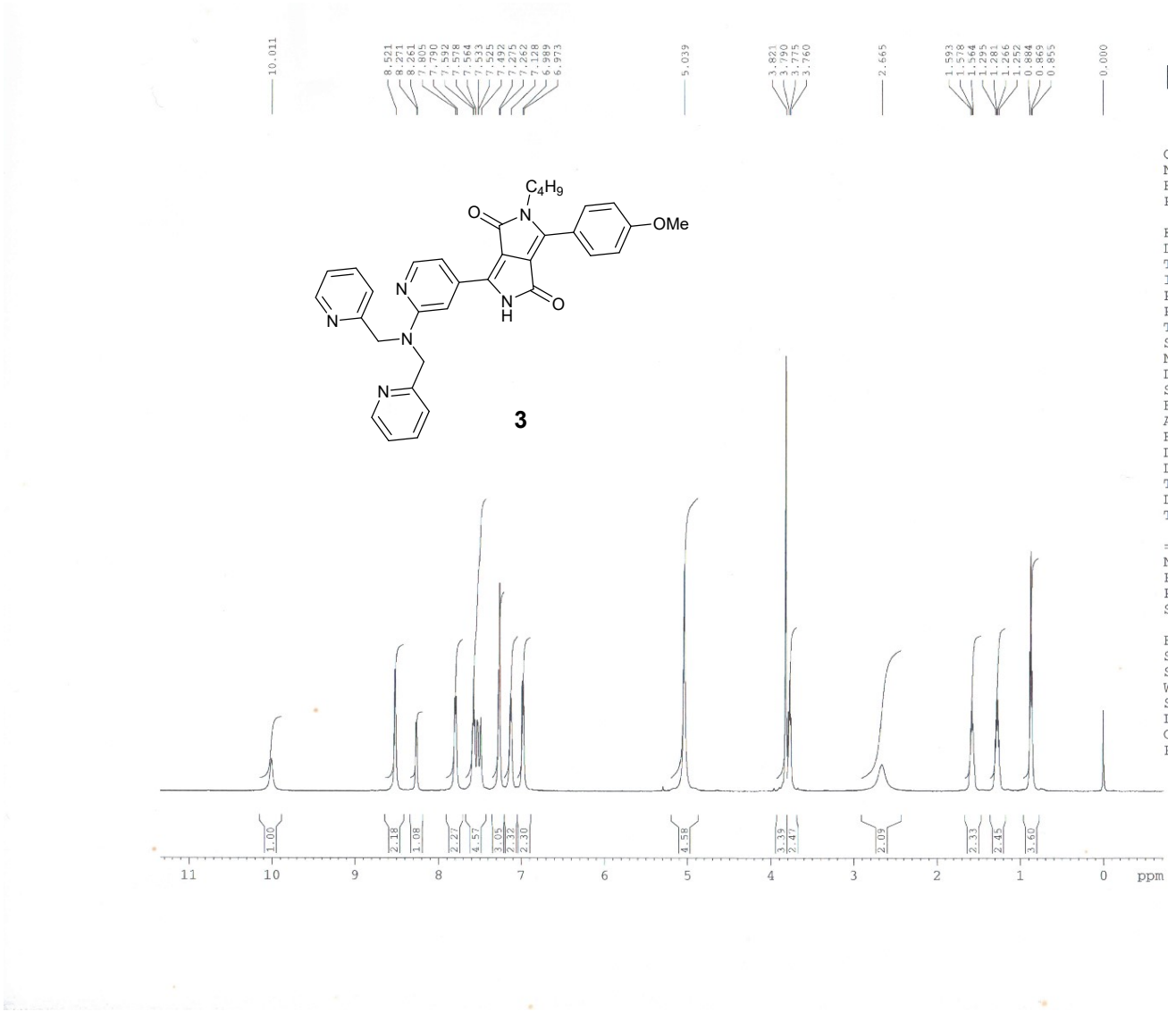

^{1}H-NMR spectra of **3** in $CDCl_3$

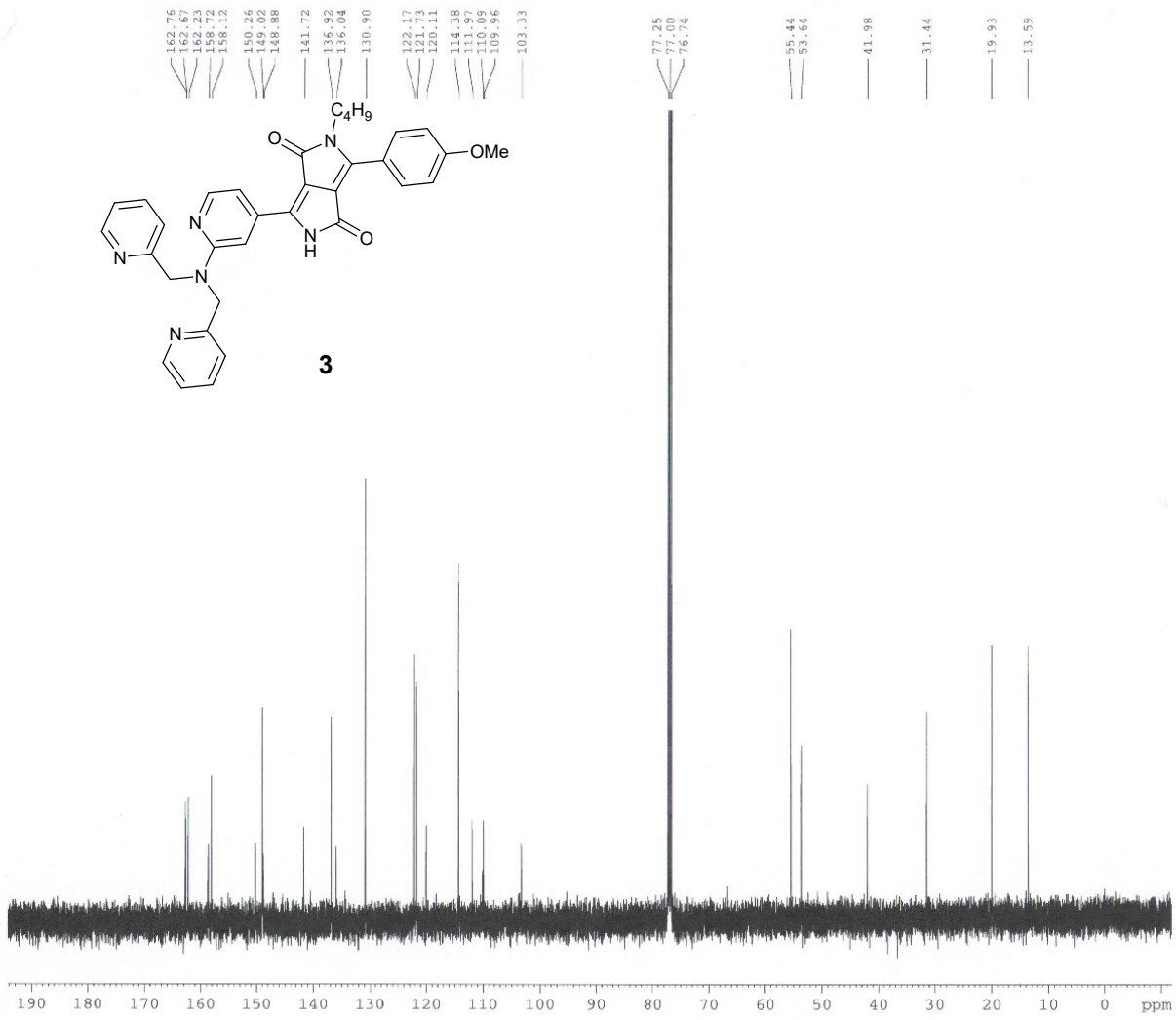

^{13}C-NMR spectra of **3** in $CDCl_3$

Elements Used:
C: 0-150 H: 0-150 N: 0-6 O: 0-3

Mass	Calc. Mass	mDa	PPM	DBE	Formula	i-FIT	i-FIT Norm	Fit Conf %	C	H	N	O
573.2628	573.2614	1.4	2.4	21.5	C34 H33 N6 O3	583.7	0.013	98.75	34	33	6	3
	573.2654	-2.6	-4.5	25.5	C39 H33 N4 O	588.1	4.384	1.25	39	33	4	1

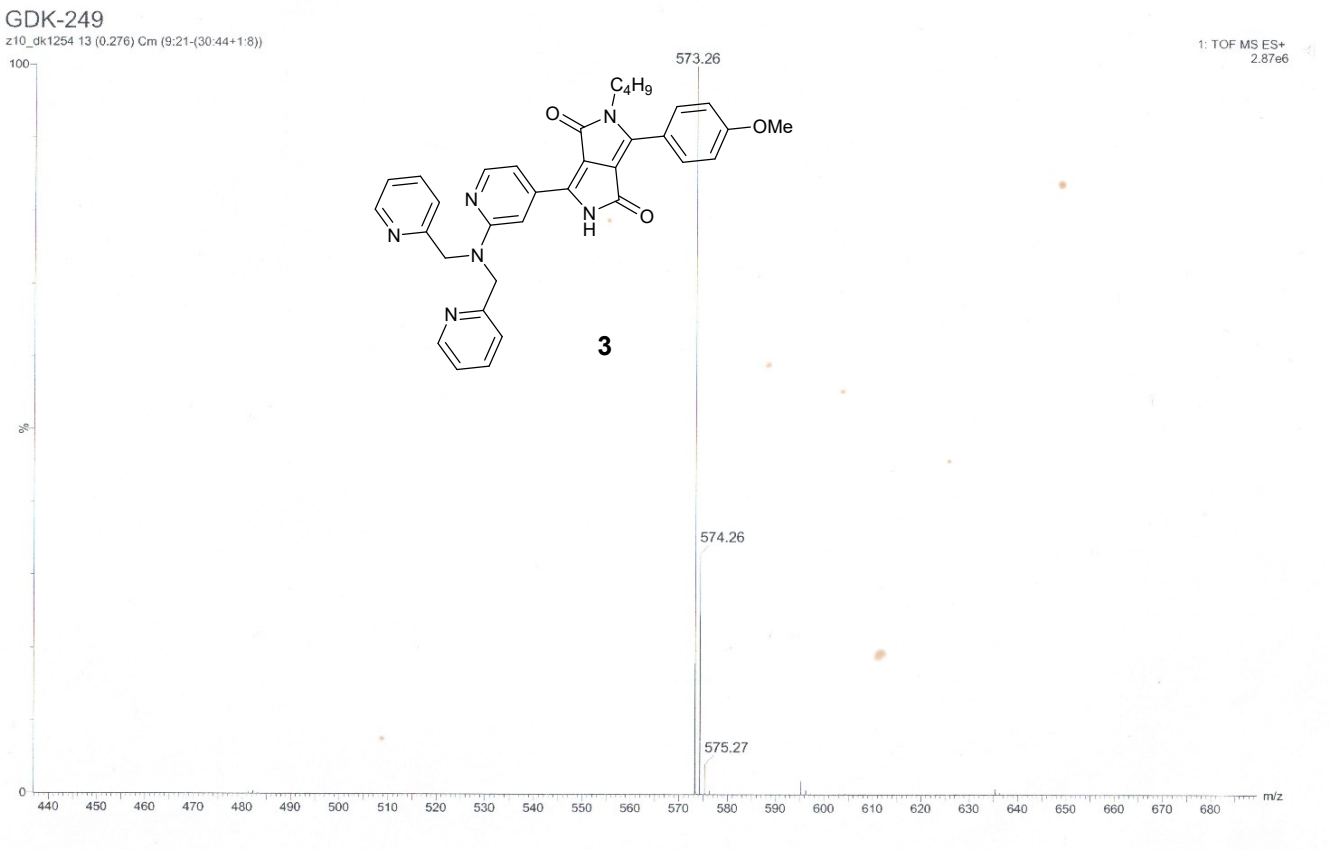

HRMS (ESI, m/z)

spectra of **3**

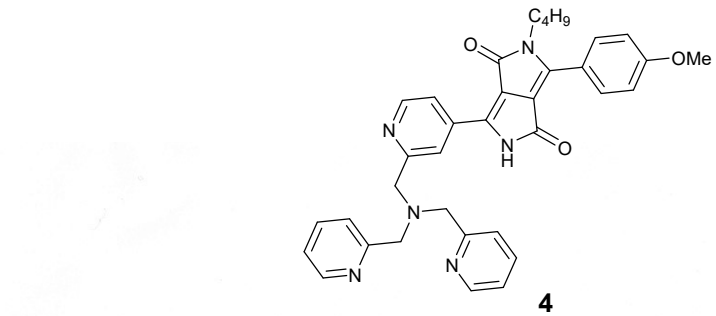

4

^{1}H-NMR

spectra of **4** in $CDCl_3$

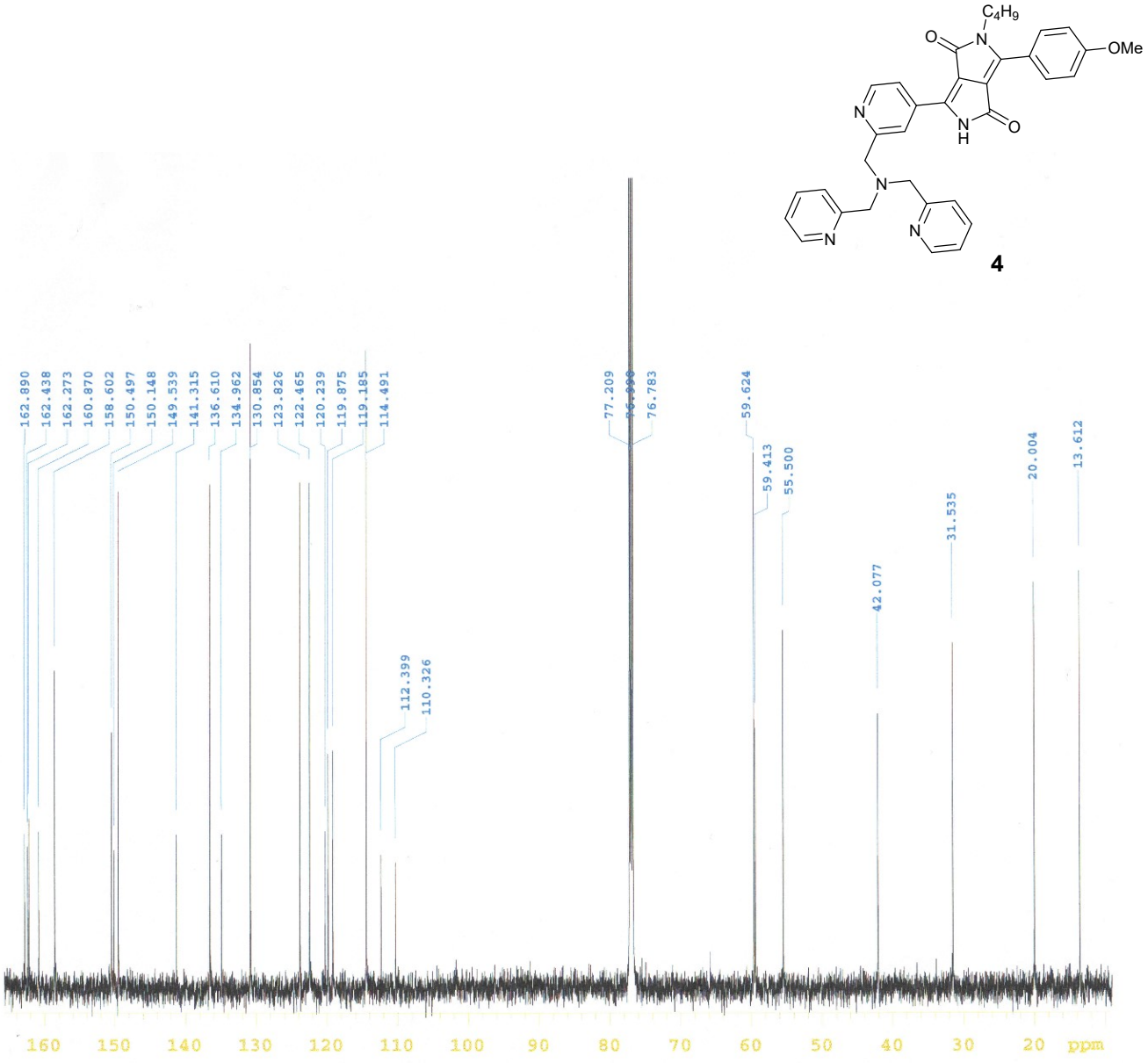
C4H9
O
N
OMe
N
N
H
O
N
N
N
4
162.890
162.438
162.273
160.870
158.602
150.497
150.148
149.539
141.315
136.610
134.962
130.854
123.826
122.465
120.239
119.875
119.185
114.491
112.399
110.326
77.209
76.783
59.624
59.413
55.500
42.077
31.535
20.004
13.612
160
150
140
130
120
110
100
90
80
70
60
50
40
30
20
ppm

^{13}C-NMR

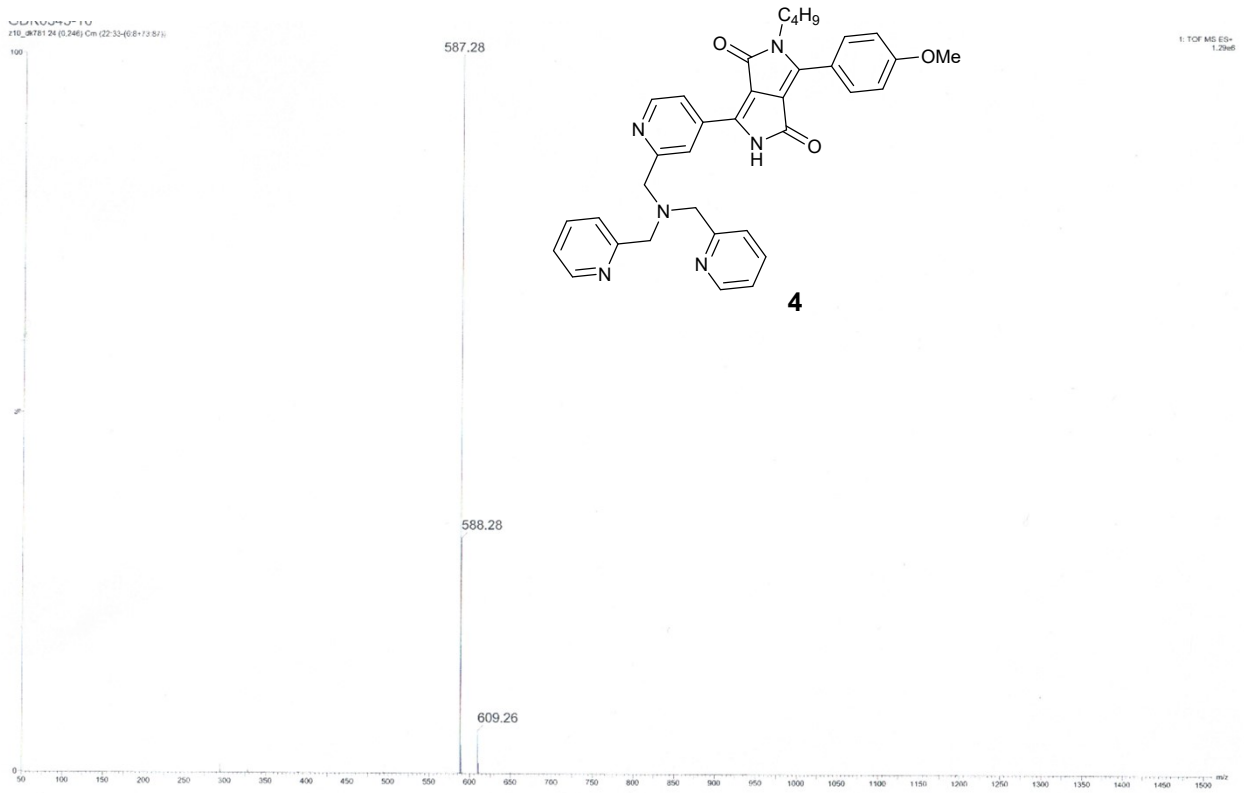

spectra of **4** in $CDCl_3$

HRMS (ESI, m/z) spectra of **4**

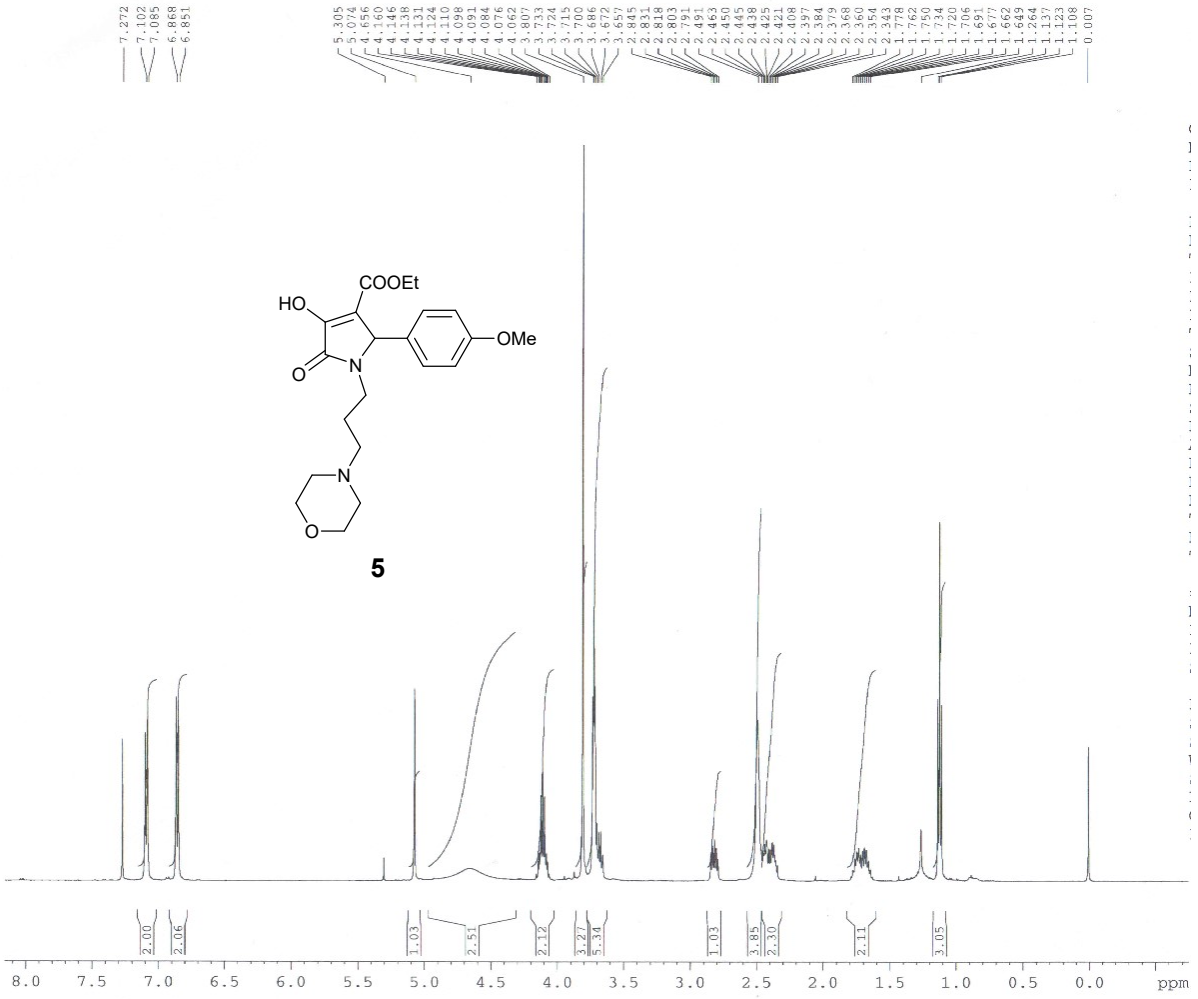

^{1}H-NMR spectra of **5** in $CDCl_3$

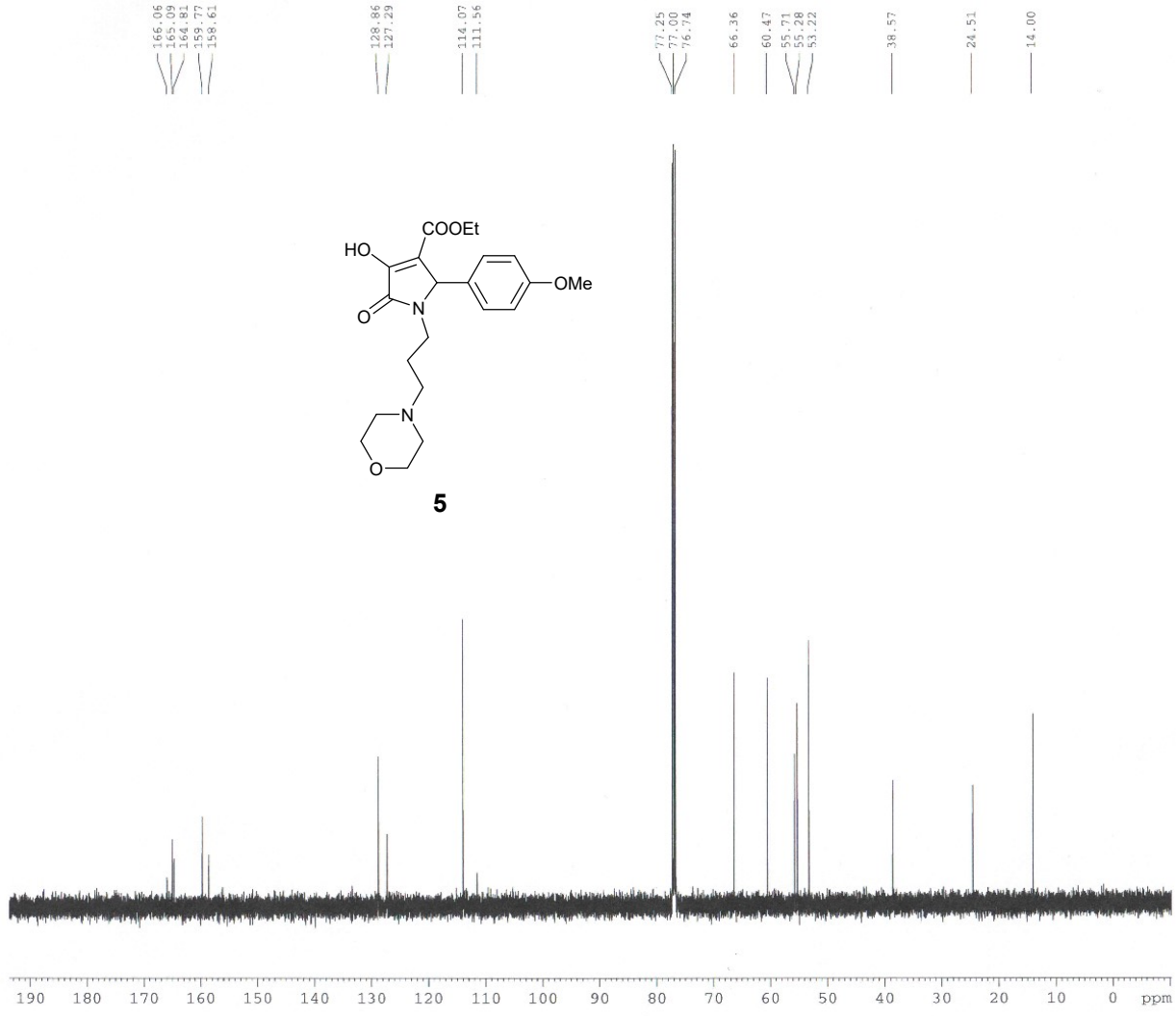
166.06
165.09
164.81
159.77
158.61
128.86
127.29
114.07
111.56
77.25
77.00
76.74
66.36
60.47
55.71
55.28
53.22
38.57
24.51
14.00
COOEt
HO
O
N
OMe
N
O
190 180 170 160 150 140 130 120 110 100 90 80 70 60 50 40 30 20 10 0 ppm

5

^{13}C-

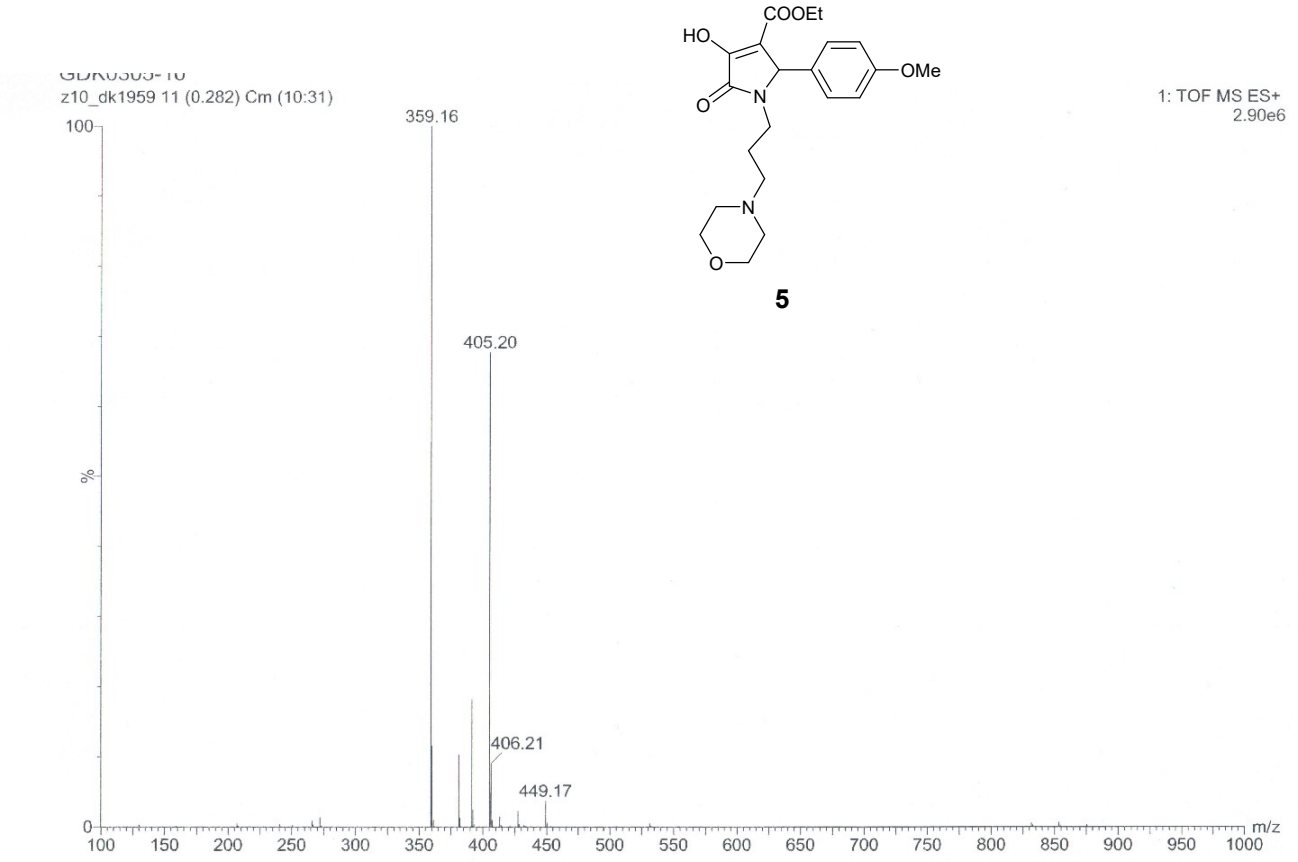

5

NMR spectra of **5** in $CDCl_3$

HRMS(ESI, m/z) spectra of **5**

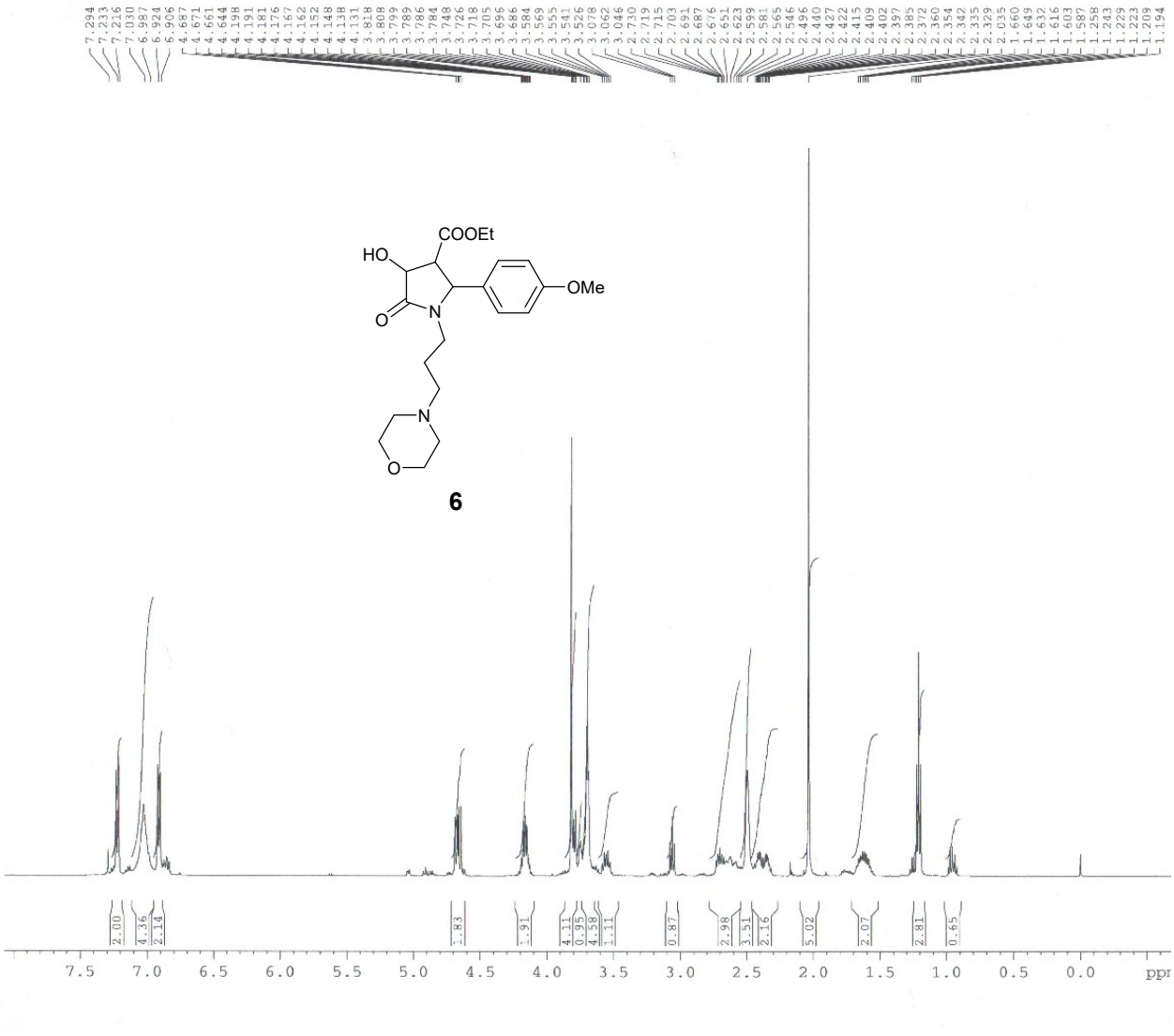

^{1}H-NMR

spectra of **6** in $CDCl_3$

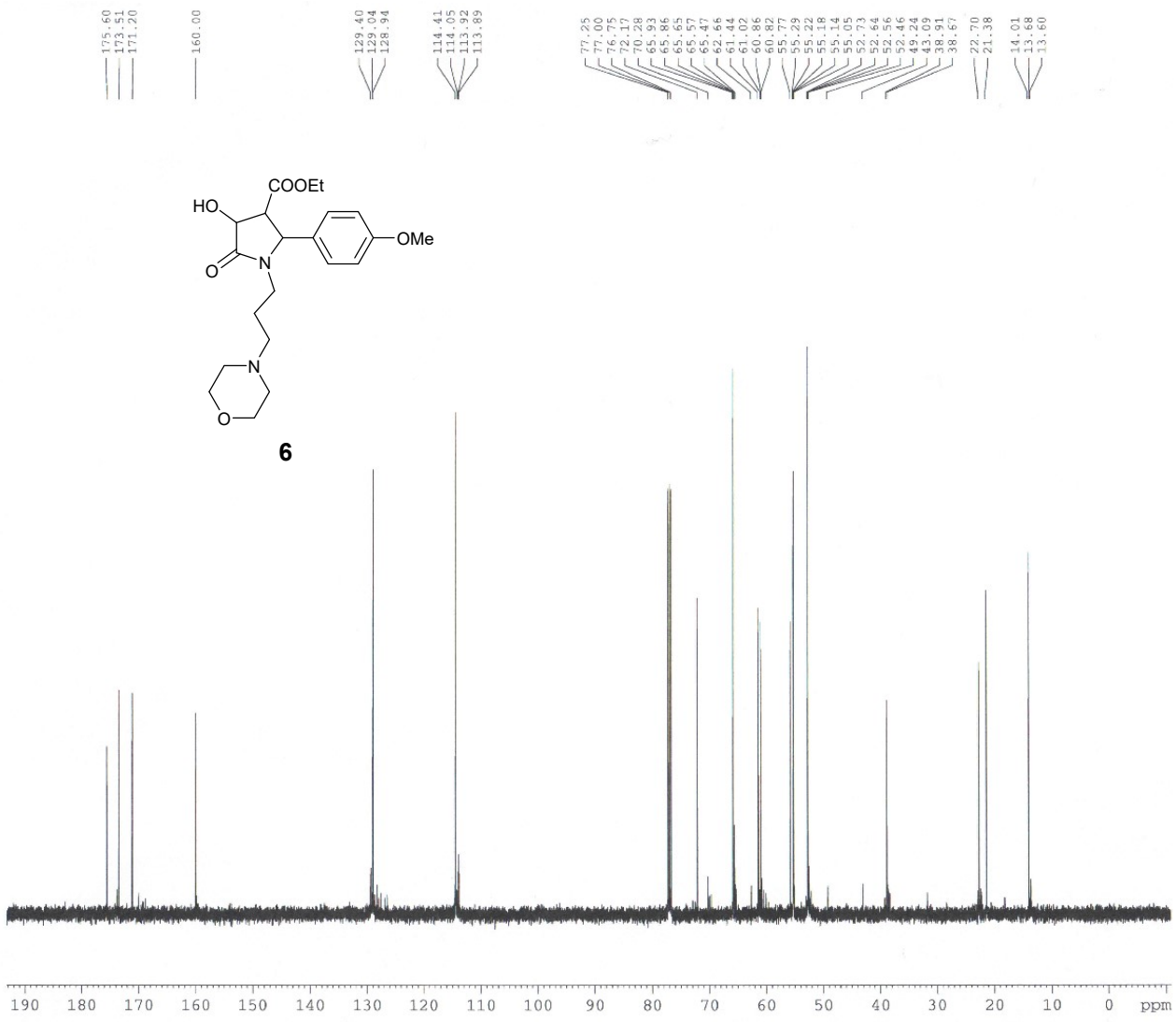
175.60
173.51
171.20
160.00
129.40
129.04
128.94
114.41
114.05
113.92
113.89
77.25
77.00
76.75
72.17
70.28
65.93
65.86
65.65
65.57
65.47
62.66
61.44
61.02
60.86
60.82
55.77
55.29
55.22
55.18
55.14
55.05
52.73
52.64
52.56
52.46
49.24
43.09
38.91
38.67
22.70
21.38
14.01
13.68
13.60
COOEt
HO
OMe
O
N
N
O
6
190
180
170
160
150
140
130
120
110
100
90
80
70
60
50
40
30
20
10
0
ppm

^{13}C-NMR

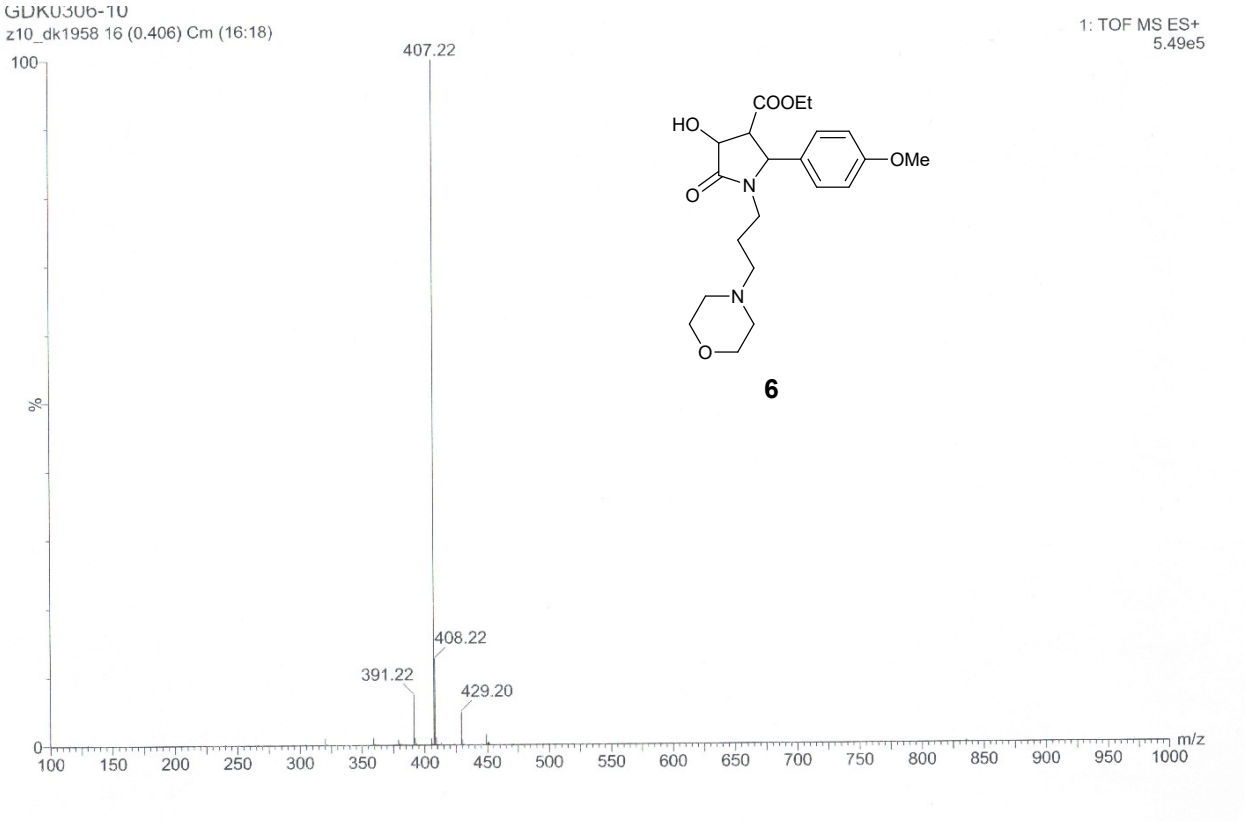

6

spectra of **6** in $CDCl_3$ HRMS (ESI, m/z) spectra of **6**

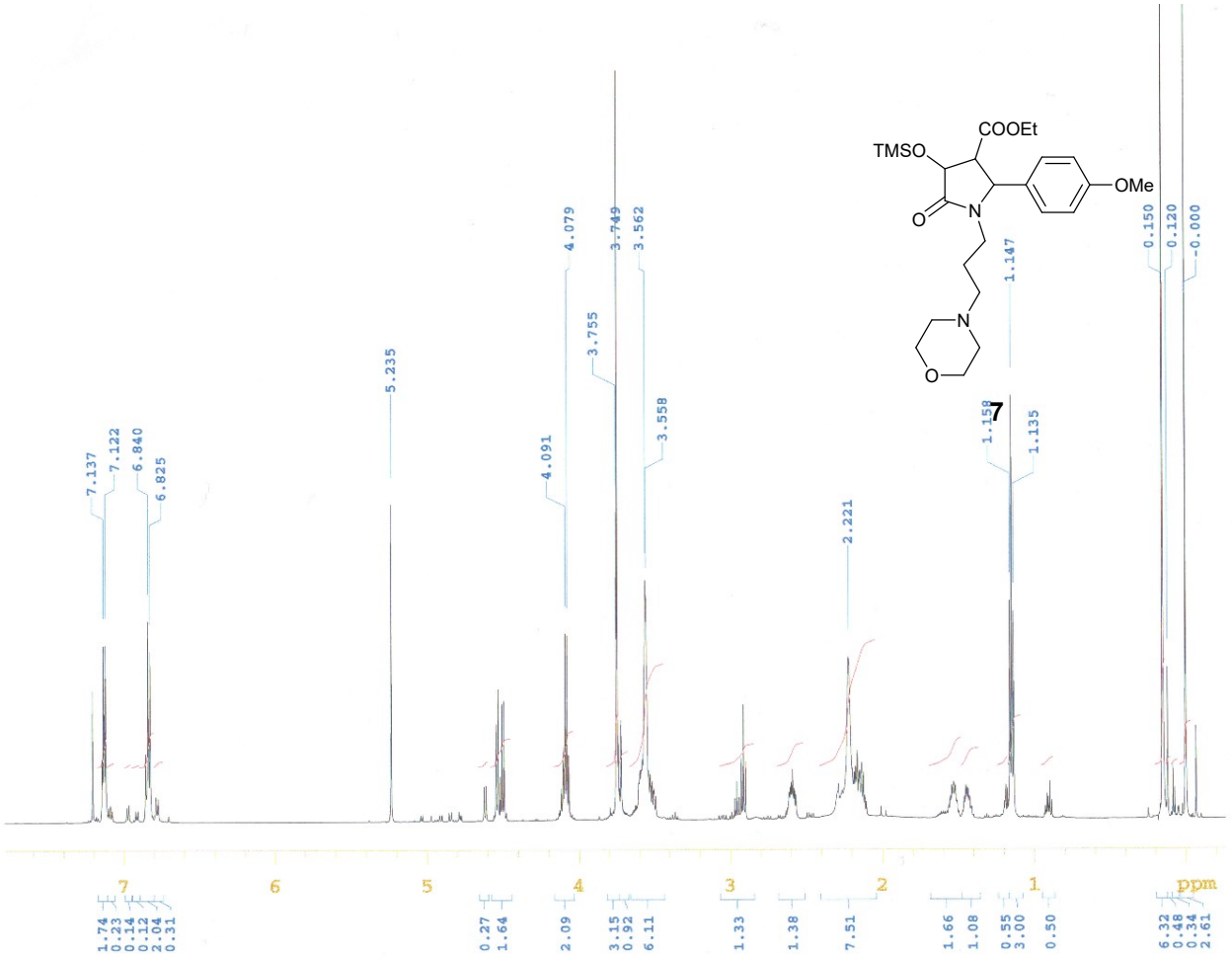

^{1}H-NMR spectra of

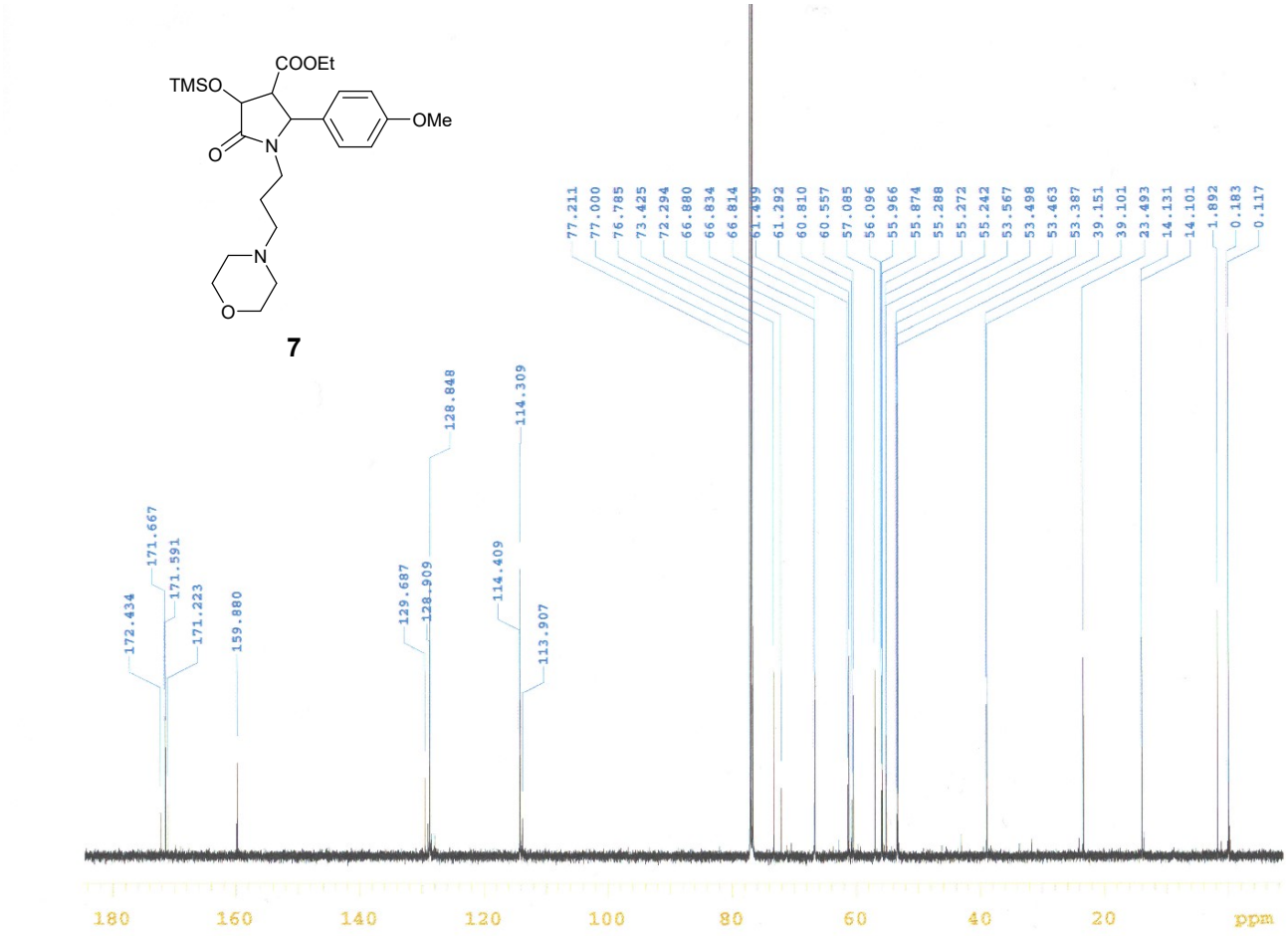

7 in $CDCl_3$ ^{13}C-NMR

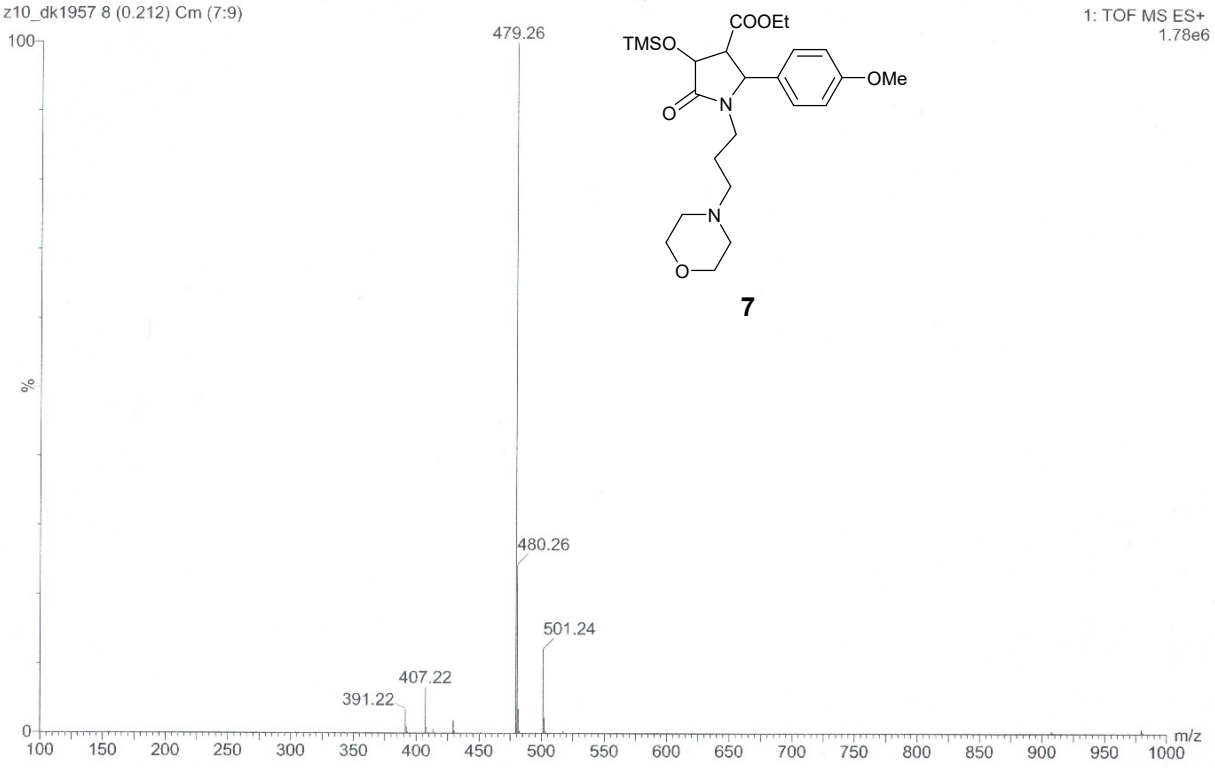

7

spectra of **7** in $CDCl_3$

HRMS (ESI, m/z) spectra of **7**

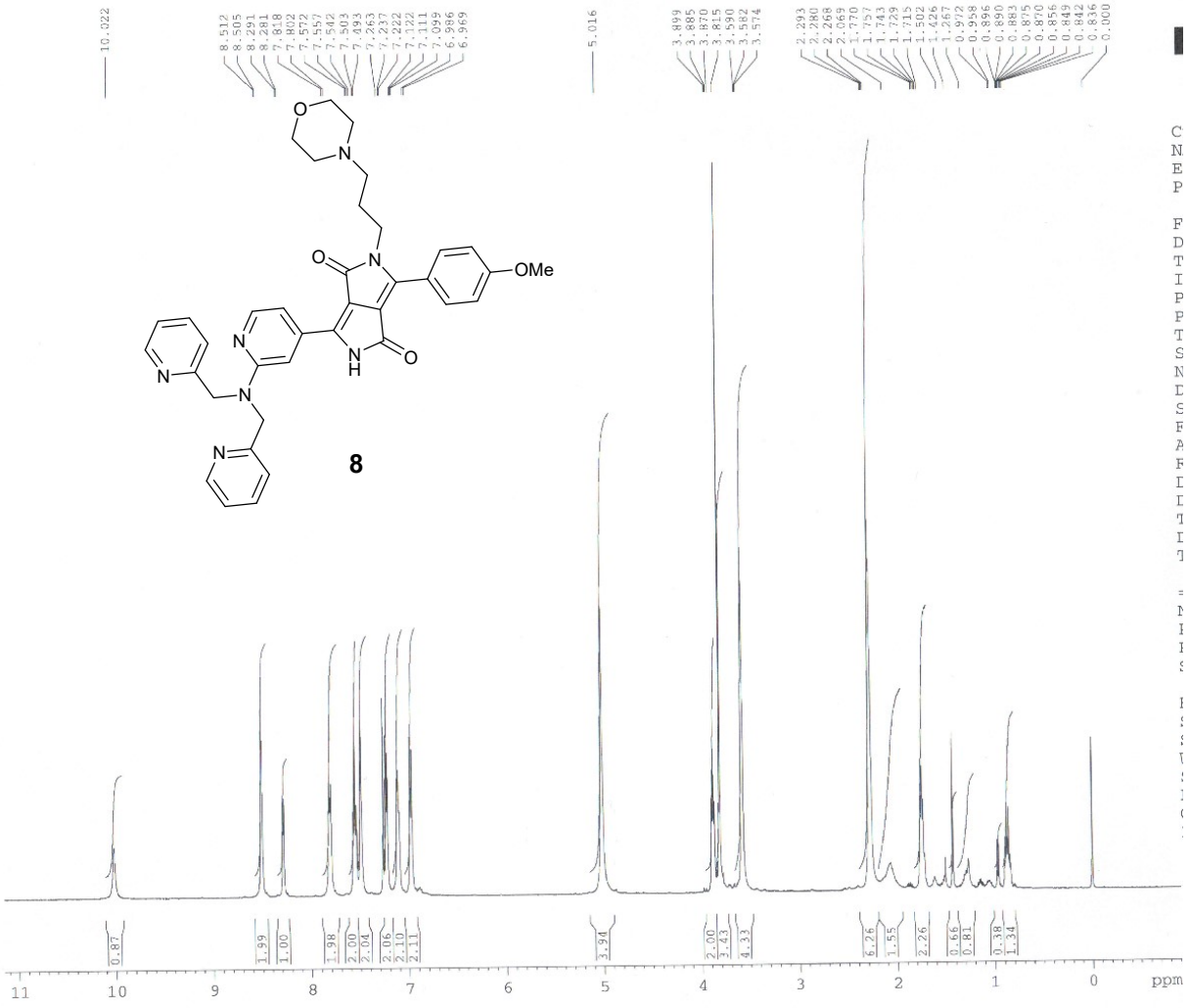

^{1}H-NMR

spectra of **8** in $CDCl_3$

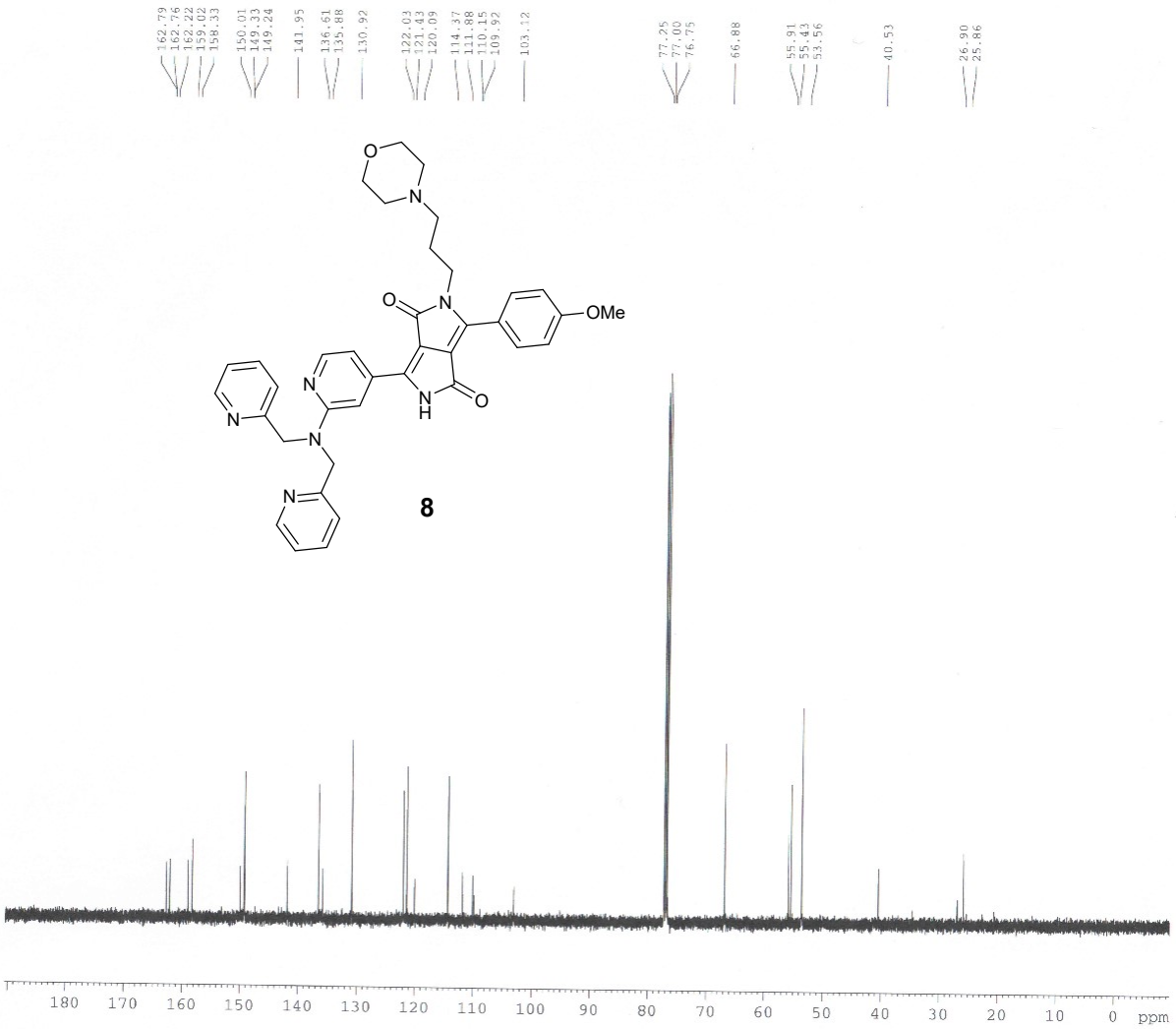
162.79
162.76
162.42
159.02
158.33
150.01
149.33
149.24
141.95
136.61
135.88
130.92
122.03
121.43
120.09
114.37
111.88
110.15
109.92
103.12
77.25
77.00
76.75
66.88
55.91
55.43
53.56
40.53
26.90
25.86
OMe
8
180 170 160 150 140 130 120 110 100 90 80 70 60 50 40 30 20 10 0 ppm

^{13}C-NMR

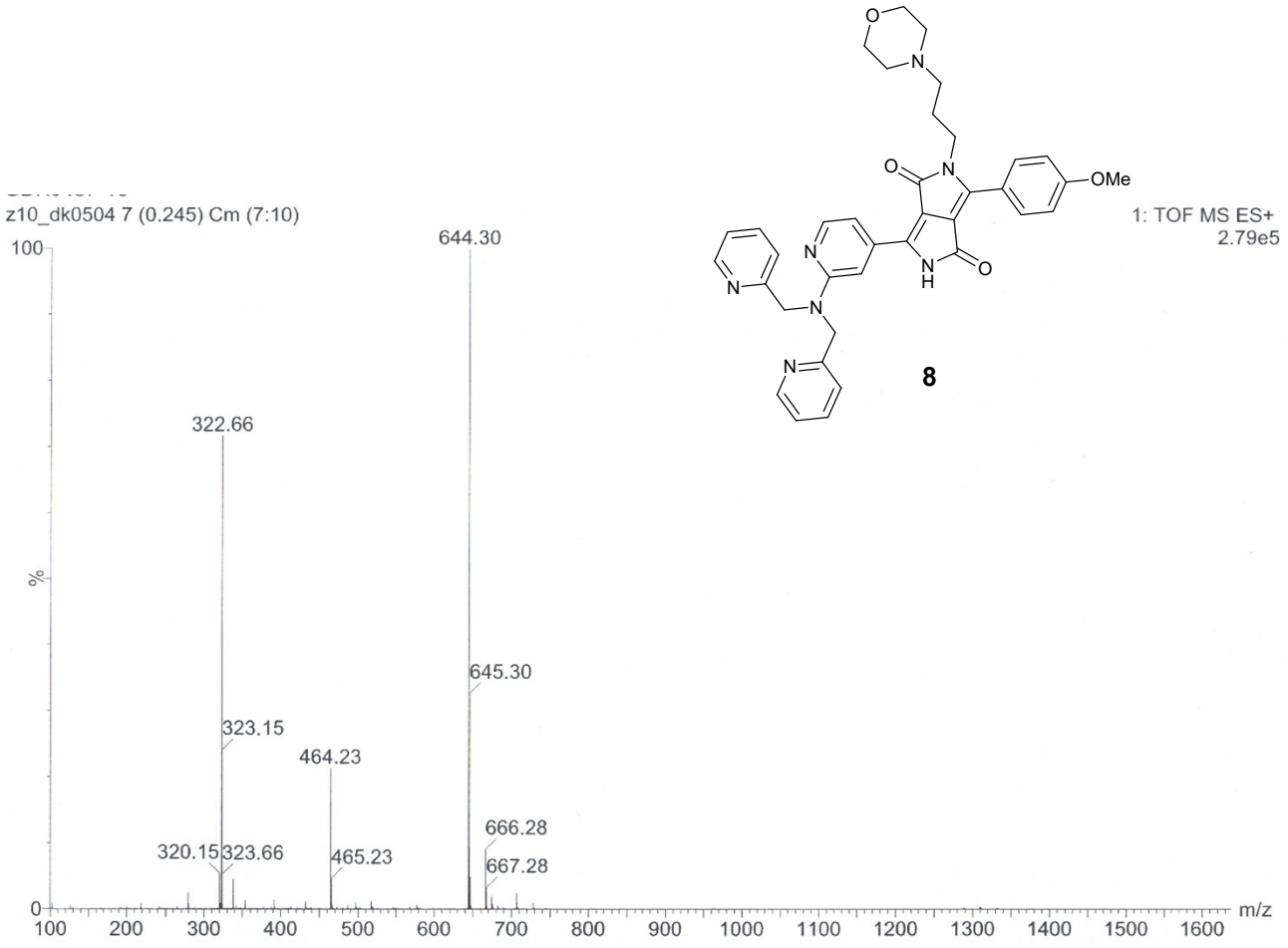

8

spectra of **8** in $CDCl_3$ HRMS (ESI, m/z)

spectra of

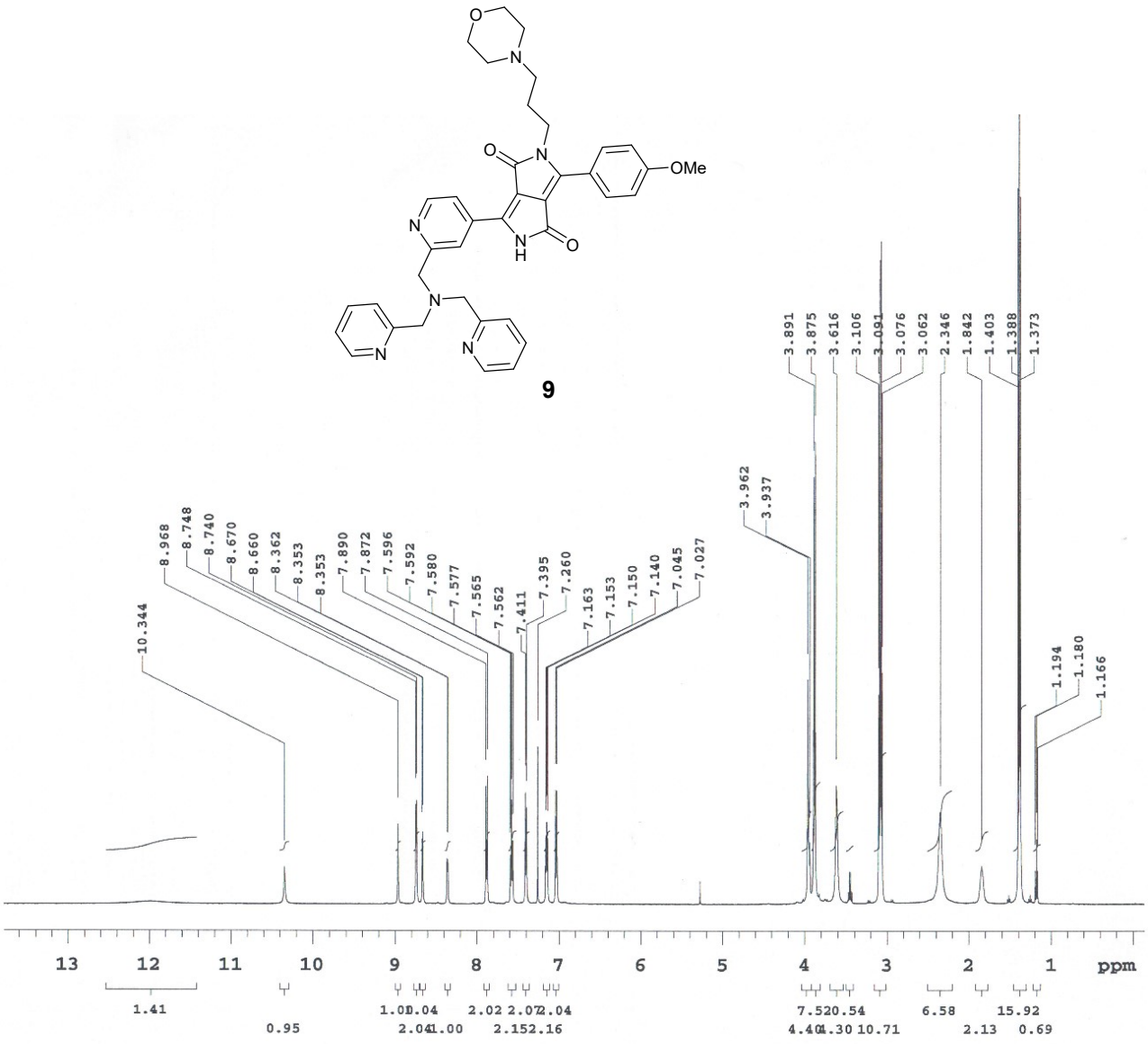

8 ^{1}H-NMR spectra of **9** in $CDCl_3$

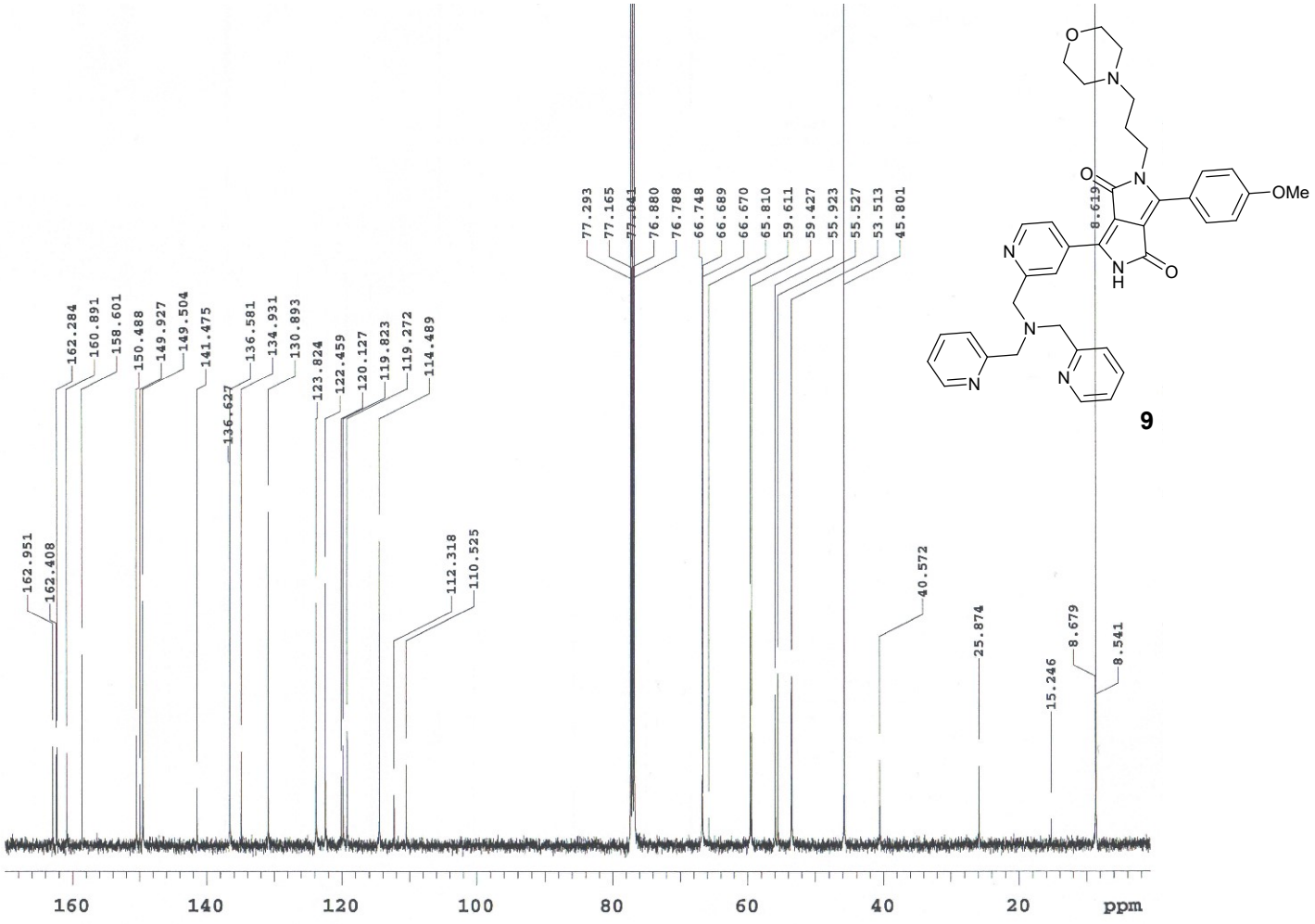

^{13}C-NMR spectra

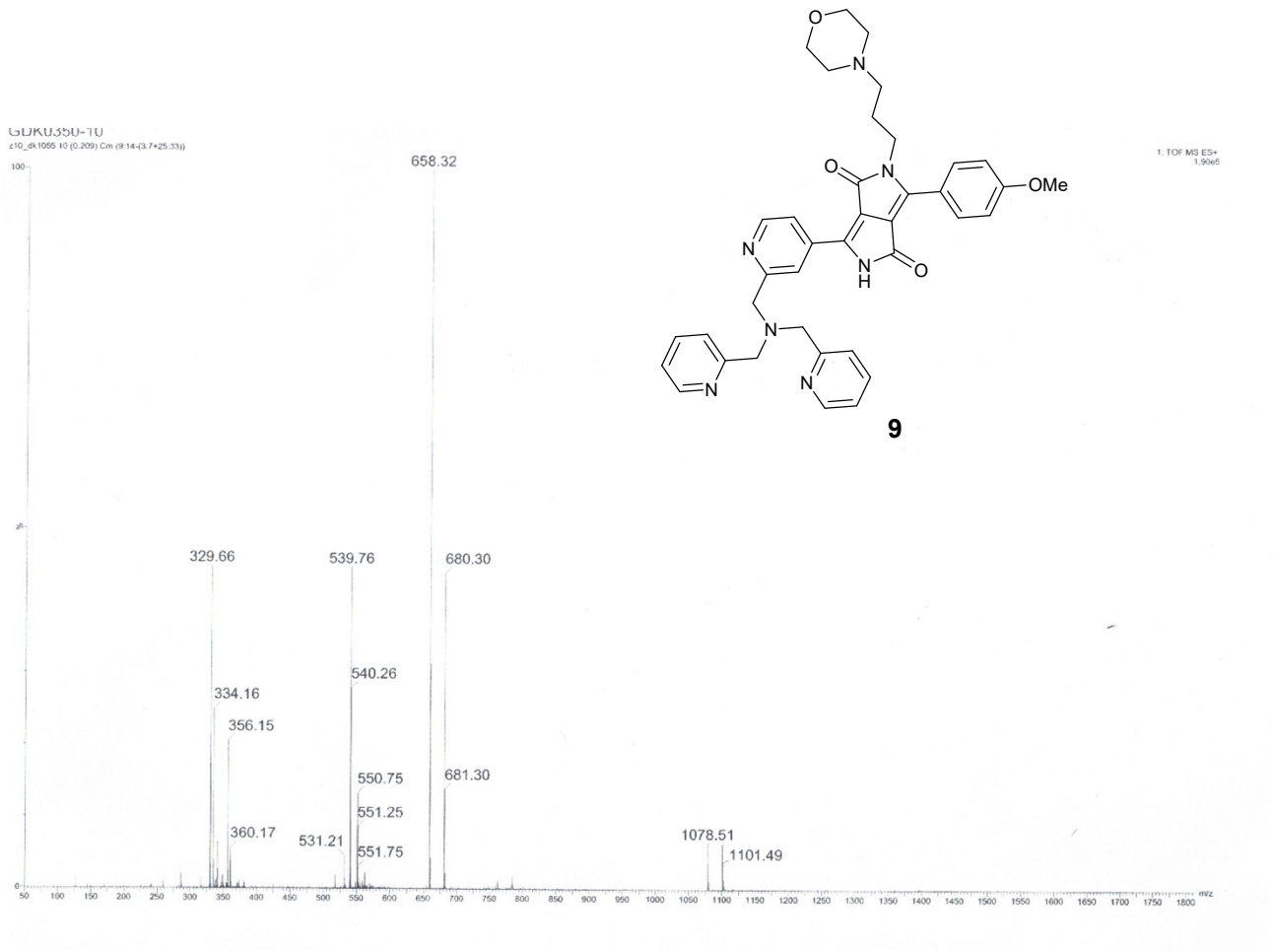

of **9** in $CDCl_3$ HRMS (ESI, m/z)

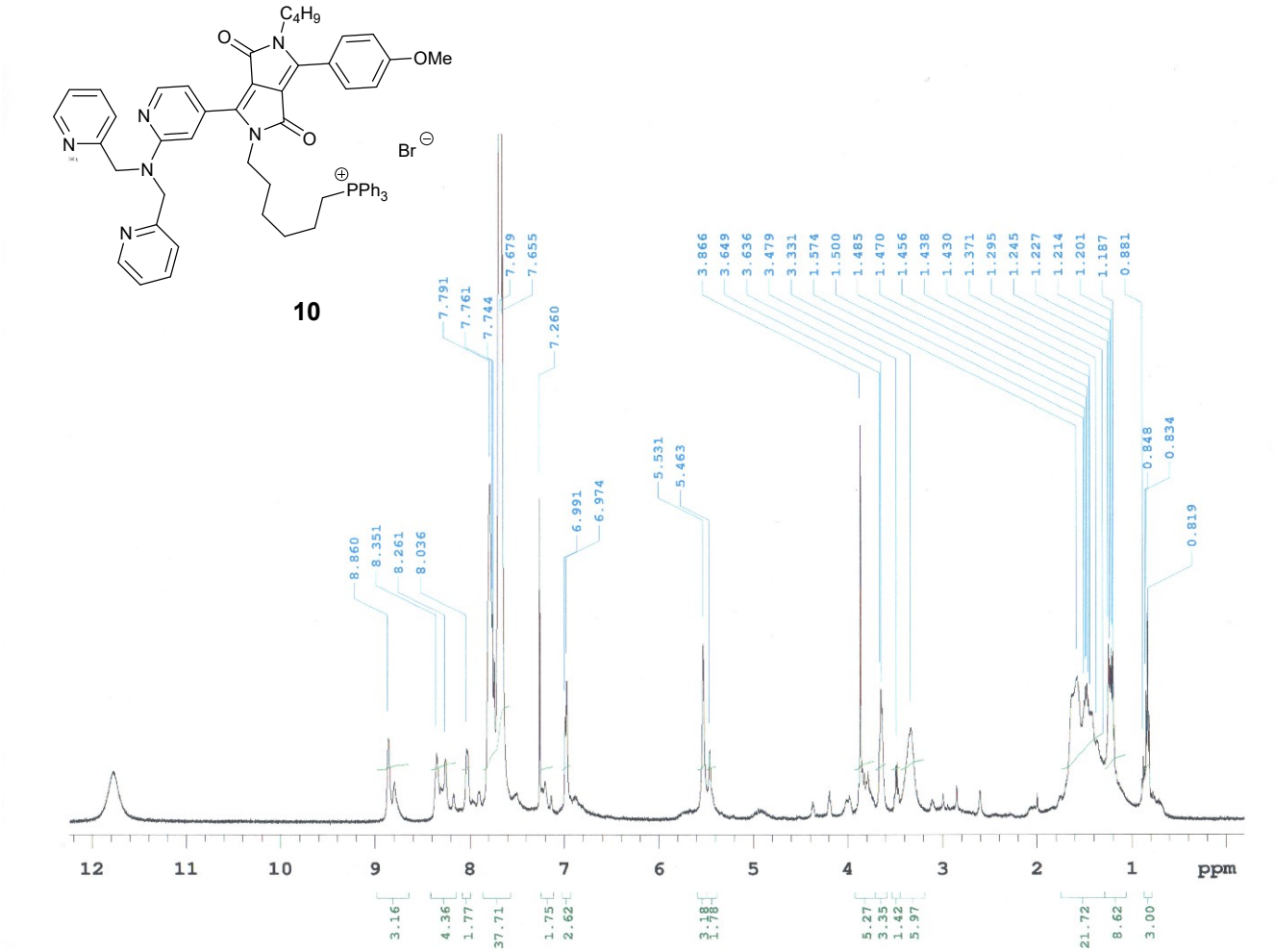

spectra of **9** ^{1}H-NMR

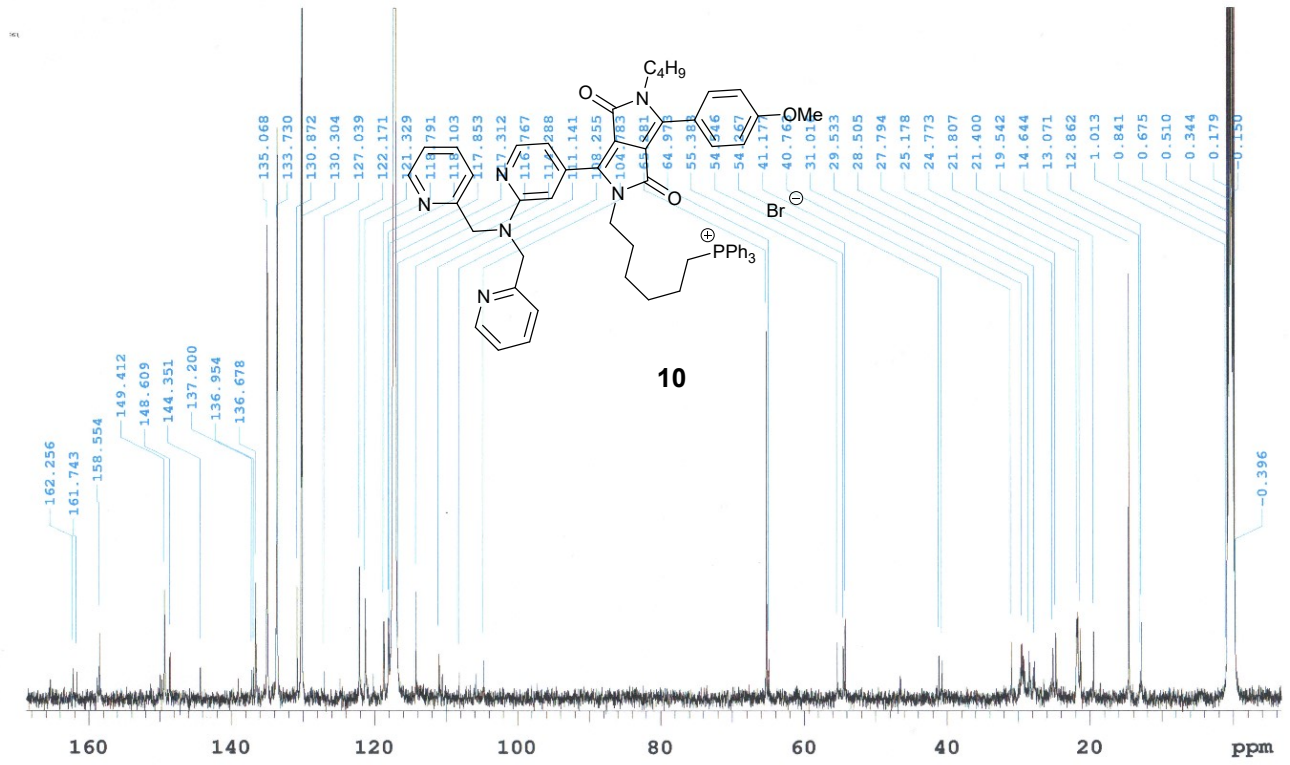

spectra of **10** in $CDCl_3$ ^{13}C-

NMR spectra of **10** in $CDCl_3$

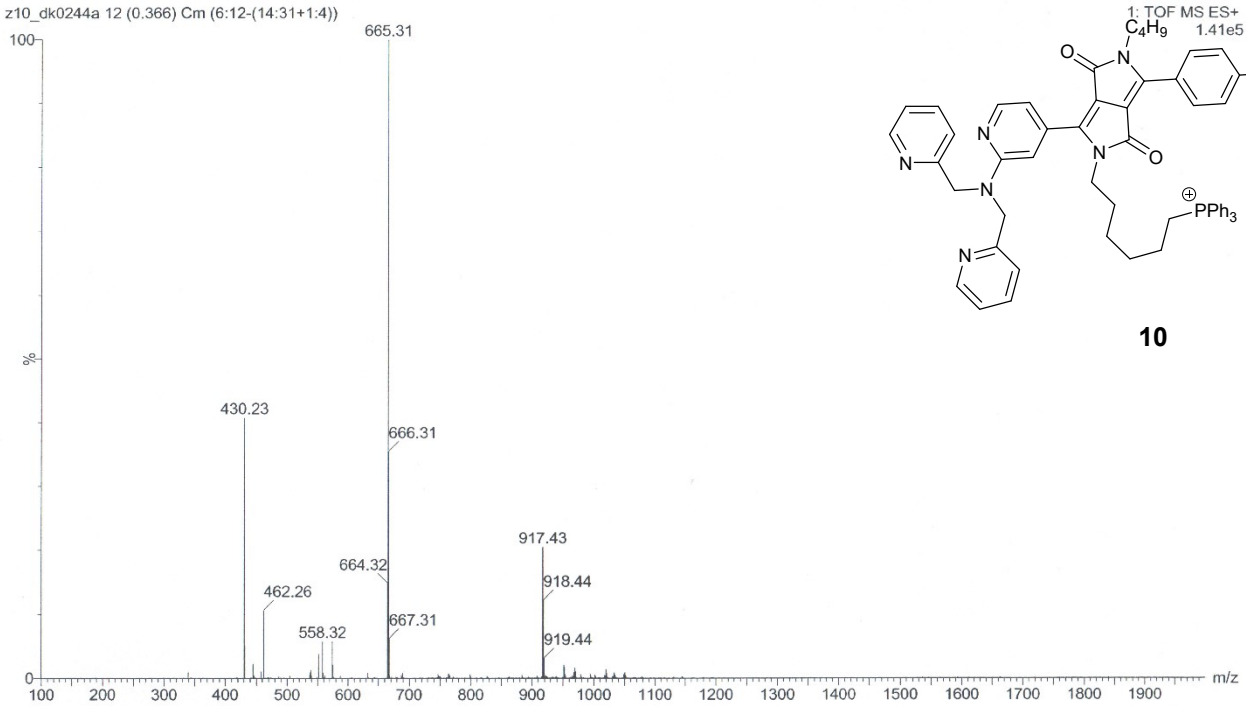

10

HRMS (ESI, m/z) spectra of **10**

Section S8: References

1. M. Pieczykolan, B. Sadowski and D. T. Gryko, *Angew. Chem. Int. Ed*., 2020, **59**, 7528-7535.